Delft University of Technology

AIRBUS

Adhesion performance on carbon fibre reinforced poly-phenylene sulphide depending on surface treatments

Miriam GOMEZ GARCIA

Master of Science
In
Aerospace Engineering

Delft, the Netherlands
September 2017

"Adhesion performance on carbon fibre reinforced poly-phenylene sulphide depending on surface treatments"

Miriam GOMEZ GARCIA

Dissertation Submitted In Partial Fulfilment of the Requirements for Master of Science in Aerospace Engineering

Company supervisor: Santiago Aranda Gallardo
Academic supervisors: Hans Poulis
Sofia Teixeira de Freitas

Company: Airbus Helicopters
Location: Donauwörth, Germany

DECLARATION

Non-disclosure note

This thesis contains internal and confidential information of Airbus Helicopters. The disclosure, publication or duplication of the thesis to third parties in parts or as a whole is strictly forbidden. It is not allowed to make any copies or transcriptions. Exceptions require a written authorization from Airbus Helicopters and the author.

The following parties are excluded from this note are:

· Hans Paulis (Technical University of Delft)

· Sofia Teixeira de Freitas (Technical University of Delft)

I hereby declare that this master thesis has been written only by the undersigned individual without any assistance from third parties.

Furthermore, I conform that no sources have been used in the preparation of this thesis other than those indicated in the thesis itself.

Date and place

Madrid, September 2017

Signature

Miriam Gómez García

Acknowledgements

I would like to thank my family and friends for their support throughout my entire education, without them it would have been impossible to reach where I am right now.

Also I would like to thank Santiago Aranda-Gallardo and the ETLO department for the opportunity to perform the master project with him and their guidance and support during this period.

Finally, I would like to thanks Hans Paulis and Sofia Teixeira de Freitas for being my supervisors at the university, their acceptance of the topic since the beginning, support during the performance of experiments and evaluation of my project.

Abstract

The use of fibre reinforced composite polymeric materials for primary helicopter structures has been increasing over the last decades due to their attractive properties; high performance and lightweight inducing more fuel savings than their metallic counterparts. With respect to the joining methods; structural adhesive bonding is preferred when cost and weight are important factors. The qualification of a bonded joint requires the determination of its durability and reliability of the bond strength, but due to the possible degradation of adhesives under certain environments, the lack of a failure criterion and in view of safety consideration, adhesive joints tends to be 'overdesign', resulting in an increase of weight and manufacturing costs.

The present project aims to evaluate and investigate the adhesive performance of carbon fibre reinforced PPS; a reinforced high performance thermoplastic qualified in Airbus and already used on certain structural parts of the helicopter. The surface topography and chemistry were evaluated using an optical microscope, XPS and contact angle measurements before and after two surface treatments; hand sanding and grinding. Adhesive joints were manufactured to analyse its single lap shear (SLS) strength and fracture energy, G_{IC} using three different adhesives and two environmental conditions.

Both surface treatments increased the surface energy, but while sanded samples showed an increase of the dispersive component, APP increased to a large extent the polar part. In addition, after hand sanding the morphology of the surface was modified. For most of test configurations, the specimens failed at the interface, however plasma treated samples showed higher values of lap shear strength and fracture toughness energy.

An accelerated ageing condition was simulated by the storage of the samples in a climate chamber at high temperature and humidity. The effect that these environmental conditions had on the adhesion performance depended to a large extent on the adhesive used; in this case all of the adhesive studied showed different trends on the adhesion properties; the epoxy adhesive designed to withstand high temperatures did not present any effect on the adhesive performance but a common epoxy for structural application showed a softening of the adhesive and therefore a decrease on the shear strength but an increase of the fracture toughness and with respect to polyurethane adhesive, the interface was degraded changing the failure from mixed to adhesive mode.

Finally, CF-PEEK samples were tested in single lap shear after these two surface treatments, showing better results than PPS with the same working parameters. However, some configurations still failed at the interface.

Table of Contents

List of figures

List of tables

Symbols and abbreviations

AID	Amaze ID (internal identification number)
AF	Adhesive failure
APP	Atmospheric pressure plasma
CohF	Cohesive failure
CF-PEEK	Carbon fibre reinforced PEEK
CF-PPS	Carbon fibre reinforced PPS
DBD	Dielectric barrier discharge
DCB	Double cantilever beam
DSC	Differential scanning calorimetry
EASA	European aviation safety agency
EP	Epoxy adhesive
FVC	Fibre volume content
GF	Glass fibre
HPTC	High performance thermoplastics composites
NDT	Non-destructive testing
PDMS	Polydimethylsiloxane
PEEK	Polyether ether ketone
PPS	Polyphenylene sulphide
PU	Polyurethane adhesive
r.h.	Relative humidity
RT	Room temperature
SLS	Single lap shear
Tg	Glass transition temperature
Tm	Melting temperature
UD	Unidirectional
UHMWPE	Ultra-high molecular weight polyethylene
XPS	X-ray photoelectron spectroscopy
γ	Surface free energy
γ^d	Dispersive component of surface free energy
γ^p	Polar component of surface free energy
θ	Contact angle

1. Introduction

The use of fibre reinforced polymeric materials for primary helicopter structures has been increasing over the last decades. With their attractive characteristics such as lightweight and high performance inducing more fuel saving than their metallic counterparts, there is a continuous investment in the development of technical and process knowledge due to their potential use in industry [1, 2].

In general composite polymeric materials lead to an increase of the customer value by enhancing mission capabilities or increasing the payload. This can be achieved thanks to the material properties; low weight, high strength or the ability to tailor the mechanical properties. Additionally, thermoplastic materials can be reworked and recycled, being beneficial for economic reasons and the fulfilment of environmental requirements [3]. The increase of the volume of thermoplastic composites is based on sustainable development and weight reduction, with the current focus on lowering the overall costs by reducing the manufacturing costs using less expensive techniques [4].

In recent years, thermoplastic composites have been successfully used in several structural parts on helicopters and aircrafts; some examples are listed below:

- The horizontal tail plane from AgustaWestland AW169 helicopter was manufactured by CF/PPS prepregs, leading to a reduction of 15% weight with respect to other fibre reinforced composites solutions [1].
- The wing leading edges in A340 and A380 are manufactured with CF/PPS prepregs.
- H160 is the first civil helicopter with all its structure made of composite material; and especially the rotor hub will be manufactured using thermoplastics [5, 6].
- The undercarriage door for the Fokker 50; the ribs and spars from this door were made from CF/PPS prepregs [7].

Along with this development, compatible joining techniques such as structural adhesive bonding are increasing their importance but they should still be improved in terms of reliability and robustness [8]. Generally, structural adhesive bonding is preferred when the costs and weight are important factors. It shows key advantages over conventional methods such as mechanical fasteners; bonded joints produce smooth contours and show superior fatigue resistance since the stresses are distributed more uniformly over a larger area reducing stress concentrations.

A bonding process is qualified after demonstrating that all the steps are reliable and repeatable. For each bonded joint, the maximum load should be proved by the evaluation of each steps leading to the study of bonding problems that might occur such as an insufficient pressure during curing or surface contamination, by the performance of mechanical tests or by non-destructive inspection methods. The last method is nowadays not reliable at a production scale, but it opens new ways for qualification in the near future [9]. In addition, the qualification of an adhesive bonded joint requires the determination of its durability and reliability of the bond strength. As a result of the possible degradation of adhesives under

certain environments, the lack of a failure criterion and in view of safety considerations, adhesives joints tend to be 'overdesigned'; in aerospace industry they are accompanied with rivets or fasteners (known as 'chicken rivets'), resulting in an increase of weight and manufacturing costs [10]. However, it is concluded by many industries that fully weight and cost saving of composites materials would only be achievable when a bonded joint can be certified without using mechanical fasteners [11].

A critical step on an adhesive bonded joint is the preparation of the surface; since the adhesion is a surface phenomenon and it was observed that the performance depends to a large on the properties of the substrate's surface. In case of thermoplastic, they are inherently inert as their chemical composition is based on carbon and hydrogen atoms with small amount of other elements such as nitrogen, oxygen and/or halogens; they show low polar component of surface energy and smooth surfaces. Due to these features, they tend to show insufficient bond strength [12, 13].

1.1. Motivation

The use of composite materials on the aircraft decreases the total structural weight due to its high specific properties, but their use could still be further optimized with the adoption of adhesive bonding as the joining technique. As it was previously stated, the achievement of a strong interface is especially problematic for thermoplastic materials due to its smooth surface and low polar component of surface free energy but this problem might be solved with the application of surface pre-treatments.

Taking into account this information, the main purpose of this project is to investigate if it is possible to obtain high bond strength and durable joints using high performance thermoplastic materials and how this can be achieved. Carbon fibre reinforced PPS material was chosen as the substrate due to its current use in some structural parts and its already qualified used by Airbus, with two of the most used surface treatments; hand sanding and atmospheric plasma treatment. The main question to answer is:

How do surface pre-treatments improve the adhesion performance on bonded joints using CF-PPS as the substrate?

The research can be split up into three sub-questions related to the three different stages of the research framework (literature review, experimental stage and interpretation of results):

- Which are the parameters that influence adhesion?
- What is the effect of the different surface pre-treatments in view of adhesion strength?
- What do we learn by comparing the results and analysis from the different types of surface pre-treatment in order to make recommendations on how to obtain the maximum adhesion strength on PPS?

By the end of the project, the information obtained will allow to:

- Increase the acceptance of adhesive bonding as a joining method.
- Optimize the design and performance of PPS composites

- Open new ways for the application of CF/PPS composites in future structural or semi-structural parts.

1.2. Scope of the work

For this project, the analysis of the adhesion performance is evaluated by the calculation of the shear strength and fracture toughness with the characterization of the surface by optical microscope, contact angle and X-ray photoelectron spectroscopy (XPS). The parameters of the different tests configurations can be seen graphically in Figure 1.1 and they are:

- Substrate

CF-PPS was the principal substrate for this project, studying its adhesive performance in all test configurations. In addition, CF-PEEK was also studied to a lesser extent to compare the effect of the substrate on a bonded joint.

- Surface treatment

The activation treatments are a mechanical method, hand sanding, and one energetic method, atmospheric pressure plasma. These methods were chosen in view of their currently use in industry with other substrates showing satisfactory results.

- Adhesive

Another parameter on an adhesive joint is the adhesive used itself; the adhesion performance should change with respect to the adhesive used. Most of the investigations found were carried out with one type of adhesive, usually epoxy. As part of the project, three different types of adhesives will be used for each surface treatment; two epoxies and one polyurethane adhesive.

- Conditioning

Finally, the ageing effect is studied and half of the samples were stored in a climate chamber for 1000h; this time was expected to be sufficient to reach the saturation point at which the weight of the sample would not increase with respect time. Previous researches have been focused on the ageing effect between the surface treatment and the application of the adhesive since the surface morphology is not stable and it tends to return to the original state over time. However, very few studies show the effect of an accelerate ageing on the adhesive performance.

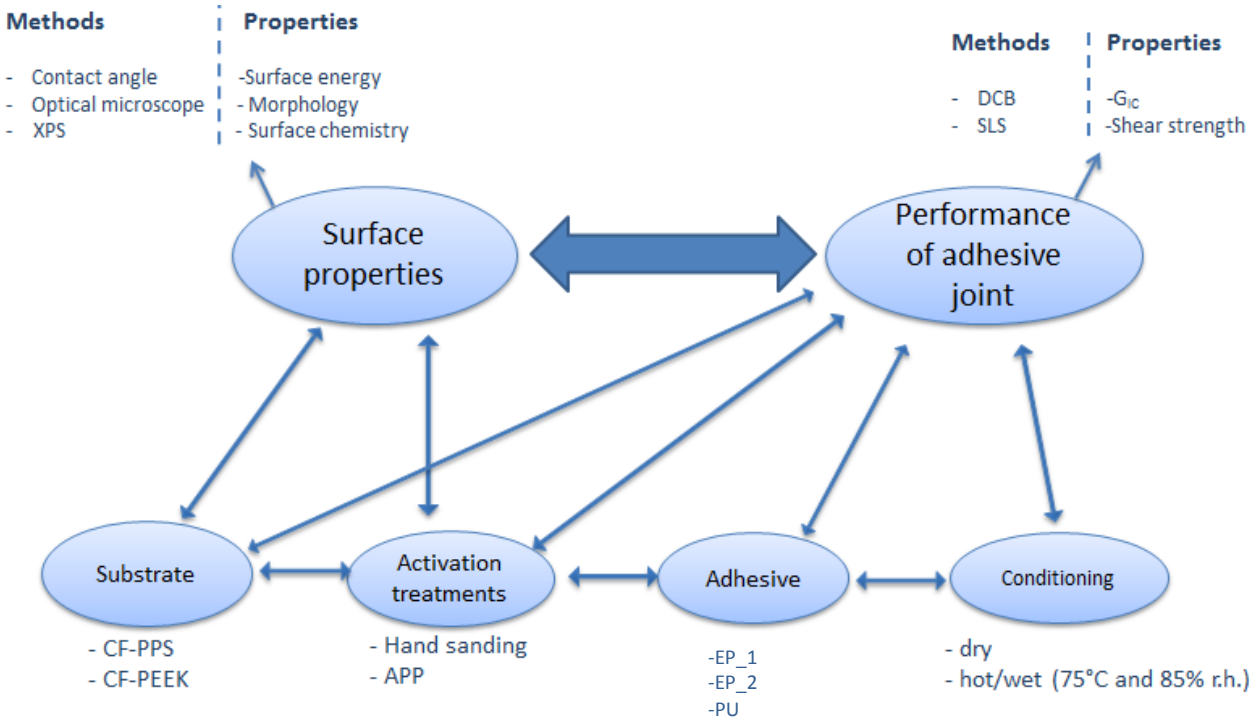

Figure 1.1: Schematic chart with the parameters and experimental activities

The structure of the project is divided into 7 different chapters; a schematic structure of how the problem is tackled is shown in Figure 1.2. It starts with the problem definition and the study of the existing documentation presented in Chapter 2. In Chapter 3, the materials used and surface preparation are detailed, whereas in Chapter 4 the experimental methods are presented. Then, the results are evaluated and interpreted on the following section. In Chapter 6, a discussion between the results is made, answering the research sub-questions. Finally, the conclusion and recommendation are presented with a brief section of suggested future works.

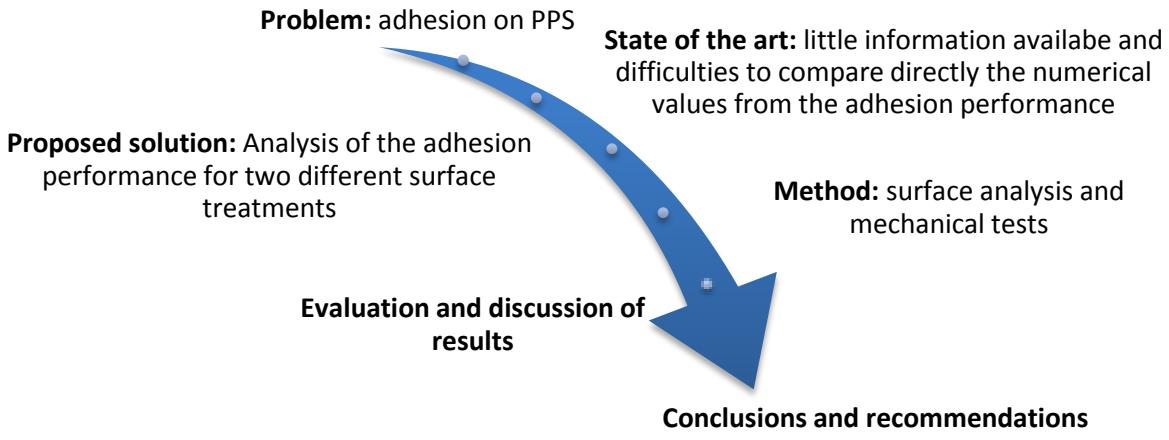

Figure 1.2: Structure of the master thesis

The test matrix is shown in Table 1.1, where the entire configurations are presented with the surface analysis.

Table 1.1: Test matrix

Material	Surface treatment	Adhesive	Conditioning-testing	Test	Analysis of the surface
CF-PPS	Hand sanding	AID 1012	Dry-RT	SLS	- optical microscopy - contact angle measurements
				DCB	
			Hot/wet - 75°C	SLS	
				DCB	
		AID 1031	Dry-RT	SLS	
				DCB	
			Hot/wet - 75°C	SLS	
				DCB	
		AID 1178	Dry-RT	SLS	
				DCB	
			Hot/wet - 75°C	SLS	
				DCB	
	APP	AID 1012	Dry-RT	SLS	- optical microscopy - contact angle measurements - XPS
				DCB	
			Hot/wet - 75°C	SLS	
				DCB	
		AID 1031	Dry-RT	SLS	
				DCB	
			Hot/wet - 75°C	SLS	
				DCB	
		AID 1178	Dry-RT	SLS	
				DCB	
			Hot/wet - 75°C	SLS	
				DCB	
CF-PEEK	Hand sanding	AID 1012	Dry-RT	SLS	- optical microscopy - contact angle measurements
		AID 1031			
		AID 1178			
	APP	AID 1012			- contact angle measurements
		AID 1031			
		AID 1178			

2. State of the art

2.1. Thermoplastic materials

Thermoplastics are polymers which can be melted and re-shaped at high temperature and when again cooled they show dimensional stability. They are classified in two groups according to its molecular arrangement; amorphous or semi-crystalline polymers. Amorphous polymers are solids below the Tg, the temperature at which can be moulded are closer to the Tg, but they might show poor resistance to solvents. Semi-crystalline polymers, such as PEEK or PPS, have two important temperatures; Tg where the amorphous polymer chains have enough energy to move relatively each other and Tm is the melting temperature at which polymer become fluid-like since the crystalline parts become liquid.

2.1.1. Poly-phenylene sulphide (C_6H_4S)

Poly-phenylene sulphide (PPS) is a high performance thermoplastic polymer made up of alternating aromatic rings and sulfur atoms in a symmetrical and rigid chain. This rigid backbone gives the material excellent balance of properties; high thermal stability with good mechanical properties up to 200°C for continuous loads and short-term loads up to 260°C. In addition, PPS shows excellent chemical resistance; there is no solvent known for temperatures below 200°C [14]. A scheme of the structure can be seen in Figure 2.1.

Figure 2.1: Scheme of PPS, in yellow there are Sulfur atoms, grey colour correspond to Carbon and white for Hydrogen (image taken from [15])

PPS is a semi-crystalline polymer with a Tg of 90°C and a high melting point of 285°C [16]. Due to its chemical structure, PPS is also inherently flame retardant as during combustion it tends to char [17], thus it is chemically inert and has a low value of surface energy, of 39 mN/m with a polar component of less than 2 mN/m in the delivered stated [18]. This low surface energy leads to a poor performance of the adhesive bond and interface failure of the bonded joint would easily occur.

2.1.2. Polyether ether ketone ($C_{19}H_{12}O_3$)

PEEK is a linear aromatic polymer consisting of aromatic rings joined by two ether and one ketone groups. A schematic picture of the monomer is shown in Figure 2.2.

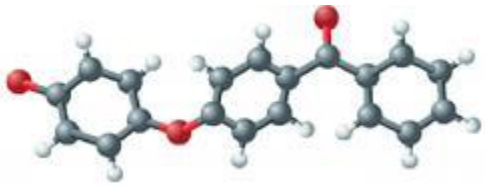

Figure 2.2: Chemical formula of PEEK monomer, in red there are oxygen atoms, grey colour is for carbon and white for hydrogens (image taken from [19])

PEEK is a semi-crystalline polymer with a glass transition temperature at around 143°C and a melting point at 343°C. It shows a tensile strength of 90-100 MPa and a Young's modulus of 3.6 GPa, and the processing conditions can influence the crystallinity and therefore the mechanical properties [20]. PEEK offers similar hydrolysis and chemical resistance compared to PPS, but some grades show an operational service temperature up to 250°C, which is higher than for PPS material.

2.2. Adhesive bonding

Adhesive bonding is a joining technique that consists on the application of an intermediate layer, which is fluid at least at some point of the process, to connect two parts of similar or dissimilar material. Adhesion refers to a thin layer between the adhesive and substrate and implies all the interatomic and interfacial forces and anchoring mechanisms to hold these two materials together [21].

The main advantages of adhesive bonding are that the stresses are distributed more uniformly reducing stress concentrations resulting in a higher fatigue resistance, no necessity of fibre breakage and the joints show a smooth contour. Furthermore, this technique is able to join any combination of solid materials with different physical properties (Young's modulus or thermal expansion coefficient), shape or thickness.

On the other hand, they show a major limitation due to the degradation of the properties of the adhesives in environments of high moisture content, solvents, or high temperature and it is necessary to determine for each type of adhesive and application how the adhesive will respond in those environmental conditions and conclude if its use is appropriate [22]. It is also a sensitive process, since its performance depends to a large extent on the surface properties; a high level of qualification is required during the bonding step. Finally, an important disadvantage is the non-redundancy load paths unless alternative paths are inserted, for example by the introduction of mechanical fasteners [23].

2.2.1. Adhesive bonding mechanisms

It is necessary to have knowledge of how the adhesive bonds are produced in order to understand the reasons and causes of the different failures modes. Nowadays, there is not one global theory accepted mainly due to its complexity involving the knowledge of different disciplines (surface chemistry, polymer chemistry, fracture analysis, rheology etc.). The principal mechanisms are [24]:

1- Mechanical interlocking

It is one of the earliest theories and states that the bond strength is achieved by the adhesive keying into the irregularities of the surface of the substrate. If the wettability of the adhesive is high enough, the principal factors that determine the adhesion are the roughness and type of porosity of the substrate [25]. This mechanism is more effective when the bond is loaded in shear with forces applied parallel to the interface; however when the joint is subjected to peel forces the strength is usually lower [24].

2- Molecular bonding

This is the oldest and most accepted theory in which the adhesive strength depends on intermolecular forces such as chemical interactions (ionic, covalent and metallic bonding), dipole-dipole interactions or van der Waals bonds between two surfaces. Therefore, the strength of the adhesive joint depends on the number and type of bonds per unit area.

3- Diffusion model

This mechanism explains the adhesion primarily for polymeric systems. The adhesion mechanism is based on the diffusion of molecular chains across the interface and into the other material [26].

4- The electrostatic attractive model

This theory is based on the creation of attraction forces between two surfaces when one has a positive net charge and the other a net negative charge. The adhesion strength is achieved by weak molecular interactions.

The gradual reduction of the adhesion performance can be explained by the degradation of the chemical bonds at the interface due for example water absorption. Therefore, adhesives joints could show high bond strength but poor service durability

2.2.2. Failure modes

An adhesive bonded joint can fail in four different ways [23]:

Cohesive failure: The failure occurs within the adhesive layer, leaving rests of adhesive on both sides of the joint. The causes are typically due to a poor joint design: excessive peel stresses, inadequate overlapping area, inadequate selection of the adhesive or service temperature etc. It could also fail due to high porosity resulting in a significance loss of strength. When a carrier is used and cohesive failure occurs, the failure is more likely to progress on that plane since this is the weakest area of the bonded joint.

Adhesive failure: The failure occurs at the interface between the adhesive and the adherend, leaving one adherend without adhesive on its surface. The main causes are:

- Ineffective generation of strong chemical bonds at the interface due to surface contamination or insufficient surface preparation
- Degradation during service of the chemical bonds at the interface

- Inadequate parameters during the curing cycle: the adhesive was cured before bonding, non-homogeneous heat distribution etc.

It is an unacceptable method and it required immediate action to identify the causes; the failure might occur at a much lower load than the design load [9].

Failure of the adherend: The failure occurs in one of the adherend, outside the joint. This failure mode is desirable since the adhesive joints achieve the maximum performance and the testing for structural certification could be reduced.

Mixed failure: It is a combination of the previous failure modes; when adhesive and cohesive failure, it usually occurs at a plane near the interface.

2.3. Surface treatments

Since the performance of adhesive joints depends to a large extend on the surface properties, substrates should show at least high wettability to ensure a good adhesion performance. The most critical step to achieve a durable joint is the preparation of the surfaces to be bonded [25].

The main objective of surface treatments is to modify the morphology and/or chemistry of the surface without changing the bulk properties of the substrate to improve adhesion and avoid adhesive failure. They are defined as one or series of treatments that remove loose material, clean the surface and modify chemically, mechanically and physically the surface to increase the surface energy of the substrates, and therefore the wettability is improved [27]. Pre-treatments should not damage the fibres or cause delamination as it will negatively affect the adherend's mechanical properties and failure is more likely to occur earlier.

In general, materials have a contamination layer consisting of release agents, grease or oils that hinder the formation of strong bonds. In addition, thermoplastic composites show low surface energy [17] and they usually present very smooth surfaces being negligible to the contribution the mechanical interlocking mechanism.

The surface treatment improves bond performance because [28]:

- It eliminates weak boundary layers such as contaminants (silicon for the release agents, fluorocarbon from release sprays and films etc.), low molecular weight species or oxidised layers.
- It modifies the chemistry of the surface by the insertion of polar functional groups or coupling agents.
- It increases the surface roughness to enhance mechanical interlocking and increase the bond area.

They can be divided into three different groups as can be seen in Table 2.1 with some examples for each group; the blue marked treatments correspond to the activation methods chosen for this project.

Table 2.1: Classification of surface pre-treatments

Predominantly effect		
Mechanical	**Energetic- Physical**	**Chemical**
Hand sanding	Corona discharge	Solvent cleaning
Grit blasting	**Plasma**	Detergent wash
Peel ply	Flame	Acid etch
Silicon carbide abrasion	Laser	Primer

Mechanical treatments are considered to be one of the simplest methods; their principal effect is a roughening of the surface increasing the bonding area and the possibility of better mechanical interlocking. Chemical treatments modify the chemistry of the surface, enhancing the formation of covalent, hydrogen, Van der Waals, dipole etc. at the interface adherend/adhesive. However, the use of these chemical treatments is becoming unacceptable due to hazardous waste generation, serious health effects and environmental considerations [29]. An alternative to the chemical methods, energetic techniques such as corona or plasma produce similar surface changes, gaining wide acceptance since their overcome the problems mentioned on the previous treatment groups.

Two methods were chosen due to its current use and qualified process on the industry:

Hand sanding: the main effect is to roughen the surface to create stronger joints than polished surfaces. It is followed by a cleaning step where all the loose particles should be removed. As it was mentioned, the rougher the surface is, the greater the area for chemical bonds is and the possibility of better interlocking occurs, therefore resulting in an increase of the adhesion performance.

Atmospheric pressure plasma: a plasma beam is produced directly from the surrounding atmosphere by the application of high electrical fields and directed towards the surface; it contains highly energetic species (electrons and ions) which have enough energy to break molecular bonds. From this interaction, free radicals are created leading to [29]:

- Removal of contaminants from the surface (surface cleaning)
- Elimination of weak boundary layers and increase of surface roughness by ablation or etching of the matrix.
- Crosslinking or branching of molecular chains near the surface.
- Modification of the surface chemistry by the reaction of the free radicals with the plasma itself or with air after the treatment.

2.4. Previous researches

In this sub-chapter, an overview of CF-PPS and CF-PEEK studies about adhesive bonding performance is presented.

2.4.1. Hand sanding

The effect on the abrasion and solvent cleaning treatment was studied as part of a research on corona treatments for different thermoplastics by A.J. Kinloch et al. [30].The data obtained was evaluated in

general for nine different fibre reinforced thermoplastics showing similarities between the results and failure modes. The chemistry of the surface was analysed in addition with its morphology by SEM pictures and the calculation of a roughness factor. The adhesion was analysed by the calculation of the adhesive fracture energy, G_{IC} by the performance of double cantilever beam tests.

After hand sanding, SEM pictures revealed a roughening on the surface without exposing the fibres. The roughening factor (r_f) for CF/PEEK substrates increased from 1.04 ±0.02 for the untreated specimens to 1.09 ±0.04; where r_f accounts for the ratio between the area and the projection area of the solid and the calculation was obtained using the following equation:

$$cos\alpha_r = r_f \cos\alpha_S \tag{2.1}$$

Where α_S is the angle observed in a smooth surface with the same chemistry and α_r is the angle observed in a rough surface. If α_S is high (~70°), the untreated specimen showed a reduction of 1° on the contact angle and after hand sanding; the contact angle would be 68.1°. However, it was observed that when these samples were additionally activated with corona treatment, the r_f increased up to 1.22 ±0.05, resulting in a decrease of 5° with respect to the smooth surface.

With respect to the chemistry, a reduction in silicon and fluorine concentrations was observed. The reduction for all reinforced thermoplastics studied was from 3-4 atom% to 1-2 atoms %. These elements are related to the contamination of the surface as they are usually associated with release agents or peel ply.

Finally, the mechanical performance of the adhesion was obtained by the calculation of the adhesive fracture energy (G_{IC}). In all the cases the fracture energy was relatively low, with a value between 0.02-0.03 kJ/m^2 and adhesive failure as the failure mode.

2.4.2. Atmospheric pressure plasma

The study of the effect of atmospheric pressure plasma (APP) surface treatment on PPS substrates was carried out by H.M.S. Iqbal et al [31] and recently by R. Hong et al. [32].

H.M.S Iqbal et al. [31] studied the effect on glass fibre reinforced PPS and carbon fibre reinforced PPS substrates bonded with a high temperature curing epoxy (DURALCO 4703). The surface energy was characterised by contact angle and surface energy estimation and the bond strength were compared by lap shear tests while the fracture area was examined with SEM microscope.

After the treatment, the specimens showed a sharp increase of the surface energy, especially on the polar component of the surface energy due to the introduction of polar groups on the surface. Lap shear tests showed an improvement by a factor of 3-4 on the lap shear strength. Treated specimens showed an increase of the polar component of the surface energy leading towards a better adhesion properties and therefore higher strength. In line with this increase, the locus of the failure mode changed from adhesive to cohesive on the substrate for both materials.

R. Hong et al. [32] investigated PPS and glass fibre reinforced PPS with a one component epoxy as the adhesive. The surface was characterized by SEM, XPS and contact angle and the adhesive strength was evaluated by the performance of single lap shear tests.

After dielectric barrier discharge (DBD) plasma treatment, the variation of the morphology was almost imperceptible. When the plasma treatment or the discharge power was higher, the surface became rougher showing a punctate structure. The surface energy increased from 16 mN/m to nearly 65 mN/m.

Similar to other pre-treatments, the chemistry of the surface was modified by the insertion of oxygen and nitrogen forming polar groups, while C and S atoms concentration decreased. Looking into S2p peak, the introduction of S=O and O=S=O groups were observed with a reduction of C-S-C and C-S-S-C groups. It was found that the surface energy increased significantly mainly due to the insertion of sulfoxide and sulfonyl groups. If the studied parameters (exposure time and power input) were higher, the height of the new chemical groups would increase.

The improvement of the adhesion was measured by lap shear strength, resulting in an increase by a factor of 3-4. The sanded specimens increased the adhesive strength by a factor of 2, with a mixture of cohesive and adhesive failure. For the plasma treated samples, the failure mode was failure on the substrate, being the value higher for GF/PPS than only PPS.

The effect of atmospheric pressure plasma on PEEK surfaces was studied also by H.M.S. Iqbal et al. [31], using the same parameters and adhesive as with PPS. After the treatment, the surface energy increased a 44% with respect to the untreated value. The improvement was slightly lower than the obtained with PPS surface.

Also in the frame of this work, lap shear tests and butt joint tests were performed to observe the mechanical properties. Due to its low polar part of the surface energy on untreated PEEK, the shear strength was 0.5 MPa, lower than PPS (6.1 MPa or 5.3 MPa, depending on the fibre reinforced material). The shear strength increased from 2.17 to 7.9 when the overlap decreased. This variation of results with respect to the overlap length was because the failure mode was substrate failure, which is independent of the overlap length. The butt joint strength increased from 4 to 22 MPa with a change on the failure area; initially the failure was located on the interface and after the treatment the adhesion was improved being the weakest area the adhesive, being the failure mode cohesive on the adhesive.

2.4.3 Conclusion

Hand sanding treatment modifies the surface topography by the increase of the surface roughness, and therefore allowing better mechanical interlocking between the adhesive and substrate and the surface area becomes larger increasing the possibility of the formation of chemical bonds. On the contrary to thermosets, this treatment appears to be insufficient on thermoplastics to obtain high strength joints and the failure mode is still at the interface.

Plasma treatment seems to be an effective method to improve the wettability and adhesive strength on bonded joints, by two main mechanisms: the roughness of the surface and the insertion of polar functional groups. In recent studies, the failure mode was usually no longer at the interface.

In this context, the present project aims to study in depth the adhesion on CF-PPS and to relate the morphological changes with the adhesion properties. These results will be compared to the existing literature to evaluate the effectiveness of these two activation methods regarding the adhesion properties. In addition, two different parameters which affect to a bonded joint performance are studied: the adhesive itself and the storage conditioning. Finally, the adhesion performance is studied by two of the most common mechanical tests; single lap shear and double cantilever beam, making a comparison between these two tests.

3. Materials and surface preparation

Since the objective of this project is to study the effect of surface treatments on CF-PPS substrates, the materials and surface preparation are presented in this section. Regarding the materials, CF-PPS and CF-PEEK has been used as a substrate for adhesive bonding with 3 different adhesives and the surface activation was done by hand sanding and atmospheric pressure plasma.

3.1. Materials

3.1.1 Substrates

The substrates are a carbon fibres reinforced thermoplastics; poly-phenylene sulphide (PPS) and polyether ether ketone (PEEK).

- **CF-PPS**
- **CF-PPEK**

CONFIDENTIAL

The Fibre Volume Content (FVC) was calculated by acid digestion according to DIN EN 2564 with the steps shown on Figure 3.1. The glass transition temperature (Tg), melting temperature (Tm) and the enthalpy (ΔH) were determined by Differential Scanning Calorimetry (DSC) following the steps of AITM 3-0027 Airbus specification. The heating cycle used consists in 2 consecutive thermal cycles:

1. First thermal cycle:
    - Increasing the temperature from 20°C to 330°C at a heating rate of 20°C/min
    - Holding the temperature at 330°C for 5 min
    - Cooling down at -10°C to room temperature (20°C)
2. Second thermal cycle (immediately after the first cycle):
    - Re-run the first heating cycle, at 20°C/min from room temperature to 330°C.

The obtained values are presented in Table 3.1, which are in accordance with the requirements for these qualified materials.

Table 3.1: Material properties

		W_f (%)	FVC (%)	Tg midpoint (°C)	T melt (°C)	Enthalpy (J/g)
CF-PPS	**Mean Value**	CONFIDENTIAL		92.95	285.63	38.85
	STD			3.22	0.85	1.03
CF-PEEK	**Mean Value**			144.30	341.69	47.58
	STD			2.06	0.25	1.53

The spectra were obtained from 6 samples, and their results are presented and analysed in the Appendix chapter. For CF-PEEK, the temperature was increased up to 370°C to pass the melting point.

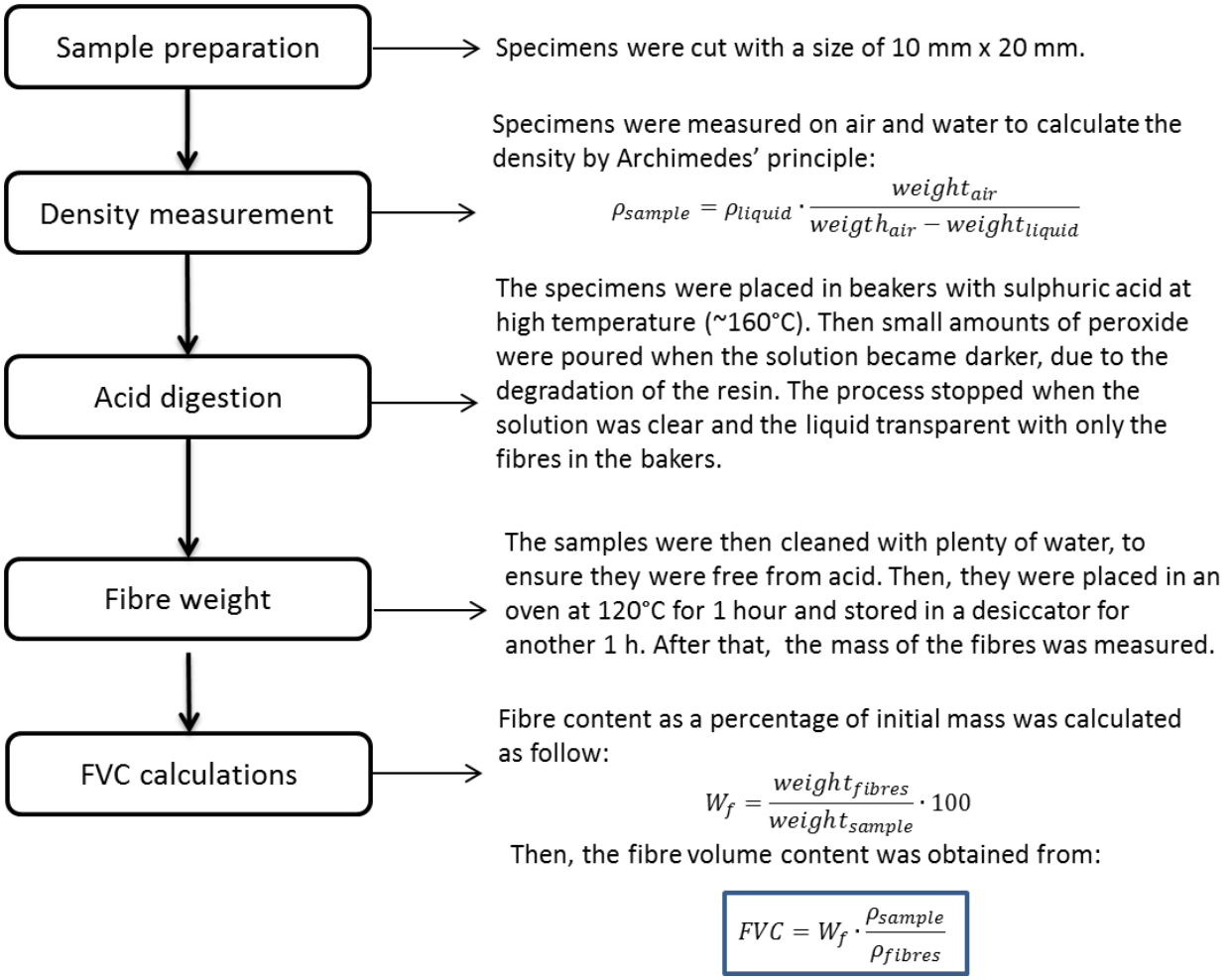

Figure 3.1: Workflow for the determination of fibre volume content (FVC)

3.1.2 Adhesives

The adhesives were selected because they are qualified materials by Airbus and commonly use on helicopter structures.

- EP_1 (ECS6054-1012): a two-component epoxy paste adhesive that offers high peel and shear strength once it is cured at room or high temperature. It shows good adhesion to a wide variety of materials; glass, metals etc. [33].
- EP_2 (ECS0044-1031): a two-component epoxy adhesive with excellent strength properties up to 177°C and higher [34]. It is a liquid shim which provides high compressive strength, good gap filling capabilities and fast cure time, being used to eliminate possible gaps or difference between two composites parts.
- PU (ECS0091-1178): a one-component polyurethane adhesive belonging to atmospheric humidity-curing polyurethanes class and used in combination with a primer. It is classified within the

adhesive sealant group, showing good impact resistance, with flexible and durable bonded joints and sealant properties.

Relevant information on the adhesives and processing parameters used in this study are summarized in Table 3.2.

Table 3.2: Adhesives and processing parameters used

Adhesive	Two-component epoxy		One component polyurethane
Trade Name	CONFIDENTIAL		
Abbreviation	EP_1	EP_2	PU
Mixing proportion	B/A = 100/27	A/B = 100/17	-
Mixing conditions	2500 rpm during 2 min	2500 rpm during 2 min	-
Curing cycle	15 days at 25°C 2 h at 65 °C	5 days at 25°C 1 h at 65 °C	Curing rate: 4 mm in 48 h at 25°C
Handling strength	2 days at RT	1 day at RT	~ 7 days at RT
Application	Manual	Manual	Air pressure gun at 6 bar
Additional information	-	-	Prior application of a primer
Tensile strength (MPa)	40	55.6	9
E-Modulus (MPa) at 25°C	2100	4940	
Elongation at break (%) at 25°C	8	2.6	>500
Tg	(Tan delta DMA) 72.3°C	(Tan delta DMTA) 73°C	

3.2. Activation of the surface

The activation of the surface can be divided into three different steps:

1- Surface preparation: Cleaning with a wetted cloth in acetone.
2- Surface pre-treatment: Activation the surface by hand sanding or atmospheric pressure plasma (APP)
3- Surface post-treatment: Application of a primer **(Only for PU adhesive)**

- **Hand sanding**

Hand sanding was performed according to the internal instruction EI045 34-9000-1 with P-120 sandpaper in two principal directions; longitudinal and perpendicular to the fibres. The pre-treatment consisted in manually sanding the surface until the first layer of resin was removed and the first carbon fibres began to

appear. Afterwards, the surface was vacuum cleaned and then cleaned with a wetted cloth in acetone until no more dust residues were visible on the cloth.

Finally, the exhausting time was at least 20 min before the application of the adhesive or primer, which was applied within the next 8 hours after the activation step. If not, the activation process should be repeated. The maximum time of 8 hours was established by the company after a research study on the adhesion performance which ensured that the effect of sanding remained at least 8 hours after the activation, being this timeframe mandatory on the production sites.

- **Atmospheric pressure plasma**

The plasma treatment equipment consisted of three different components: a FG5002 power generator, a high voltage transformer and a rotatory tool with a rotatory nozzle head. The gas from a compressed air network and the high voltage were combined into the plasma jet chamber. Due to the rotation of the nozzle, a vortex-like structure was formed leading to the formation of highly reactive species. Then, the plasma beam was directed towards the surface changing the surface properties of the substrate. In Figure 3.2, a picture of the atmospheric pressure plasma set-up is shown.

The working parameters used are listed in Table 3.3. The geometric parameters such as the speed, air pressure or treatment width were chosen according to recent studies carried out in the company: an evaluation of the plasma parameters on an epoxy thermoset resin (internal document name ECD-TN-EDVLO-2013-0135) and a co-curing bond research with GF-PPS as a substrate (internal document name ECD-TN-EDVLO-2013-012).

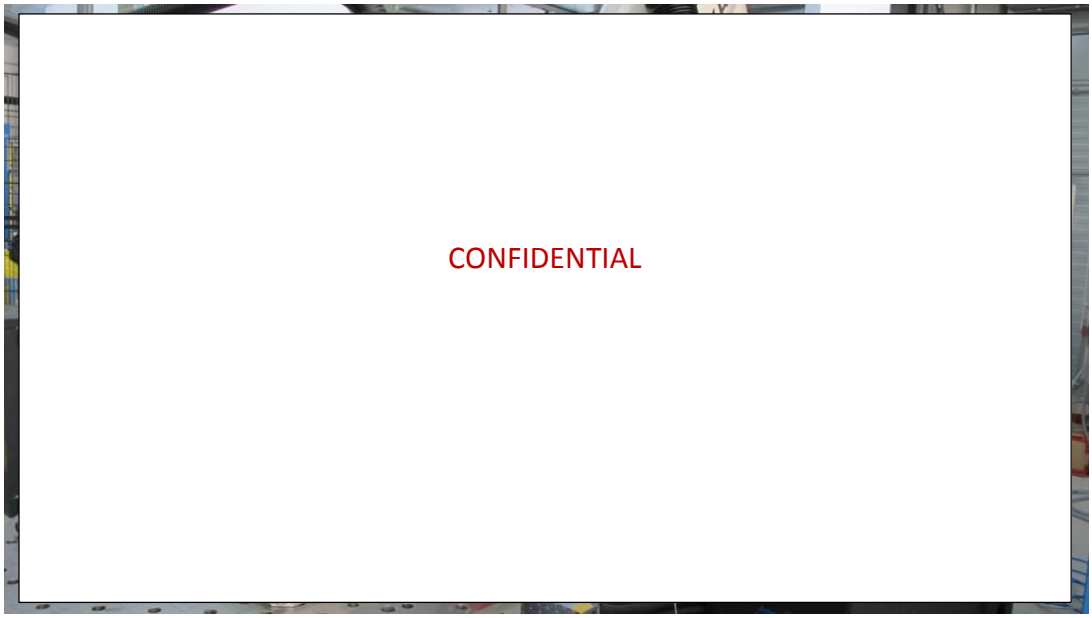

Figure 3.2: Surface activation of G_{IC} specimen by atmospheric pressure plasma.

The area activated with plasma treatment was sufficiently larger than the bonding surface to ensure a homogenous activation on the entire bond area. All samples were activated the same day and covered

separately in aluminium foil for their storage, in order to decrease chemical reaction with the environment and the exposure to reactive materials. In this case, the hydrophilicity remains higher than normal condition storage, as it was concluded by M. Kilinc et al. in their research [35].

Table 3.3: Working parameters of APP

Basic characteristics of the Generator	
Input voltage	CONFIDENTIAL
Generator output	
Frequency	
Operational parameters	
Voltage	CONFIDENTIAL
Intensity	
Nozzle rotation	
Air pressure of plasma	
Nozzle distance	
Speed	
Step over	
Treatment width	

The preparation of the samples was carried out within two weeks after the treatment, and the contact angle was measured to observe the loss of effect over time of this activation method (see Figure 5.6). The information about the days passed between the activation treatment and bonding step is summarized in Table 3.4.

Table 3.4: Information about the time passed between the activation surface and the bonding stage.

Sample		**Days passed after bonding**
Single lap shear	EP_1	1
	EP_2	0
	PU	7
Double cantilever beam	EP_1	4
	EP_2	14
	PU	2 and 7

4. Experimental methods

In this chapter, the experimental techniques used for analysing the surface after the activation treatments and the mechanical properties resulting of these treatments are presented. These methods can be divided into two categories: surface analysis and mechanical tests.

4.1. Surface analysis

The surface analysis is an important aspect in the study of surface treatments and adhesion performance. As it was mentioned earlier, adhesion is a surface phenomenon being its performance dependent on the surface properties, and the main objective of activation treatments is to change the surface properties without affecting the bulk properties. So, three techniques were used to evaluate the surface properties: optical microscopy, XPS and contact angle measurements.

Surface analysis was performed on the same substrates as the mechanical tests; i.e. the samples were obtained from the same laminate ensuring the same properties at the surface. In case of XPS analysis, the size of the samples was 10 mm x 20 mm and for the microscope and contact angle, the size was variable having an approximately value of 80 mm x 80 mm.

- **Optical microscope**

The morphology of the surface plays an important role on the performance of an adhesive bonded joint, as several adhesion mechanisms depend directly or indirectly on the roughness of the adherend such as mechanical interlocking or molecular bonding theory explained in section 2.2.

The analysis of the morphology and roughness profile of the surface was carried out by an optical microscope. The micrographs were taken at high magnification being possible to observe the morphology in detail and a roughness profile of an arbitrary straight line was obtained.

- **X-ray photoelectron spectroscopy (XPS)**

The surface chemistry of the adherend plays a major role on the adhesion performance since the molecular bonding mechanism depends directly on the chemical composition of the surface. As it has been stated, this mechanism is one of the oldest and most accepted theories of adhesion and is based on the intermolecular forces between adhesive and substrate. Additionally, plasma treatment is a popular method to improve the adhesion by changing the morphology and chemistry of the surface [36].

Therefore, the surface composition of two different samples (untreated and plasma treated CF-PPS) was evaluated and compared. XPS is a quantitative technique consisting on the irradiation of an X-ray beam to the material and the measurement of kinetic energies from the ejected electrons allowing the determination of the surface chemistry. The electrons are emitted from the surface (up to 10 nm depth), being a popular method used for the chemical analysis of the upper-most surface layers [37].

The analysis was carried out in the facilities of Airbus group in Ottobrunn (Munich). The untreated specimen was cleaned with acetone and stored at ambient temperature, while the plasma treated sample was first cleaned with acetone, then activated by plasma and covered in aluminium foil for storage at ambient conditions for 3 weeks. The time between the surface activation and the analysis of the chemical composition was an important parameter to take into account, owing to the ageing effect on surfaces treated with plasma.

- **Contact angle measurement**

Contact angle measurement is a widely used technique for obtaining information about surface properties. The direct determination of the surface energy of a solid presents certain difficulties, so indirect approaches have been studied. Among these techniques, contact angle measurement is considered the simplest, and consists in measuring the contact angle between a solid and a liquid [38-40]. High energy surfaces are easier to wet resulting in a lower contact angle, being favourable to achieve a strong adhesive bond because there is more intimate contact between adhesive and adherend [41].Young's equation provides the relation between surface energies and contact angle [42]:

$$\gamma_S = \gamma_{SL} + \gamma_L \cos\theta \tag{4.1}$$

Where γ_S is the surface tension of the solid, γ_L represents the liquid surface tension, γ_{SL} corresponds to the solid-liquid interfacial tension and θ the contact angle. In this equation, the only value that can be measured with accuracy is γ_L. It could be seen that surface energy of the solid and contact angle are inversely proportional.

The change of wettability after sanding and atmospheric pressure plasma treatment was evaluated by sessile drop contact angles. The measurements were performed at room temperature by a "drop shape analyser – DSA100 Krüss" machine. The measurements were analysed with the software DSA4, in which the baseline was changed manually. The program calculated the contact angle between the liquid and the substrates 10 times for each drop and angle (left and right), being the total time needed less than 8 s. In addition, at least 6 water drops were used for each surface condition.

Three liquids were used (water, ethylene glycol and diiodomethane) to calculate the surface free energy of PPS and PEEK after each surface treatment from the contact angle and the surface energy of the liquids (Table 4.1). The surface energy was calculated according to Owens-Wendt-Kaelble equation, in which the surface energy is divided into a polar and dispersive component. The polar components accounts for hydrogen interaction, dipole-dipole, dipole-induce dipole, while the dispersive parts accounts for van der Waals interactions [43]:

$$(1+\cos\theta)\gamma_{LV} = 2\left(\gamma_S^d \cdot \gamma_{LV}^d\right)^{\frac{1}{2}} + 2(\gamma_S^P \cdot \gamma_{LV}^P)^{\frac{1}{2}} \tag{4.2}$$

Where γ_{LV}, γ_{LV}^D and γ_{LV}^P are the total, disperse and polar part of the surface energy of the liquid respectively, θ is the contact angle between the liquid and the solid surface obtained by the sessile drop analysis. The unknown values are γ_S^D and γ_S^P which represent the dispersion and polar components of the

surface free energy of the surface. Then the total surface energy (γ_S) was calculated by the sum of its components:

$$\gamma_S = \gamma_S^d + \gamma_S^P \tag{4.3}$$

Table 4.1: Surface free energy of the test liquids

Liquids	γ^p_{LV} (mN/m)	γ^d_{LV} (mN/m)	γ_{LV} (mN/m)
Water	51	21.8	72.8
Ethylene glycol	16.8	30.9	47.7
Diiodomethane	0.0	50.8	50.8

The Owens-Wendt-Kaelbe equation can be solved by using two different liquids and obtaining a system of two equations with two unknowns (γ_S^D and γ_S^P), but it was observed that the results varies with respect to the pair of liquids used. The calculation of the surface free energy was obtained according to BS EN 828:2013 by rearranging the formula (4.2) to the general form of a straight line:

$$\frac{(1+\cos\theta)\gamma_{LV}}{2\sqrt{\gamma_{LV}^d}} = \sqrt{\gamma_S^P} \cdot \frac{\sqrt{\gamma_{LV}^P}}{\sqrt{\gamma_{LV}^d}} + \sqrt{\gamma_S^d} \tag{4.4}$$

$$y = m \cdot x + b$$

The disperse component is the square of the intercept in the ordinate axis (b) and the polar part is the square of the slope (m). In Appendix section, the data of the contact measurements and the step for the calculation of the surface free energy are presented.

In case of APP treated samples, a series of measurements using water were executed over time at 0, 3, 8, 10 and 14 days after the surface activation. The evolution of the contact angle over time was investigated since the bonding step of specimens was conducted in the following two weeks after the plasma treatment (see Table 3.4).

4.2. Mechanical tests

The adhesion performance for each configuration was evaluated by two different mechanical tests: single lap shear and double cantilever beam tests. The performance of these tests provided numerical values for comparison with the analysis of failure modes. Half of the samples were stored in a climate chamber during 1000 h at 75°C and 85% r.h. to simulate an accelerated ageing conditioning.

4.2.1. Double cantilever beam specimens

The double cantilever beam test is a mechanical destructive method commonly used for the study of the adhesive strength, by calculating the fracture resistance on mode I. Mode I refers to the applied force to enable the propagation of the crack, in this case the stress applied is perpendicular to the plane of the crack [44].

Adhesive joints are heterogeneous due to contamination on the surface, local variation of the surface energy, presence of voids or because the adhesive could be filled with solid particles. These heterogeneities could be assessed by fluctuation in force-displacement curves from the theoretical curve and analysis of the fracture surface.

DCB tests allow the analysis of the adhesive performance by the calculation of the fracture toughness energy according to DIN EN 6033 [45].

$$G_{IC} = \frac{A}{a \cdot w} \cdot 10^6 \ \ (J/m^2) \tag{4.5}$$

Where G_{IC} is the fracture toughness energy, *A* is the energy to achieve the propagation of the crack (integration of the area of load-displacement) in J, *a* is the propagated crack length in mm and *w* is the width of the specimen in mm.

- **Sample preparation**

The manufacturing of the DCB specimens consisted of several steps summarized graphically in Figure 4.1.

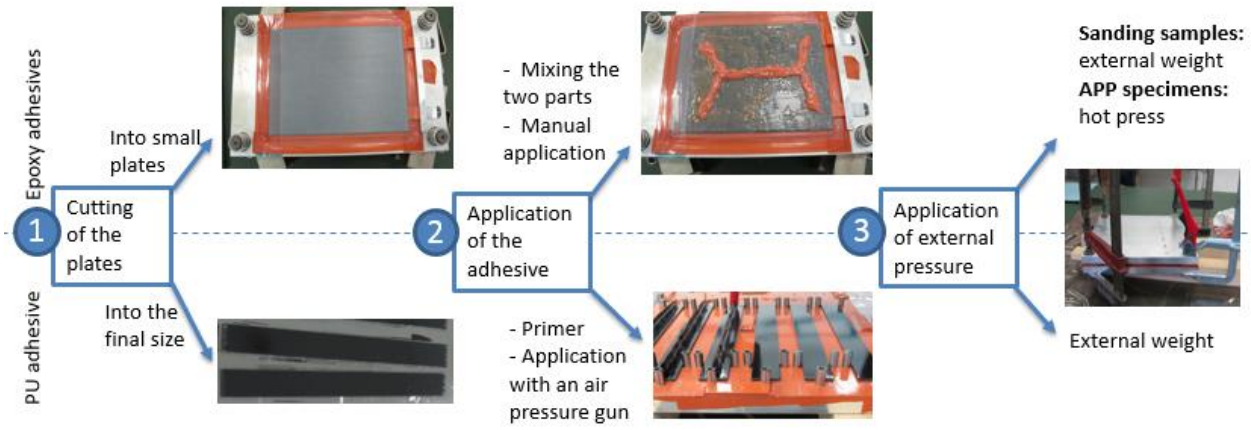

Figure 4.1: Manufacturing steps of double cantilever beam specimens.

Firstly, the samples were cut from a big CF-PPS consolidate panel having a dimension of 250 x 180 mm for epoxy adhesive (6 final specimens from each plate) and 250x25 mm for polyurethane adhesive (final size of the specimen). This difference was because this polyurethane adhesive was classified within moisture-cure polyurethanes. Since the curing process took place from the outside to the inside of the adhesive bond, the width of the bond should not be too large. Then, the entire surface was activated and the samples were placed into the moulds.

The next step was the application of the adhesive. The epoxies paste adhesives used were a two-component system so a mixing step took placed. The parts were mixed according to their respective datasheet (see Table 3.2) with the mixing conditions of 2500 rpm during 2 min. The thickness of the adhesive layer was controlled by the placement of a fabric (nylon knitted cloth with the internal name:

ECS6071-1090), with a thickness of 0.1 mm. The required adhesive thickness for the samples bonded with PU adhesive was 0.8 mm and thin metal strips were placed on the mould to achieve the desired adhesive thickness. The difference in thickness is related to the configuration in which the adhesive achieves its optimal performance.

Finally, the mould was closed and external pressure was applied until the adhesive was cured. In case of samples activated with APP and bonded with epoxies adhesives, the external pressure was applied by a Bürkle press at high temperature (65°C) during 2 hours. This ensured a uniform thickness throughout the plate; in contrast with the samples activated by hand sanding, where the adhesive thickness was higher than the required and the value was not constant; being maximum in the centre and minimum in the edges.

An scheme of a DCB specimen is shown in Figure 4.2, where the substrates, adhesive, activation of the surface and applied force are indicated.

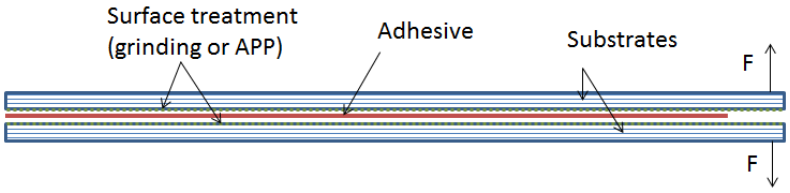

Figure 4.2: Scheme of the DCB specimen

Certain incidents have occurred during manufacturing, which must be taken into account when the results were analysed.

Table 4.2: Incidents during manufacturing of DCB samples

Sample			Incidents
Adhesive	**Treatment**	**Conditioning**	
EP_1 and EP_2	Hand sanding	Dry	The external pressure was not sufficient, resulting in the bond thickness larger than required.
EP_1	Hand sanding	-	The activation process was repeated
PU	Hand sanding	Dry	The size of the samples was out of tolerance and an extra cutting step before bonding was necessary.

- **Experimental set up**

The specimens were tested in a Zwick/Roell machine with a load cell of 10kN; using a crosshead speed of 10mm/min obtaining force vs displacement values. The geometric dimensions such as width, thickness, crack length etc. were introduced manually and the data was processed by TestXpert software. The samples without conditioning were tested at RT and the samples stored in the climate chamber were tested at 75±3°C with a dwell time of 7 min at that temperature before the beginning of the tests.

The application of the force differed from the standard DIN EN 6033; instead of bonding metallic tabs at the edges, a metal tool as it is shown in Figure 4.3 was used. This tooling allows a direct application of the

force without the necessity of a bonding step, but in contrast a pre-crack is created while the specimens are forced into the metal clamp. The length of the pre-crack cannot be controlled and its value depends on the properties of the substrate, adhesive and the interface.

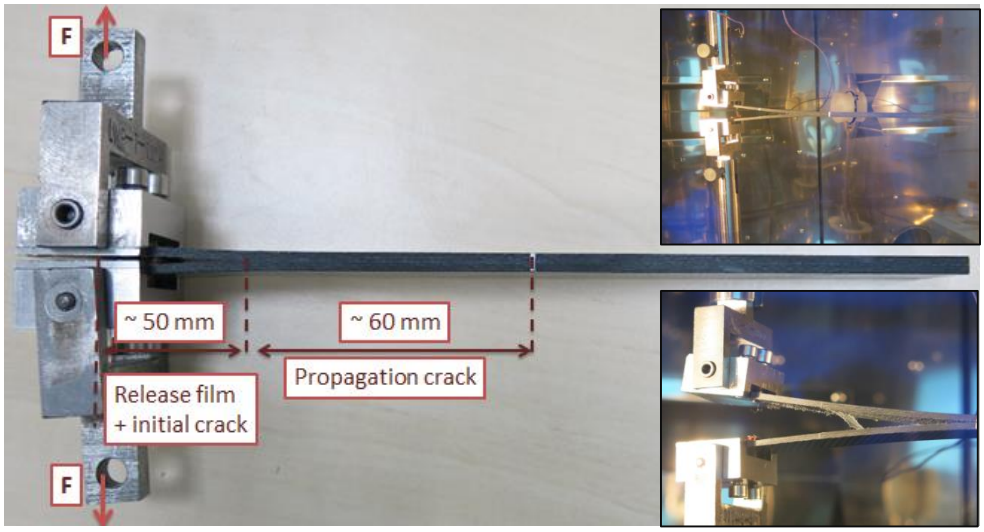

Figure 4.3: DCB test specimens

4.2.2. Single lap shear specimens

Single lap shear tests are a widely used destructive test for the determination of the "apparent" shear strength of an adhesive bonded joint. Test specimens are easy to prepare, but the shear distribution is not uniform along the bonding area and there are high peeling stresses at the edges of the bond-line which could thus be the first cause for failure [46].

The obtained value of shear strength is not a material property of the adhesive as it depends on the joint geometry, but it is a design value for joints. The values were used to compare different test series from this project and from other previous studies with the same geometry and testing parameters.

Single lap shear tests were performed according to DIN EN 2243-1, in which the applied force vs the displacement was obtained. Then, the shear strength was calculated using the following equation:

$$R = \frac{F}{L \cdot W} \tag{5.2}$$

Where R is the shear strength in MPa, *F* is the failing load in N, *L* is the overlap length in mm and *W* is the width in mm. The results are shown graphically for each adhesive with an analysis of their failure mode.

- **Sample preparation**

The manufacturing of the single lap shear specimens consisted of several steps summarized graphically in Figure 4.4. Firstly, the raw material, which was a big consolidated laminate, was cut into small plates

according to DIN EN-2243, having a dimension of 100 x 180 mm. Then, the bonding area was activated and the plates were placed into the mould.

Secondly, the application of the adhesive was done similar to DCB tests. For PU adhesive samples, a primer was applied before the adhesive using a brush and covering uniformly the entire bond area. The bondline thickness was the same as DCB specimens; 0.1 mm for EP_1, EP_2 and 0.8 mm for PU.

Thirdly, the mould was closed and external pressure was applied by the placement of weight on top of the moulds or by the use of clamps. Finally, the plates were taken out of the mould after curing, the alignment tabs were bonded and the plates were cut to the final dimension.

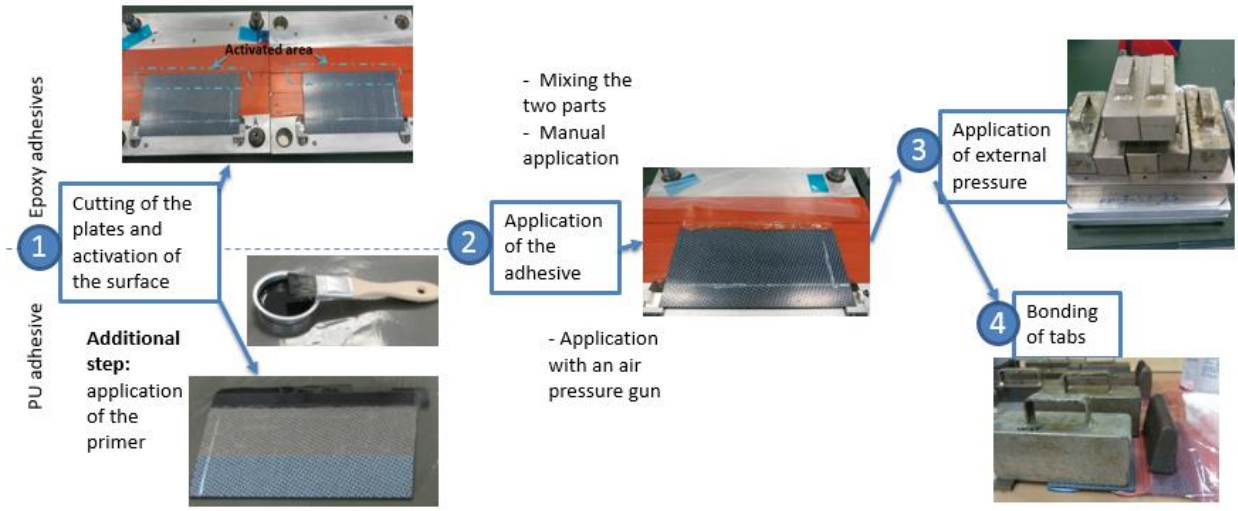

Figure 4.4: Manufacturing steps of single lap shear samples

The performance of lap shear tests depends on the boundary conditions at the grip of the tensile machine. In this project, an alignment tab with the same thickness as the substrates was adhesively bonded to reduce the bending moment on the bond area during the mounting of the sample [47]. A scheme of the test specimen is shown in Figure 4.5, indicating the important components and the direction of the applied force.

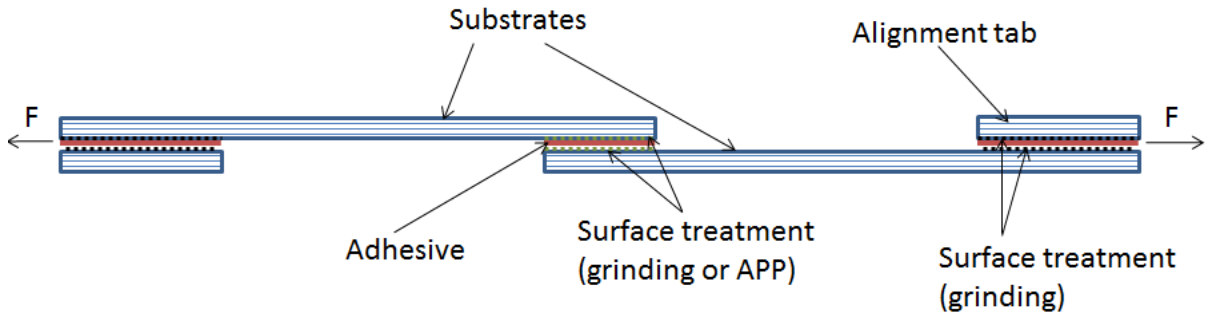

Figure 4.5: Scheme of the SLS specimen

- **Experimental set up**

The mechanical tests were carried out in a Zwick/Roell machine with a load cell of 250kN obtaining a graph of force vs displacement. The parameters during testing were a preload of 50N and the crosshead speed of 2 mm/min. In case of hot/wet specimens, they were removed from the climate chamber and storage at RT for 2h. The test temperature was 75 ±3°C with a waiting time at that temperature prior to the start of the test of 7 min.

The geometrical parameters such as the overlap length, thickness of the adhesive and wide of the specimens were introduced manually into the TestXpert software programme.

5. Results

In this chapter, all the experimental results are presented and analysed. They can be divided into two categories; in the first group, the information related to the analysis of the surface is explained and the second group gathers the data about the bonding properties after the performance of mechanical tests.

5.1. Analysis of the surface

The analysis of the surface provides essential information for the evaluation of the effect of different surface treatments on the adhesive performance.

5.1.1. Morphology

The surface was analysed with an optical microscope as explained in Chapter 4, obtaining a micrograph and a roughness profile from an arbitrary horizontal line. Figure 5.1 shows this information for the reference (untreated), sanded and plasma treated CF-PPS specimens.

The reference sample presents a smooth surface with several small scratches, which might have been produced during handling and cutting. It has a greyish colour due to the PPS matrix with darker areas where the upper fibres were located. The surface profile shows small peaks and valley corresponding to the scratches observed; the surface is practically flat with a difference in height of 6.5 µm approximately.

After sanding, the morphology of the surface differs. The surface becomes rougher and straight lines can be observed corresponding with the final direction of grinding. The glow characteristic from a smooth surface is no longer visible and the upper fibres are partially exposed due to the removal of the thin layer of resin. The roughness profile consisted on peaks and valleys distribute regularly through the entire surface, having a difference of 17 µm.

The specimen treated with plasma shows slightly visible changes on the surface with respect to the reference; the surface is also even with small scratches. It can be noticed areas with different colours which might be due to a non-homogeneous surface treatment. With respect to the roughness profile, the general trend is similar to the reference specimen since it also showed a flat surface with a maximum difference of 8 µm and small sharp peaks where the scratches are located.

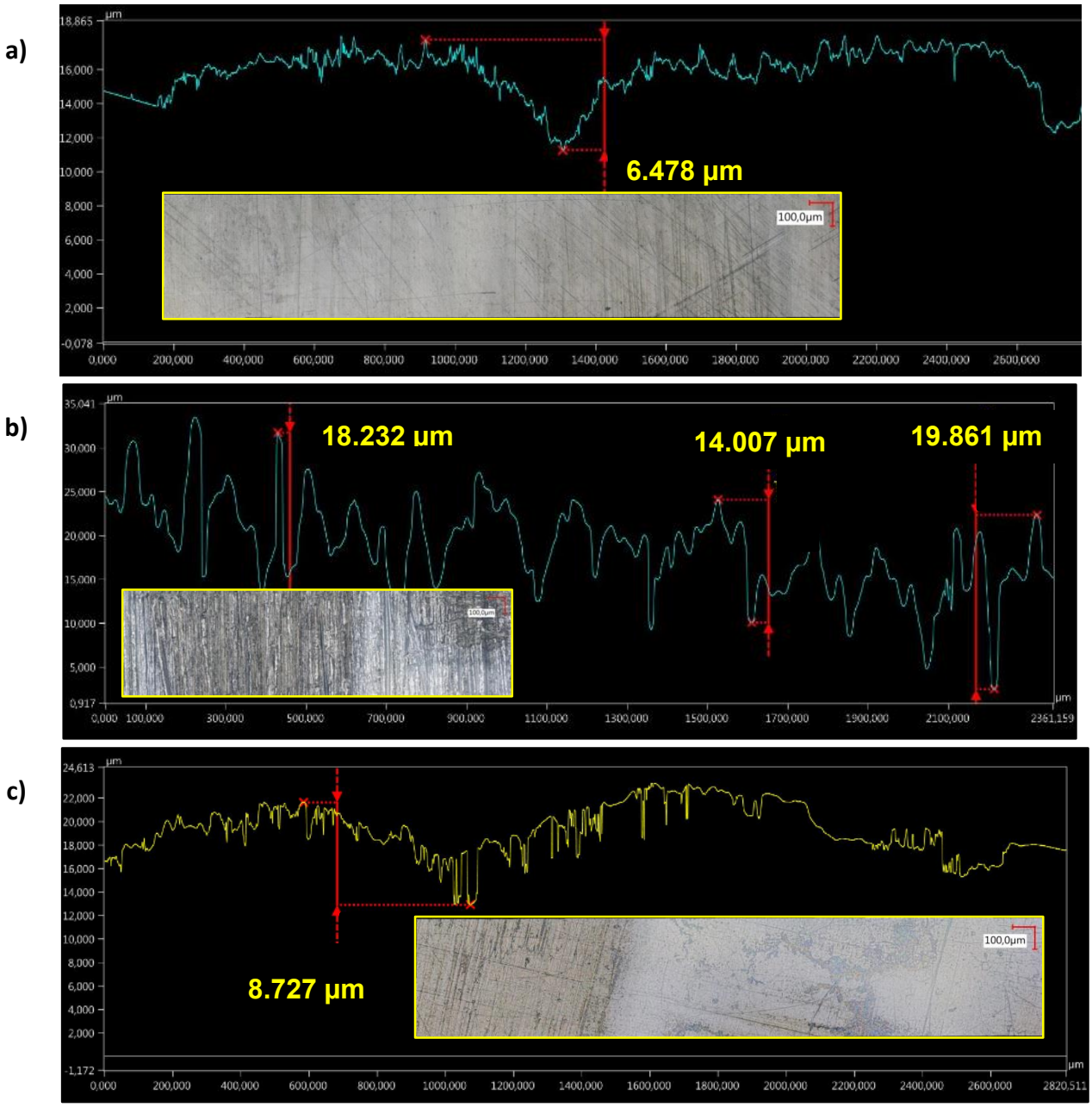

Figure 5.1: Surface topography of CF-PPS of a) reference, b) sanded and c) plasma treated samples.

The surface morphology was also studied on CF-PEEK substrates for two cases; untreated and after hand sanding shown in Figure 5.2.

The surface of the untreated sample is uneven, showing broad peaks and valley of 20 - 40 µm height. This macro-roughness was visible with the naked eye and by obtaining the distribution of heights in the area of analysis, but not with the micrographs, where the background has a uniform greyish colour with small scratches. This surface should have been similar to the plasma treated sample, since the morphology of the surface hardly changed.

Hand sanding sample shows similar topography to sanded CF-PPS substrates; uniformly distributed peaks and valleys with an approximate difference in height of 10 µm. The fibres started to be exposed and the macro-roughness almost disappeared; there were certain areas where parts of the broad valleys were still observed.

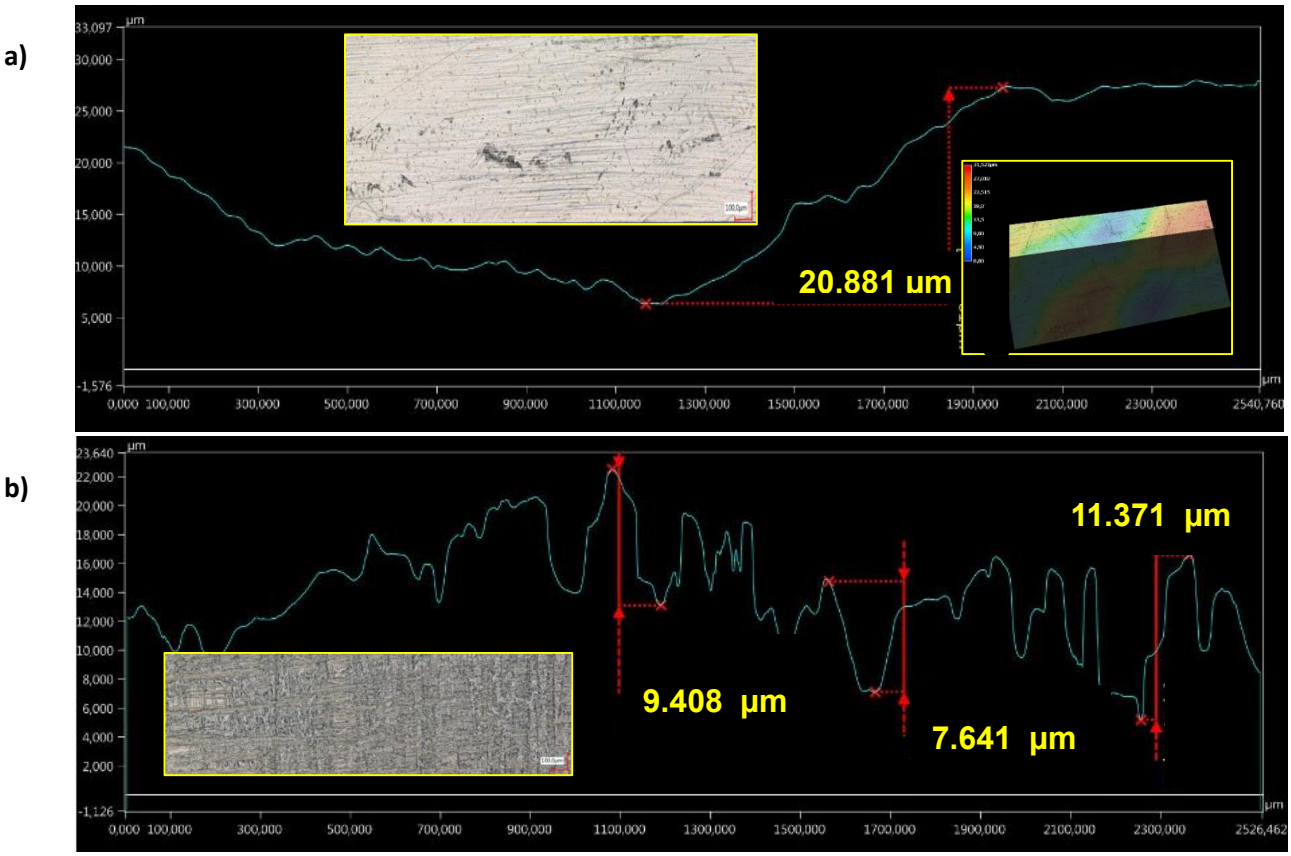

Figure 5.2: Surface topography of CF-PEEK from a) untreated sample and b) the sanded sample

The main changes observed on the morphology of the surface are:

- CF-PEEK and CF-PPS specimens show different surface morphology in the as-received state, due to the difference in the parameters and tooling during consolidation. While CF-PPS presents very smooth surface, CF-PEEK surface shows a macroscopic roughness.
- After APP on CF-PPS, the surface remains similar to the untreated sample by the evaluation through an optical microscope. However, previous researches [32] observed through SEM microscope that the micro-roughness increased as a consequence of ablation of the matrix and removal of low molecular weight species.
- In case of hand sanded sample, the surface profile changes considerably with respect the untreated specimen since it consists in uniformly distributed peaks of approximate 10-17 µm for both samples, increasing the roughness and the bond area.

5.1.2. Chemistry

Plasma pre-treatment modifies the chemistry of the surface by the insertion new elements and the consequent formation of different functional polar groups, as explained in section 4.1, being beneficial for the improvement of the adhesive joint due to stronger interatomic forces at the interface. The chemical composition of the surface was obtained from an untreated and a treated plasma specimens to evaluate and compare the surface chemistry. For each sample, the chemical composition was measured in 3 different areas obtaining the mean value and sample standard deviation for each atom concentration.

Table 5.1 shows the atomic percentage of elements on the surface except hydrogen. Hydrogen is an element very difficult to detect with XPS due to its small cross section (5000 times smaller than the 1s orbital of a carbon atom) and the non-existence of core-electrons. As the hydrogen element only has valence electrons, these orbitals appear as broad bands in the spectrum being usually impossible to distinguish from the other elements [48]. Due to the equipment resolution, concentrations of elements lower than 1% should not be taken into account and for this reason they are between brackets.

Table 5.1: Surface composition (in percent atomic concentration) of CF-PPS specimens before and after plasma treatment obtained by XPS analysis

Sample		C	N	O	F	Na	Mg	Si	S	Ca
Reference	**Mean (%)**	**85.7**	**1.1**	**6.4**	**-**	**-**	**-**	**(0.3)[1]**	**6.5**	**-**
	STD	1.2	0.6	0.5				0.3	1.1	
Plasma treated	**Mean (%)**	**48.1**	**4.5**	**34.3**	**(0.4)**	**1.5**	**(0.4)**	**3.0[2]**	**7.0**	**(0.8)**
	STD	2.9	0.7	1.4	0.2	0.3	0.1	0.2	0.6	0.2

The reference sample shows high percentage of carbon and sulphur atoms; these two elements together with hydrogen are the theoretical chemical composition of PPS polymer. However, N and O atoms were additionally in the chemical composition and could have been introduced during manufacturing, cutting or cleaning of the specimens. It must be noted that the existence of O and N atoms on the surface is beneficial to the adhesion performance as they form functional groups increasing the wettability. The existence of N and O atoms on the surface was also found in previous investigations [32]. A deeper analysis on C1s peak (Figure 5.3) was made to evaluate the different covalent bonds with carbon atoms; the untreated sample shows that carbon was predominantly bond in C-C or C-H structures, with only 3% in C-O bonds. It can also be deduced that the surface did not present contamination, since only a small amount of Si was found in the form of PDMS (C_2H_6OSi; big molecules used for release functions).

After plasma treatment the surface composition changes significantly; the concentration of C atoms decreases from 85.7% to 48.1% as a result of the insertion and increase of other elements. The principal effect of plasma treatment is a large increase of oxygen atoms from 6.4 to 34.3%, being the most important contributor parameter for the improvement of adhesion. The rise of nitrogen concentration is smaller

[1] Binding energy of 102,6 eV corresponding to PDMS (Polydimethylsiloxane)
[2] Binding energy of 103.3 eV corresponding to silicates

(from 1.1 atom% to 4.5%.) since this element is thermodynamically less favourable than oxygen [49]. Small amounts of Ca and Na are found which could be related to the sizing of the fibres or impurities on the matrix.

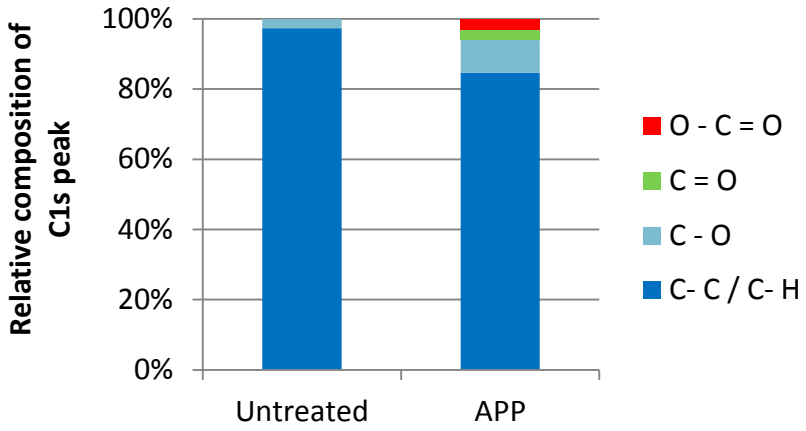

Figure 5.3: Relative amount (atom %) of carbon species in untreated and plasma treated CF-PPS specimens

Figure 5.3 shows that most carbon atoms are still bonded in C-C or C-H structures, but C-O bond increased its relative amount together with the introduction of new functional groups: carbonyl (C=O) and carboxylic acid (O-C=O) groups.

Although the content of sulphur remains similar, a significant peak shift is observed after plasma treatment (Figure 5.4). A reduction of the concentration of C-S-C and C-S-S-C groups occurs at the same time as new functional groups are introduced, such as sulfoxide and sulfonyl groups (S=O).

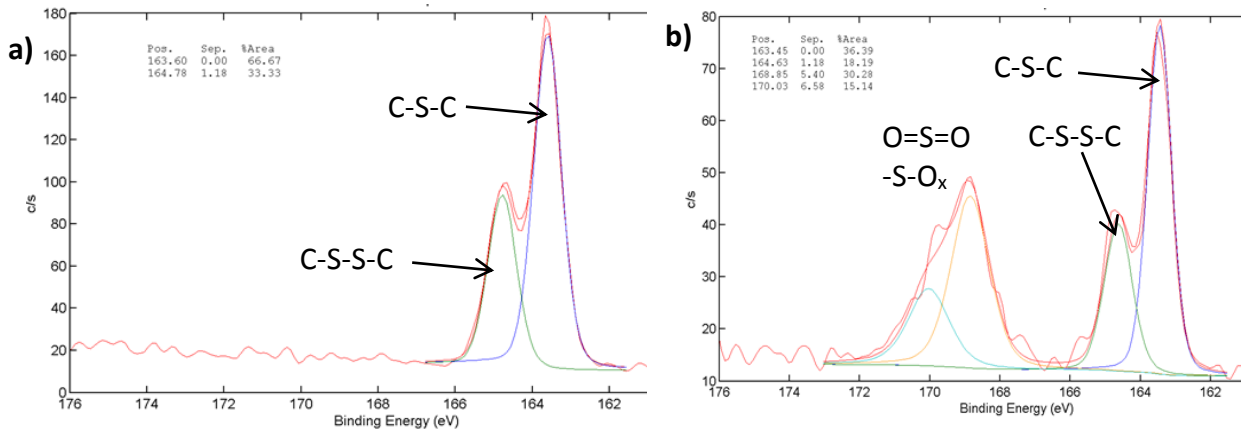

Figure 5.4: High resolution of S2p spectra; a) untreated and b) APP treated sample

Therefore, the main changes on the chemistry after plasma treatment are:

- Large increase in the concentration of oxygen atoms.
- Introduction and increase of functional polar groups.

The direct consequence on the adhesion performance is an increase on the possibility of the formation of chemical bonds at the interface. According to the chemical bonding theory explained in sub-section 2.2.1, the strength of the adhesive joint depends on the number and type of chemical bonds per unit area. Increasing the chemical interactions at the interface, might result in a change on the failure mode avoiding the adhesive failure.

5.1.3. Contact angle

The contact angle values using water as wetting liquid for CF-PPS are plotted graphically in Figure 5.5. The reference value is 80.7 ± 1.35°; which is in agreement with the obtained results from previous researches (84 ± 5°) in [50]. After sanding, the contact angle increases up to 95.8± 4.01 ° and on the plasma treated substrates the value decreases to 28.7 ± 2.91 °.

Regarding the sanded specimens, a decrease of the contact angle was expected, as the surface became rougher and the water drop would spread in a larger extent over the surface. However, an increase of the contact angle of approximately 15° is obtained with a large dispersion of values, due to the final grinding direction and water drop observation. After grinding the drop does not spread on the surface uniformly, on the contrary it spreads with oval shape being the major axis parallel to the grinding direction. If the drop spreads more (major axis), the contact angle will decrease.

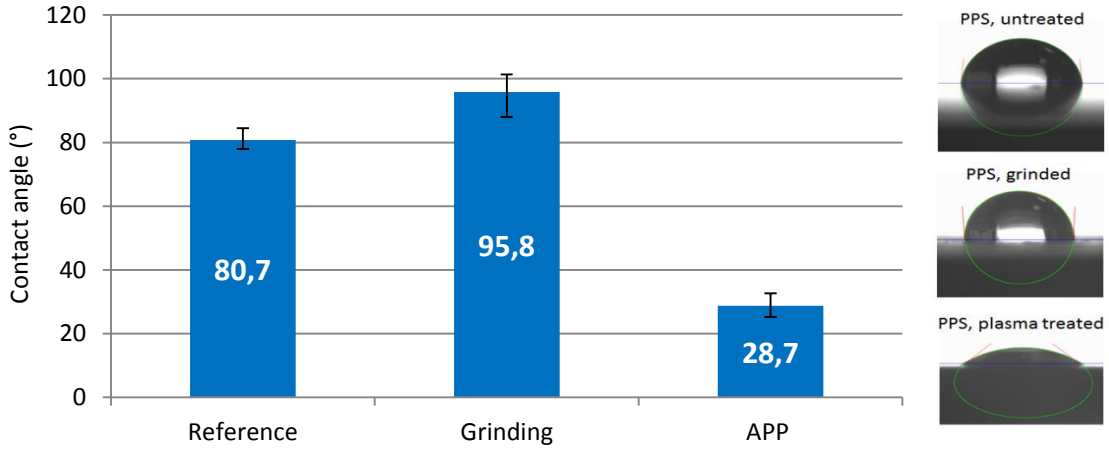

Figure 5.5: Contact angle before (reference) and after the surface treatments on CF-PPS substrates

A previous investigation carried out by H.J. Busscher et al. analysed the contact angle of a water drop on different polymers with different degrees of roughening. In that research, the results showed that for most of the specimens, the contact angle increased when the initial contact angle from a smooth surface was higher than 86° and in turn there would be a decrease of the contact angle if the initial angle was lower than 60°. Between 60° and 86° the surface roughness did not appear to have an general trend [51]. It was recently observed in a study that an increase of the contact angle occurred after sanding on epoxy resin reinforced with carbon fibres when the fibres were exposed and damaged; in this case the contact angle increased from 64° to 88° [13].

With respect to plasma treatment, a sharp decrease on the contact angle is observed from 80.7° to 28.7°. The chemical modifications (addition of O and N elements) are the reason for the improvement in wettability; since the surface free energy increases due to new polar functional groups, scission of molecular chains or creation of free radicals.

At ambient conditions, polymer materials have certain mobility on their molecular chains to respond to interfacial forces, being possible a rearrangement of their polymer chains by rotation or translation movements. Therefore, the surface chemistry will vary in order to minimize its free surface energy between the polymer and the environment [52] as stated in section 3.2. This loss of effect is known as "ageing" and occurs due to the inter-diffusion of high energetic groups into the bulk material and the reaction with the environment, reducing the effectivity of the treatment.

The "ageing" effect was evaluated by measuring the contact angle over time only on plasma treated samples, as it is shown in Figure 5.6, since the bonding step took place on the following weeks after the surface activation. The contact angle increases from 28° to 46° when 3 days have passed and it remains nearly constant during the next two weeks. At that time, the effect of plasma treatment is still noticeable since the contact angle was lower than the reference value (~80°). The small loss of effect was partly owing to the storage conditions, since the samples were wrapped on aluminium foil decreasing the interaction with the environment and possible reactions. After 14 days, it was observed high dispersion on the measurements so a new specimen (marked in red colour) with the entire storage time covered in aluminium foil was used having a similar contact angle to the third day measurements.

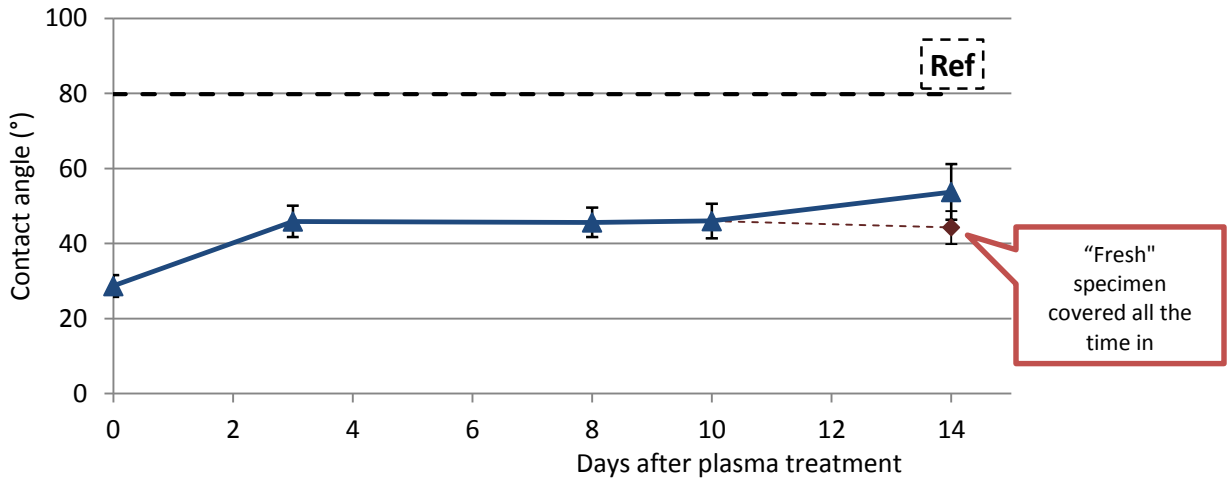

Figure 5.6: Variation of contact angle over time after plasma treatment

The analysis of the contact angle was also performed on CF-PEEK samples (Figure 5.7). The effect on the contact angle for different surface treatments is similar to CF-PPS substrates; in both cases the untreated sample shows high contact angle being unsatisfactory to achieve high bonding strength. After plasma treatment, there is a big decrease on the contact angle down to 18° but with a large scatter. It should be noted that the software did not show high resolution when the contact angle was lower than 20° since it could not reproduce with precision the drop contour showing generally a higher value than the real one. The sanded specimen shows a similar value as the reference but with higher scattering of results, due to

the morphology of the surface since the depth valleys from the untreated sample were still observed as it is shown in Figure 5.2.

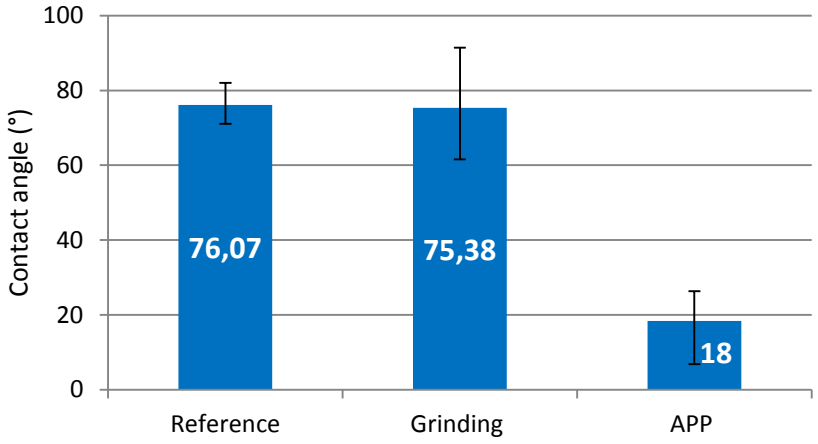

Figure 5.7: Contact angle before (reference) and after the surface treatments on CF-PEEK substrates

In addition, the contact angle was measured with three different liquids (water, ethylene glycol and diiodo-methane), for the calculation of the surface energy of the substrate with the Owens-Wendt-Kaelble equation (eq. 4.2) [46]. The free surface energy, with its polar and dispersive component, is plotted in Figure 5.8.

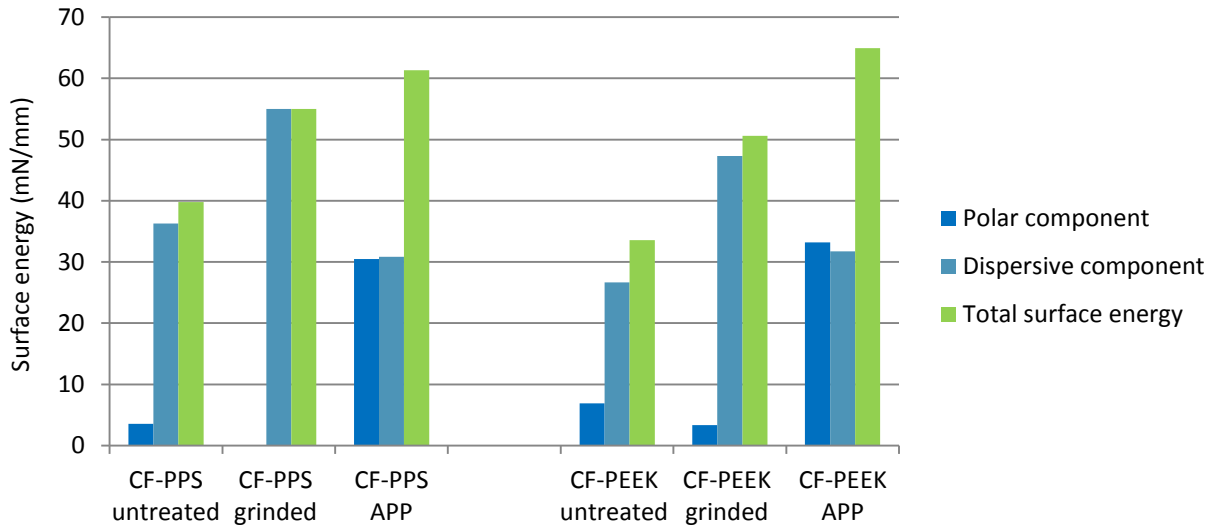

Figure 5.8: Surface energies of reference (untreated), sanded and atmospheric pressure plasma treated CF-PPS (left side) and CF-PEEK (right side)

It can be seen that both substrates show a similar trend:

- The surface energy increases after the application of the surface pre-treatment being beneficial to the bonding performance. The higher the surface energy, the better the wettability.
- Samples after sanding shows an increase of the surface energy by increasing the dispersive part, since the polar component might decrease slightly. The polar part may have decreased because

the surface could have been contaminated by the insertion of oxygen atoms during manufacturing and cutting the specimens, as it was observed in untreated CF-PPS. Therefore after sanding this contamination should be partially removed, decreasing the oxygen content and consequently the polar part. The disperse part increases due to a larger area for the formation of disperse forces.

- After plasma treatment, the polar component increases to a large extend while the dispersive part decreased slightly. This large increase was induced by the introduction of new elements and polar functional groups on the surface, enhancing the formation of dipole-dipole, covalent bonds etc. at the interface.

5.2. Mechanical tests

The adhesion performance was evaluated by two mechanical destructive tests: double cantilever beam and single lap shear. The samples stored at ambient condition were tested at RT while the specimens stored in the climate chamber were tested at high temperature (75°C). The results are shown separated for each adhesive used, first for DCB and then for SLS.

5.2.1. Fracture toughness

The results are presented for each adhesive in a different sub-section with an analysis of their failure modes. The fracture toughness is calculated from the force-displacement curve with the equation presented in section 4.2.1.

- **EP_1 adhesive**

The results obtained are plotted in Figure 5.9; both pre-treatments give similar average values of fracture toughness in both storage conditions. This value is around 200 J/m^2 after manufacturing the samples and increases up to 350 J/m^2 after an accelerated ageing condition.

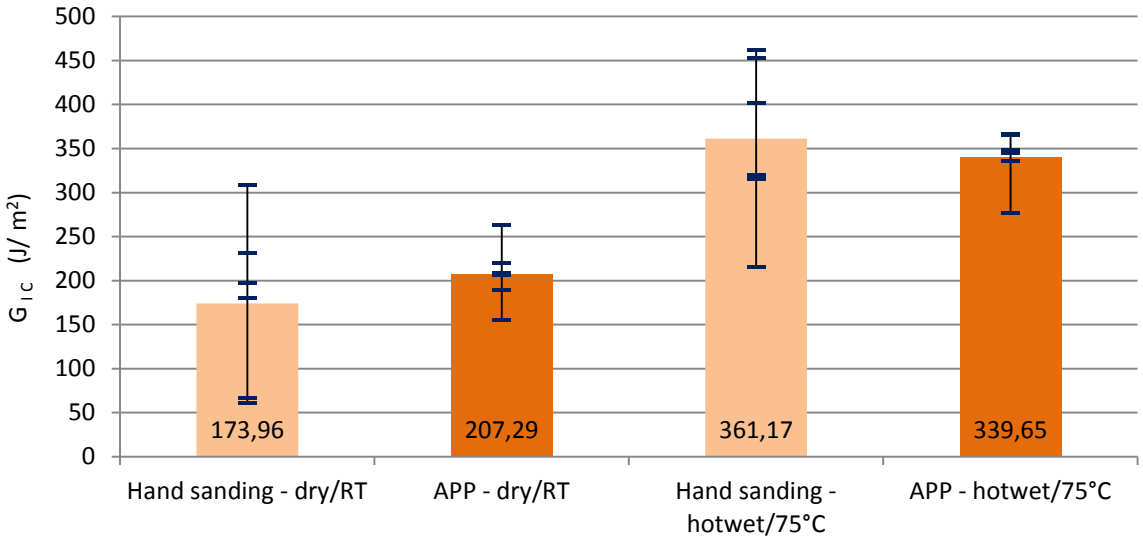

Figure 5.9: DCB tests results of CF-PPS substrates bonded with EP_1 adhesive

After hand sanding, the obtained results present high scattering reaching a value of coefficient of variation of 55% and 26% respectively on the dry and hot/wet test series. The principal reason might be a non-uniform activation of the surface, since it was done manually, the centre or some areas could had been more grinding than the edges. Although an especial care was taken to avoid this problem by the detailed observation of each plate, it was hard to detect any heterogeneity.

Therefore, the high dispersion can be related to the difference in failure modes, as it is shown in Figure 5.10. Looking into the dry samples after sanding, the failure is always at the interface, showing the lowest G_{IC} value when the adhesive is only on one side. The fracture toughness energy increases when part of the adhesive is on one side and the rest on the other side of the specimens and finally the highest value corresponded to the sample where the adhesive is divided into small areas between the two sides, therefore length of the adhesive "fractured" was higher. With respect to hot/wet conditioning analogous things happens; the fracture energy is higher when the area of cohesive failure (CohF) becomes larger.

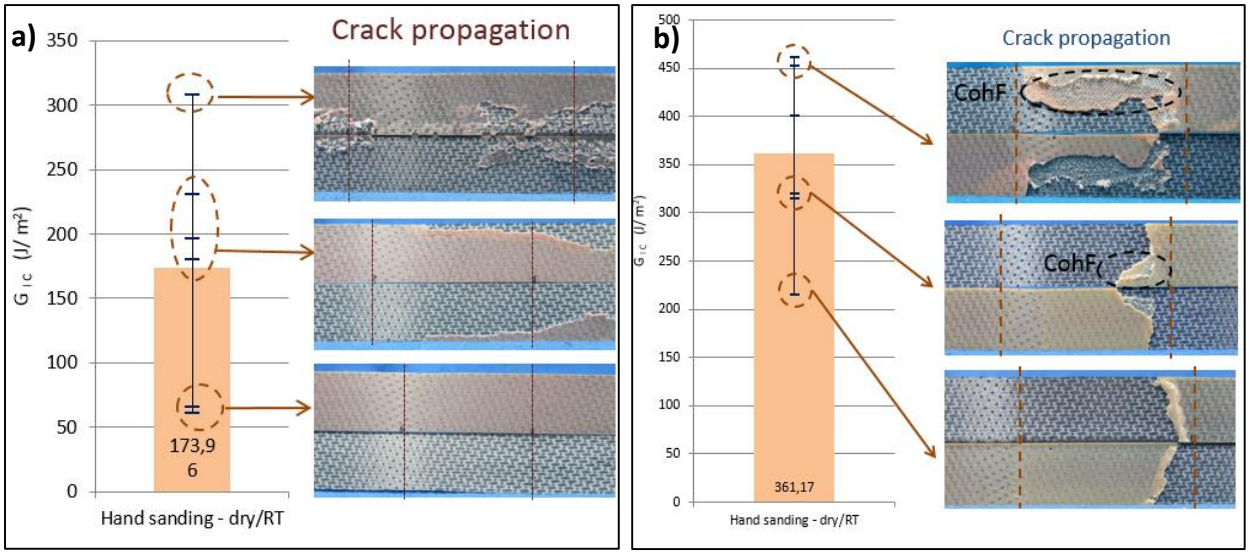

Figure 5.10: Relation between the fracture toughness energy values with their failure mode on hand sanding samples bonded with EP_1

Plasma treated samples show higher value on dry samples compared to grinded samples but lower value after hot/wet, and their failure mode are shown in Figure 5.13. These values are lower than expected and in some test configurations the failure mode is still at the interface.

Dry samples presented an unusual behavior during testing; the propagation of the crack is unstable meaning that the load was increased without noticing a propagation of the crack until it reached a certain critical value where the sample broke catastrophically, increasing suddenly the crack length. Therefore, load-displacement graph was a straight line reaching the maximum and then the load decreased sharply. In this case, it would be inaccurate to calculate G_{IC} since the propagation of the crack was not progressive, but the values were calculated to compare the numerical value with other test series. At the beginning of the propagation crack, there is a small area showing damage on the adhesive (crazing of the adhesive and delamination of the substrate), and then the samples failed 100% adhesively.

With respect to the hot/wet samples, the specimens fail cohesively showing similar G_{IC} values, except one specimens. The pre-crack was formed during the introduction of the test specimen into the metal clamps, so the failure mode in this part varied significantly; adhesive, cohesive, delamination on the substrate or a mixture between these failure modes. The specimens with the lowest G_{IC} shows cohesive failure on this initial pre-crack, being the weakest link on the joint, therefore lower load was necessary to propagate the crack.

APP_dry-RT	APP _hot/wet-75°C
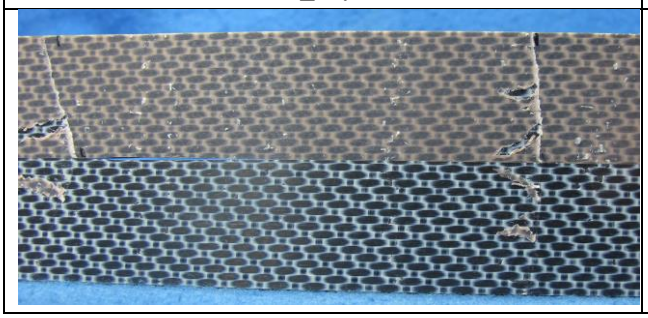	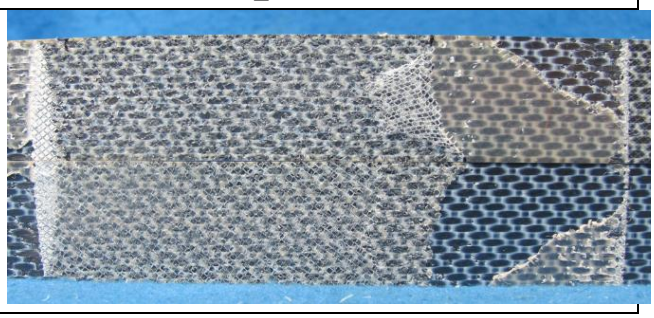

Figure 5.11: Fracture pattern from specimens treated with plasma and bonded with EP_1

- **EP_2 adhesive**

The test results for the samples bonded with EP_2 are plotted in Figure 5.12 and a picture of the failure modes in Figure 5.13. The values are very low in all the configurations with average fracture toughness energy lower than 100 J/m^2 and adhesive failure mode. The main cause for these results was an inadequate surface activation, being impossible the creation of strong chemical bonds or the interlocking between the adhesive and the substrate to improve the adhesion at the interface.

Sanded samples show very low value since the main objective of this surface treatment is to roughen the surface and this modification is insufficient to achieve a good adhesion performance. After an accelerated ageing condition, the value was null because the samples were debonded while they were placed in the specimen clamping. This clamping configuration defers from the standards (see Figure 4.3); instead of bonding tabs, the samples have to be introduced into a metal clamp with a thickness of approximately 2 mm. Therefore, the initial crack is formed while the samples are introduced in this tooling. The length of this pre-crack will vary according to the strength of the adhesion among other parameters; and in this configuration the interface was degraded resulting in the complete debonding of the specimens before the set-up of the mechanical test.

Plasma treated specimens show a small improvement on the adhesive performance with respect to hand sanded specimens and some samples show a mixed stable and unstable crack growth . Although the failure mode is still the same, the interface becomes stronger due to the higher possibility of creation of chemical bonds. It should be noted that this configuration was bonded two weeks after the activation of the surface due to an unexpected problem on the workshop. This might be the reason for its low value because as it was stated plasma treatment increased considerably the surface energy; but this effect is lost over time.

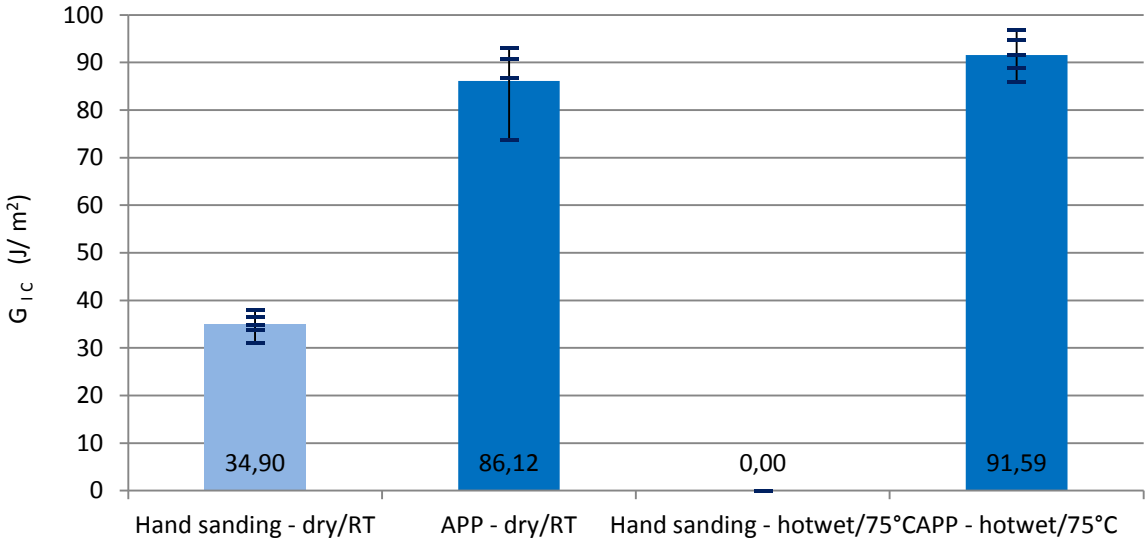

Figure 5.12: DCB tests results of CF-PPS substrates bonded with EP_2 adhesive

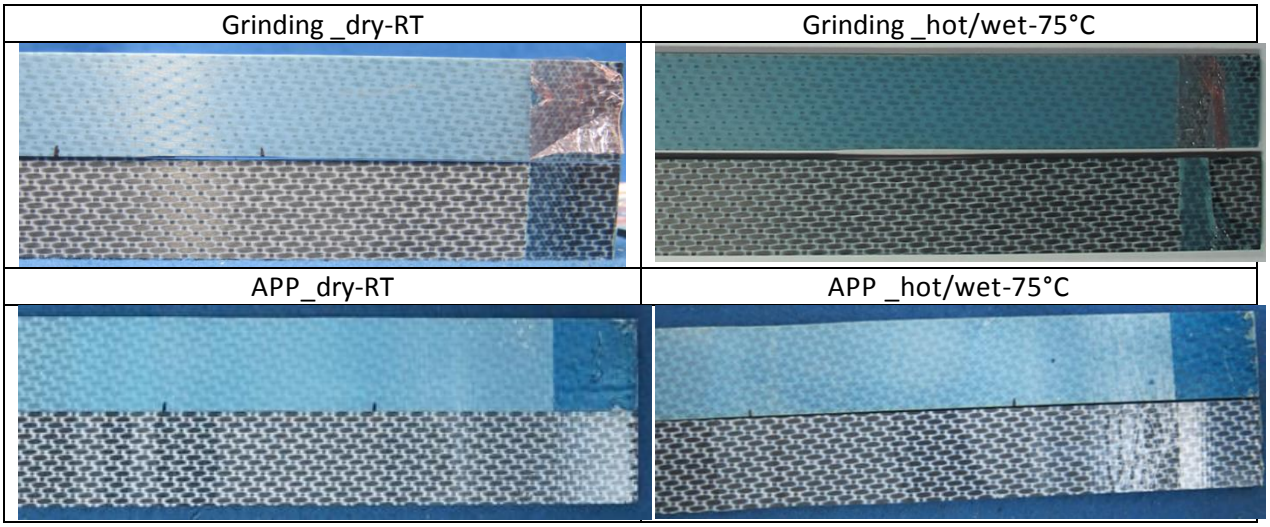

Figure 5.13: Fracture pictures from double cantilever beam tests bonded with EP_2

It should be noted that after the storage on the climate chamber and a higher temperature during testing, G_{IC} remained similar, suggesting that the adhesive and the interface are not degraded after the storage on high temperature and humidity. The weight was controlled during the storage increasing its value only 0.04% with respect to weight of the samples before conditioning.

- **PU adhesive**

Double cantilever beam tests were also performed using a polyurethane adhesive with an adhesive thickness of 0.8 mm, higher than with epoxy adhesives (0.1 mm). The results are shown graphically in Figure 5.14 with a picture of their failure modes in Figure 5.15. All four test series show very different performance, having high dispersion in their results and different failure modes.

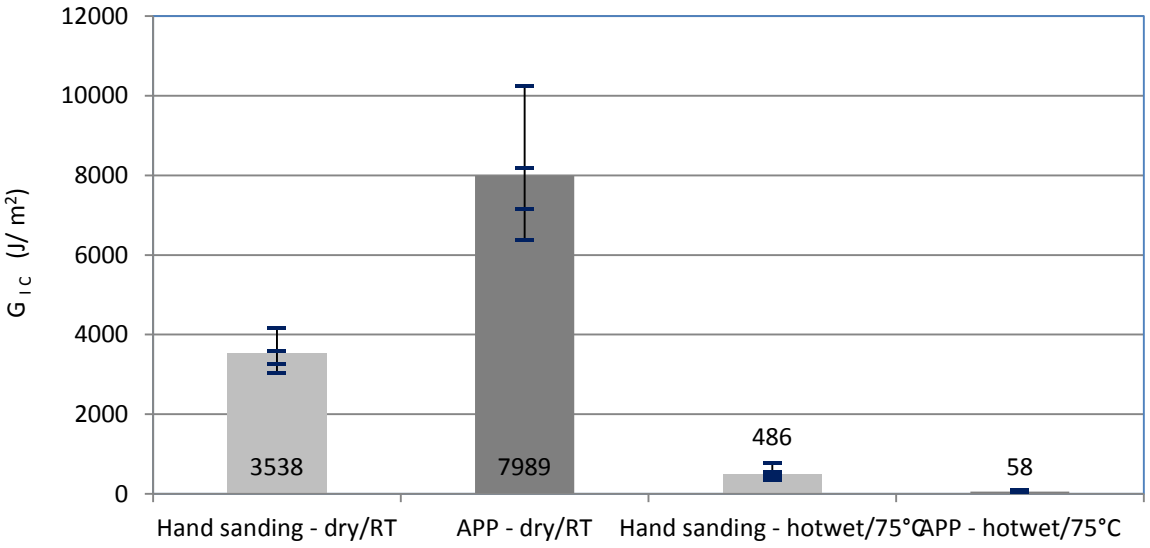

Figure 5.14: GIC results for CF-PPS substrates bonded with PU adhesive

Samples without conditioning have very high values compared with the previous test configurations, with an increase of 2 to 3 orders of magnitude. This behaviour can be explained by two reasons:

- Cohesive failure mode
- The inherent flexibility of the PU adhesive

This induces the necessity of greater deformation from the substrates to be able to propagate the crack; therefore the applied load needs to be much higher than with epoxy adhesives. It was observed during testing a high curvature on the substrates despite of their high bending stiffness reaching a value of at least 80 mm between the two edges of the specimen, whereas the epoxies specimens at RT shows an approximately value of 10 mm. This non-linear behaviour can lead to an overestimate G_{IC} when the adherent suffer large deformations leading to energy dissipation, as it was observed Y. Sekiguchi et al. [53].

However, the values of fracture toughness dropped considerably after the storage in the climate chamber and high test temperature. The obtained values are similar to the ones obtained previously using epoxy adhesives. This sharp drop is mainly related to the change on the failure mode; from cohesive or a mixed failure to 100% adhesive failure between the adherend and the primer by visual inspection. This change of the failure area is produced due to the degradation of the interface between the substrate and primer. This degradation takes place during the storage at the climate chamber; high temperature and humidity weakened the chemical bonds at the interface, resulting in an earlier failure. This could be seen on the failure mode (100% AF after conditioning) and on the initial crack since it was larger than RT specimens.

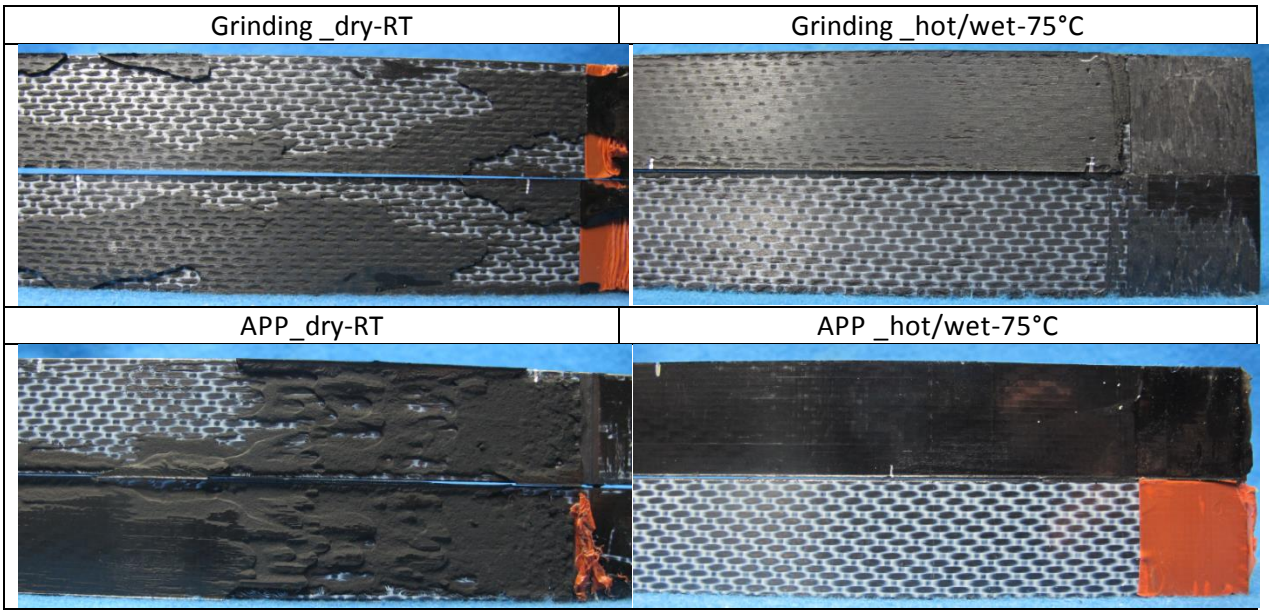

Figure 5.15: Fracture pictures from double cantilever beam tests bonded with PU

5.2.2. Shear strength

The results are presented for each adhesive in a different sub-section with an analysis of their failure modes. The shear strength is calculated from the equation presented in section 4.2.2.

- **EP_1 adhesive**

The results for the specimens bonded with EP_1 on CF-PPS substrates are shown in Figure 5.16 and their failure mode in Figure 5.17.

After hand sanding, the average shear strength at RT is 14.26 MPa with adhesive failure mode and after plasma, the shear strength increases reaching an average value of 21.17 MPa. This increase occurred because the interface was improved by the generation of stronger chemical bonds, as a consequence of the insertion of oxygen atoms on the surface as it was seen in section 5.1. It could be noted that this test configuration showed high dispersion and could be related to their failure modes; the specimens failed in a mixed mode between adhesive and delamination (Figure 5.17_3). Since adhesive failure occurs, the activation of the surface is not sufficient and the interface is still the weakest area. Higher values usually have high percentage of delamination failure; this delamination took place only on the resin and it was debonded from the carbon fibres. In some areas the adherend shows a scratched surface where the resin was damaged; showing cuts perpendicular to the applied force.

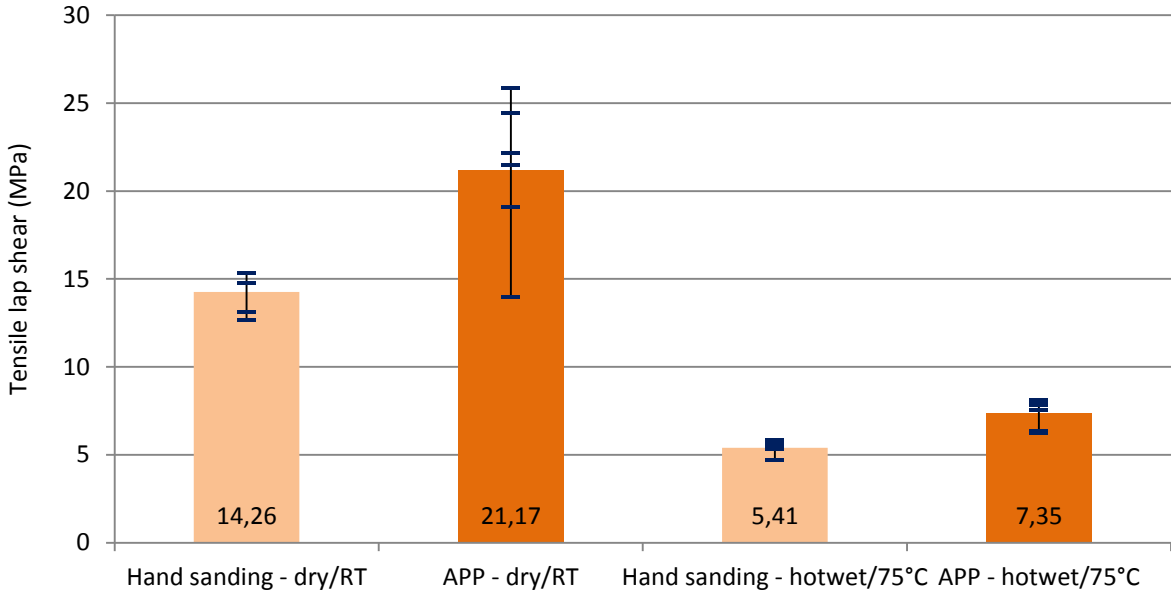

Figure 5.16: Test results for single lap shear test with EP_1 adhesive

After simulating an accelerated ageing by the storage of the samples in a climate chamber during 1000 h, the shear strength decreases considerably, approximately by a factor of 1/3 with respect to the specimens tested at RT. The prolonged exposure at high temperature and humidity suggests to have produced irreversible chemical and physical changes within the adhesive such as plasticization or degradation on the interface resulting in a loss of bond strength and additionally the high testing temperature (75°C) might have had an effect on the properties of the adhesive, generally they will soften at high temperature. It was observed in a previous internal research, that the E-modulus (MPa) decreased from 2100 to 30 MPa after hot/wet conditioning.

Looking into sanded samples, the failure mode is still on the interface but the failure pattern differed with respect to the specimens tested at RT (Figure 5.17_2). The adhesive is distributed mainly on one part of the specimen with the carrier fabric, and the other part showed only small areas distributed uniformly, where the fibres were located. So, the adhesion failure occurred on both sides and usually on the areas with PPS resin, which appeared to be the weakest link in this joint. In case of APP samples, the failure mode was also altered. The pattern looks like the scales of a fish; where the adhesive is broken in planes at approximately 45° with respect to the applied force.

The test results for CF-PEEK substrates are presented graphically in Figure 5.18 with a picture of the failure mode. Both pre-treatments provide high shear strength value, 24 MPa for hand sanding and 26.91 for APP. The values are higher than CF-PPS, especially after hand sanding, due to the composition of its monomers containing two ethers and one ketone functional groups. As it has been seen, the presence of functional groups is essential to achieve a structural joint since strong chemical bonds can be formed. During the analysis of the surface energy, an increase of the polar component was observed, meaning a higher concentration of polar interactions such as dipole-dipole, hydrogen bonds etc. Despite the high shear strength values, the failure mode is still at the interface after grinding and a mixed failure (AF + CF) after plasma.

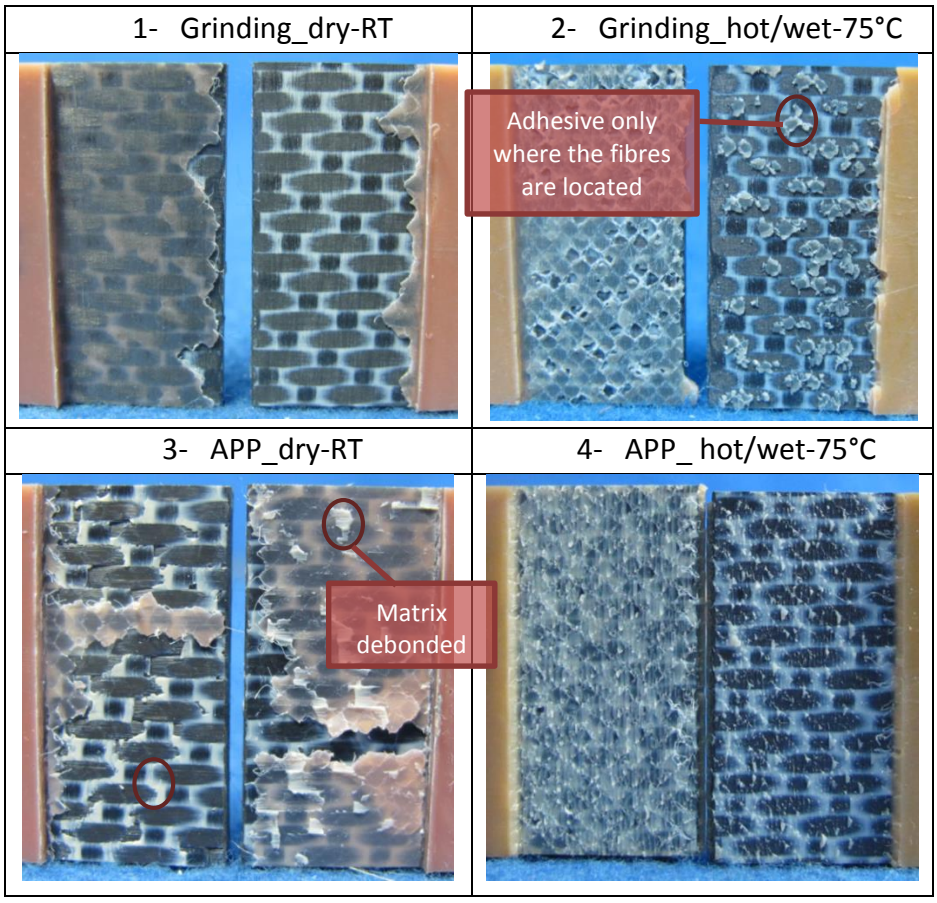

Figure 5.17: Fracture pictures from single lap shear tests bonded with EP_1

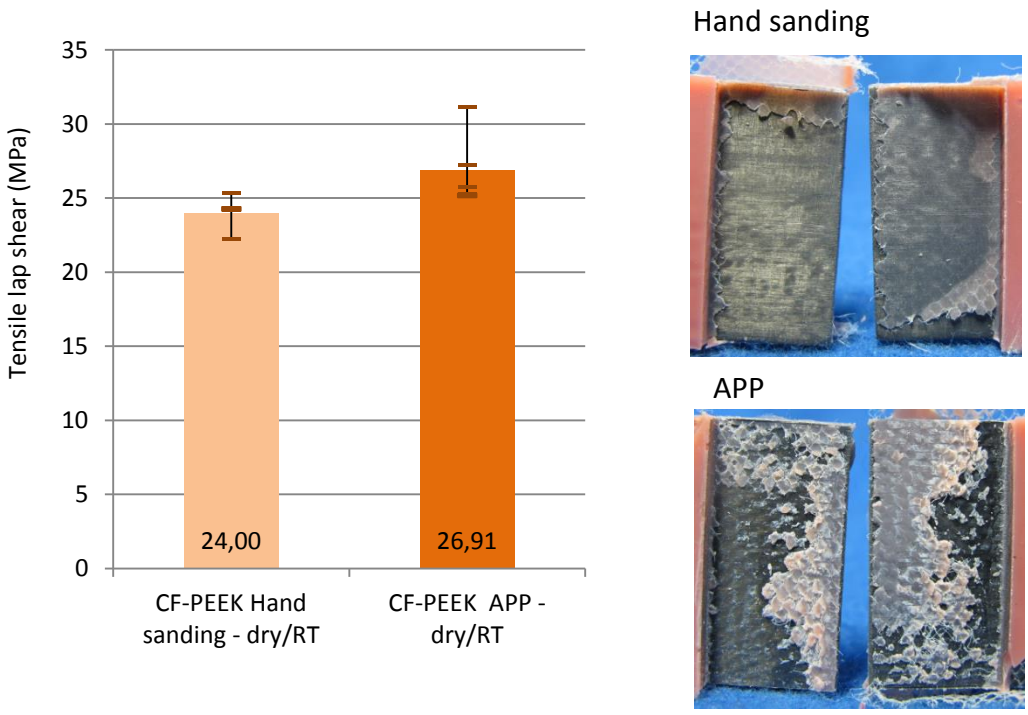

Figure 5.18: Single lap shear tests results and failure mode of CF-PEEK samples bonded with EP_1

- **EP_2 adhesive**

Test results are shown graphically in Figure 5.19 with their failure modes in Figure 5.20. All tests configurations showed similar value of tensile lap shear, being relatively low with failure at the interface.

After hand sanding, the shear strength reaches a value of 9.18 MPa and with hot/wet conditioning and 75°C of test temperature the obtained value is 9.75 MPa. In both cases the coefficient of variation is less than 5%, so the test series show high reproducibility. Looking into the APP treated samples; the average shear strength value increases slightly up to 11.04 MPa for the samples tested at RT and 10.88 MPa after the storage in the climate chamber and high test temperature.

After plasma treatment, the chemistry of the surface is modified by the insertion of oxygen and nitrogen atoms forming new functional groups on the surface as it was seen in Section 5.1.2. As a result the interface becomes stronger and the shear strength increased slightly, but this modification was not sufficient since the weakest area was still at the interface. In addition, this improvement on the shear strength can be also observed with the failure modes; all samples fail adhesively but there are some differences with respect to the pre-treatment. Specimens treated with plasma show cuts perpendicular to the applied force on the substrate, especially on the resin part as it is shown in Figure 5.20. In very few small areas, this damaged resulted in a delamination failure, where the resin was debonded from the substrate. As a consequence of this damage to the surface, these two test configurations had higher coefficient of variation, especially after hot/wet conditioning. In this case, on sample showed half of the value with respect to the rest of the test series with a failure mode 100% adhesive and no damage or scratches on the surface of the adherend.

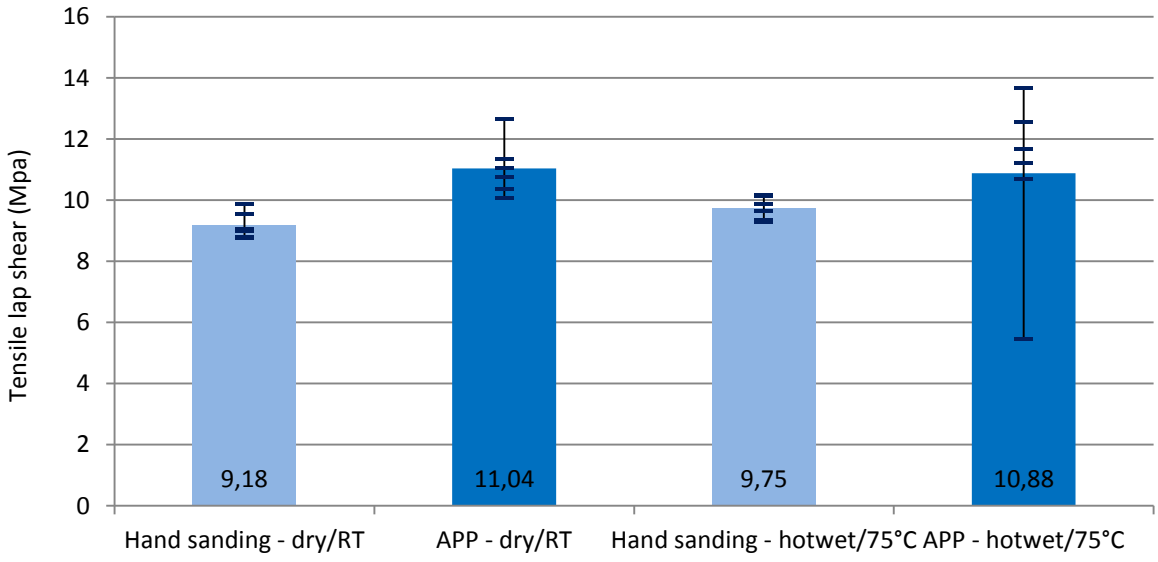

Figure 5.19: Test results for single lap shear test with EP_2 adhesive

The adhesive joint maintained its behaviour after hot/wet conditioning and high test temperature. The accelerated ageing condition appears not to have any effect on the adhesive and adhesion performance, since the shear strength value and failure mode remain similar.

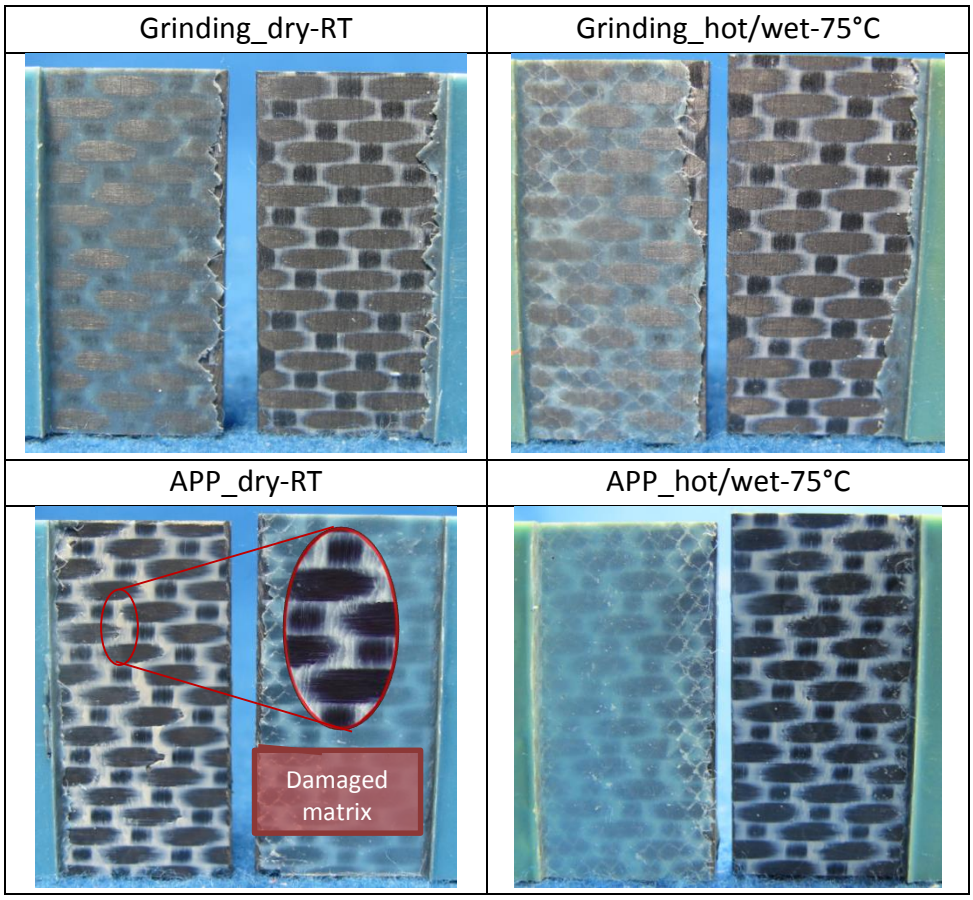

Figure 5.20: Fracture pictures from single lap shear tests bonded with EP_2

The results for CF-PEEK substrates are shown in Figure 5.21, and a similar shear strength value was obtained with both pre-treatments with the same failure mode; 100% AF.

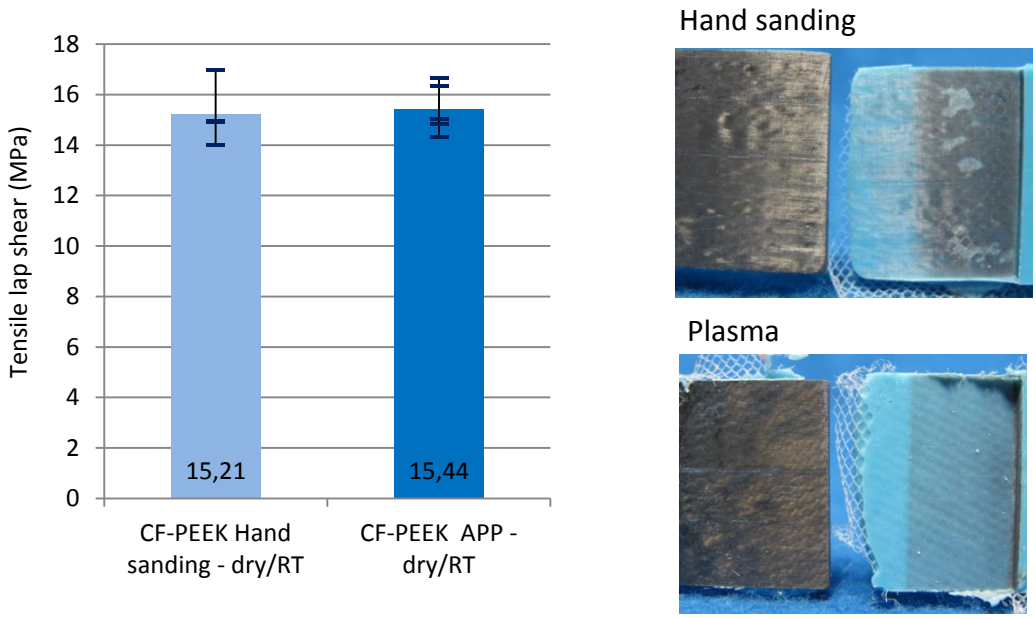

Figure 5.21: Single lap shear test results and failure modes of CF-PEEK bonded with EP_2

Both activation treatments show similar improvement on the shear strength reaching a value of 15 MPa; this value is lower than using EP_1 but it increases with respect to CF-PPS substrates. As it was also observed with EP_1, the presence of oxygen on the chemical composition of PEEK increases the likelihood of formation of strong covalent bonds with respect to PPS, resulting in higher shear strength at the interface. However, after both pre-treatments, the activation of the surface is insufficient since adhesive failure still occurs.

- **PU adhesive**

The adhesive performance of PU sealant-adhesive after single lap shear tests is shown graphically in Figure 5.22 with a picture of their failure modes in Figure 5.23.

The highest shear strength is achieved after hand sanding reaching a value of 5.85 MPa. In this test series, samples show a mixed failure mode; it is cohesive failure where the fibres are located and adhesive failure between the fibres where there is only PPS resin. After grinding, some carbon fibres were exposed showing good adhesion properties compared to the thermoplastic resin; where the pre-treatment was insufficient to avoid adhesive failure.

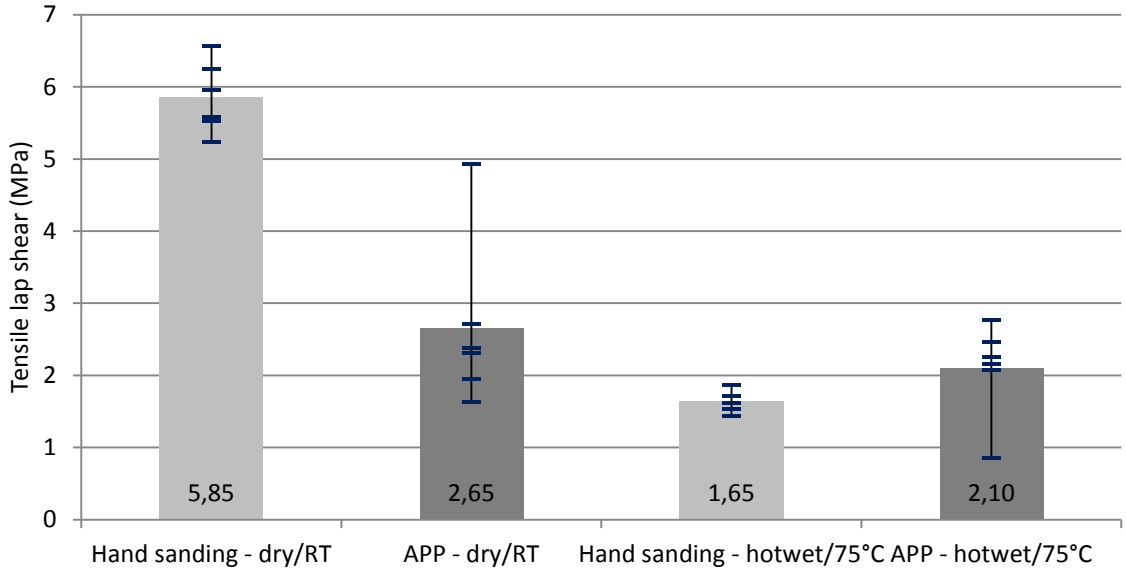

Figure 5.22: Test results for single lap shear test with PU adhesive

This behaviour changes after an accelerated ageing on the climate chamber, since the shear strength decreased up to 1.65 MPa with a change in the failure mode, similar to the behaviour in DCB tests. This change takes place due to the degradation at the interface; the adhesive failure occurs predominantly between the substrate and the primer, except at deep scratches where a black colour is observed. Therefore, the humidity and high temperature has an irreversible effect at the interface carbon fibre-primer, since the interface was weakened.

Plasma treatment specimens fail adhesively between the substrate and the primer, showing that the activation of the surface was not enough to avoid the failure at the interface. It should be noted that the specimens were bonded one week after the activation of the surface, although the samples were wrapped on aluminium foil, a loss of effect occurred as it was seen in Figure 5.6. Some specimens had small areas or scratches were the failure was cohesive near the substrate, showing a good adhesion between the primer and adhesive. In both cases, the coefficient of variation was more than 30% due to a specimen in each configuration showing a complete different value than the rest of the series; in case of APP-dry/RT configuration, one sample showed a mixed failure mode (~80% AF and 20%CF) and for APP-hot-wet/75 the sample had any small area or scratch where cohesive failure occurred.

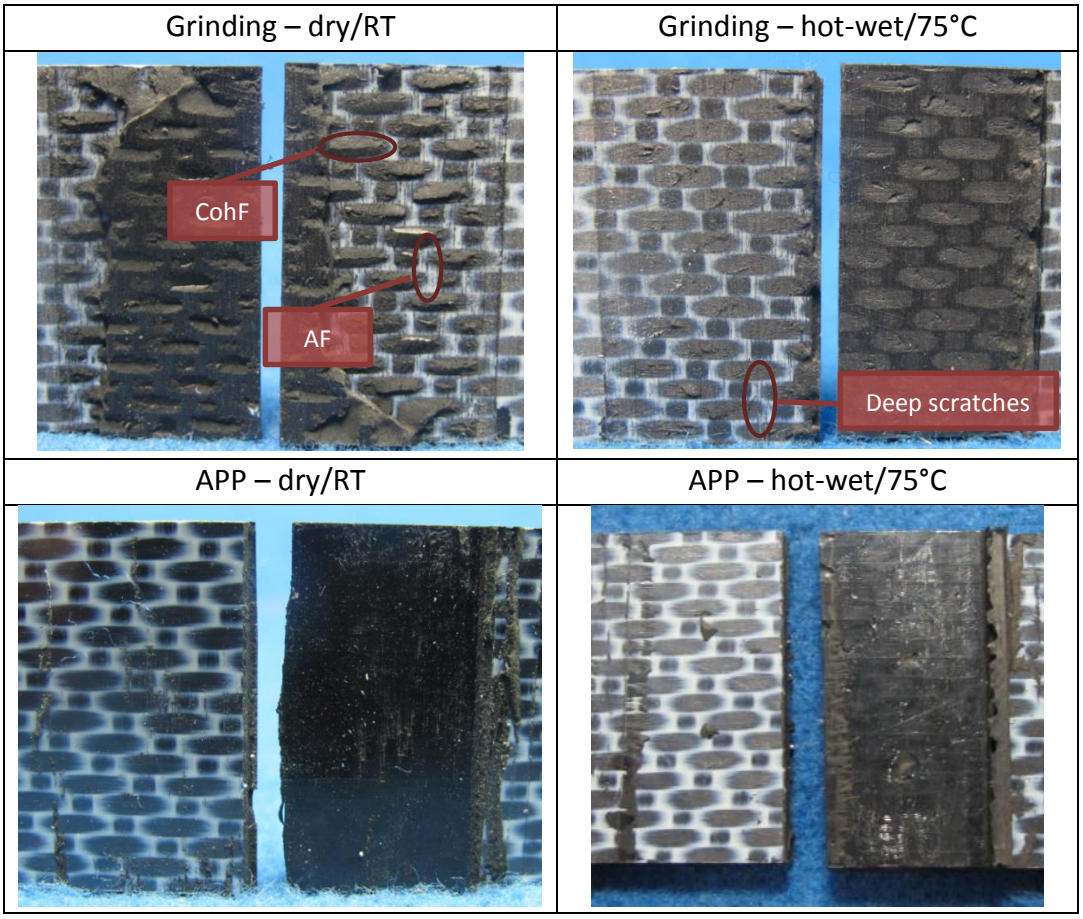

Figure 5.23: Fracture pictures from single lap shear tests bonded with PU

Analogous to the other adhesives, the results from CF-PEEK are presented in Figure 5.24. Contrary to the behaviour of epoxy adhesives, the use of a polyurethane adhesive sealant with a primer gave better results after sanding than plasma treatment.

After sanding, the shear strength reached a value of 6.85 MPa with a failure mode 100% cohesive. Therefore, this surface treatment was sufficient to move the weakest area from the interface to the adhesive. As it was observed with CF-PPS substrates, the primer created a strong link with the areas where the fibres were located resulting in a mixed failure. A similar behaviour is expected to have happened with CF-PEEK; in which the laminate was built up by UD plies having the top ply at 0° orientation. So, after

grinding, the area where the fibres are exposed is larger and distributed uniformly resulting in an increase of the interatomic and intermolecular forces at the interface.

In contrast, plasma treated samples showed a lower shear strength value; 4.89 MPa due to a mixed failure mode. In this case the plasma treatment appeared to be sufficient in certain areas; which ranged from 10% to 50% of cohesive failure. So adhesive failure occurred predominantly and took place between the primer and the substrate by visual inspection.

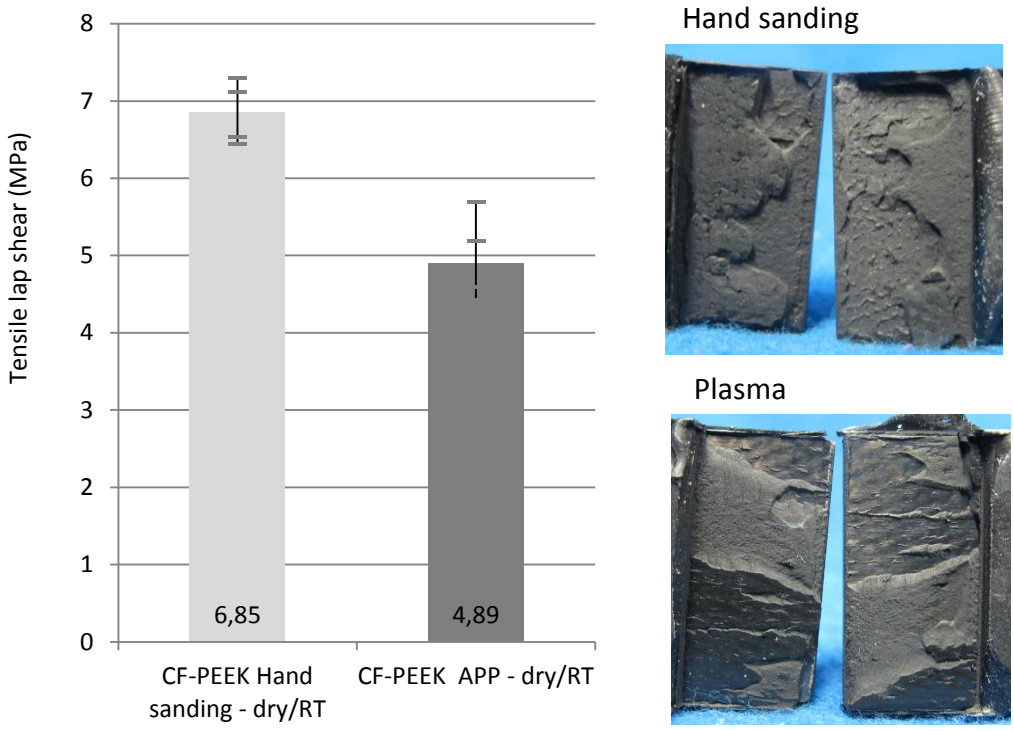

Figure 5.24: Single lap shear test results and failure modes of CF-PEEK bonded with EP_2

6. Discussion

6.1. Relation between surface morphology and adhesion performance

Since adhesion is a surface phenomenon, a comparison between the surface properties and the adhesion properties are made in greater depth:

- **Hand sanding**

Sanding treatment is classified within the mechanical methods and was done manually with P-120 sandpaper (fine grade) until the first layer of resin was removed. The main objective is to roughen the surface and the morphology was evaluated using an optical microscope. Both substrates (CF-PPS and CF_PEEK) showed similar surface profile with small peaks distributed uniformly with a value of 10-17µm. The surface energy increased after this pre-treatment, especially the disperse part. The dispersive part accounts for the dispersion forces which are non-additives forces and the increase can be related to a larger area for these forces to act.

In general, the adhesion performance is unsatisfactory because the shear strength and fracture toughness values are still low and all failure modes occur in the interface except one configuration: PU adhesive without conditioning. In this case, a good adhesion occurrs where the carbon fibres are located:

- PPS laminate were made out of fabric plies, and after grinding in certain areas, carbon fibres started to be exposed. This lead to a mixed failure50% cohesive near the substrate and 50% adhesive failure.
- The plies used on PEEK laminate were unidirectional, so larger areas with only resin were difficult to detect. Similar to PPS, good adhesion to carbon fibres should be expected and as the exposure of carbon fibres was uniformly throughout the surface, the interface was not the weakest link. In this case, the failure mode was 100% cohesive.

Chemical bonding mechanism would only make a small contribution after mechanical treatments because thermoplastic polymers are inherently chemically inert as their molecular chains are made out of C and H, with small quantities of other atoms; S or O. This leads to a low concentration of strong chemical bonds.

With respect to the interlocking theory, the roughening of the surface has two main effects:

- It enhances the introduction of the adhesive into the irregularities of the substrate.
- The bonding area becomes larger, increasing the possibility of creating chemical interactions.

In this case, the adhesive keying into the substrate might have improved adhesion strength, but this, together with the increase of bonded surface area were not sufficient to change the failure mode. The diffusion model cannot be applied to this configuration since the polymers were not compatible; the

molecular chains must be very similar. And finally the electrostatic attraction model is based on weak molecular interactions that results in a low contribution to the improvement of adhesion strength.

Therefore, hand sanding is not a suitable treatment for thermoplastics since the adhesion properties are relatively low and the predominant failure mode is at the interface. According to the certification specification provided by EASA stated in Chapter 1; adhesion failure is unacceptable and immediate action is needed when this occurs in a bonded structure. The modifications of the surface by a roughening of the surface with an increase of the dispersive component of the surface free energy were not sufficient to achieve high strength and avoid adhesive failure mode, obtaining similar results to Kinloch's study [30]. Due to the chemistry of the molecular chain and considering molecular bonding as the main mechanism to achieve high strength, the likelihood of formation of strong covalent bonds is not high enough to avoid interfacial failure.

- **APP**

Atmospheric plasma treatment is an energetic method whose objective is to change the chemistry and morphology of the surface. The main surface change is big increase of oxygen atoms, from 6.4 to 34.3% atomic concentration with the subsequent formation of functional groups such as carbonyl, carboxylic acid, sulfoxide or sulfonyl groups was leading to chemical bonding being the main mechanism. Mechanical interlocking and electrostatic attractive model should have only make a small contribution and the diffusion model cannot be applied because of the different nature of the polymers.

In this case, the adhesion performance is still unsatisfactory and most of the failure modes continued to take place at the interface or if a mixed failure occurred; adhesive failure is usually the predominant failure mode. This behaviour was unexpected since the surface characterization after the treatment seemed to be very promising; the contact angle decreased more than 62% with respect to the untreated sample and the oxygen content increased to a large extent forming new functional groups. The unsatisfactory performance can be attributed to:

1. The "ageing effect"

In this project, the ageing effect was evaluated by the contact angle measurements, showing an increase of 55% after 3 days, then the contact angle levelled off and after 2 weeks the effect was still noticeable since the contact angle was 50°.

From a logistic point of view and the implication in the production chain of the company, all the samples were activated the same day and wrapped in aluminium foil for storage before bonding. The time passed between the activation and bonding step was less than 1 week, except for DCB using EP_2. During storage, the polymer tries to minimize its surface energy by reacting with the environment and by the inter-diffusion of functional groups into the bulk material; this loss of effect resulting in a decrease of the surface energy is known as "ageing effect" and can be prejudicial for adhesive performance. The ageing of effect was study by Moritzmer et al. [36] taking into account two parameters: temperature and time. He studied three different thermoplastics resulting in a loss of bond properties with increasing the studied factors, however a function with the ageing parameters could not be detected. Additionally, Comyn et al. [54]

studied the loss of effect of corona treatment on PEEK samples stored at ambient conditions resulting in a slightly fall (~17% after 90 days) of shear strength over time.

2. Inadequate plasma parameters

Some samples were bonded on the same day as the activation treatment and also failed at the interface. This suggested an inadequate selection of plasma parameters which resulted in a non-homogeneous or insufficient activation. However, the morphological changes seemed very promising with a sharp decrease on the contact angle similar previous researches using atmospheric and low pressure plasma on different high performance thermoplastics with a value of ~30° [55, 56] and similar chemical composition compared to R.Hong study [32].

Despite this, the adhesion performance after APP is generally improved with respect to sanded specimens. The interface strength improves showing a tendency to change the failure area to delamination on the substrate; especially in SLS configurations using epoxy adhesive. In these cases, adhesive failure is the predominant failure mode but the surface of the substrate is damaged due to shear stresses, showing small cuts as can be seen in Figure 6.1 with certain areas with delamination failure.

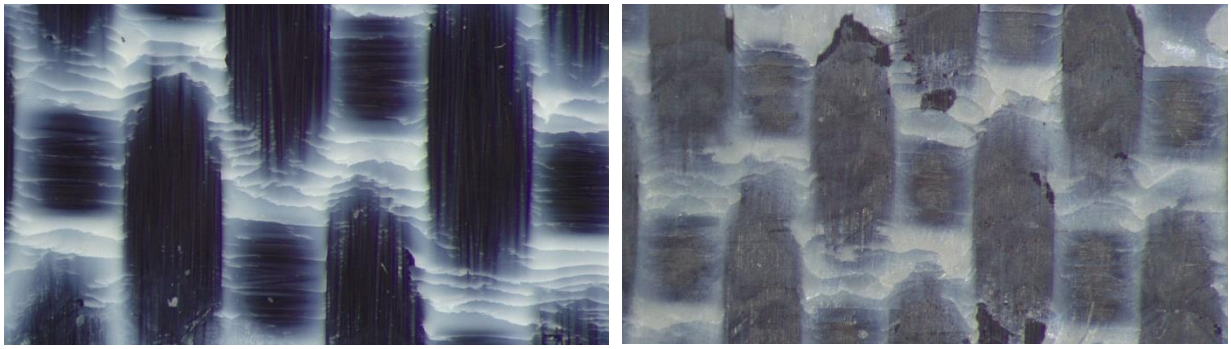

Figure 6.1: Micrographs from SLS tests with EP_1, plasma treated and RT testing.

This trend means a possibility of further improvement on the interface, increasing its strength to avoid interfacial failure, as it has occurred in previous researches carried out by H.M.S. Iqbal [31] and R. Hong [32]. These two previous investigations lead to the conclusion that an improvement on the adhesion performance on PPS was observed with a change on the failure mode from the interface to delamination on the substrate. The morphological changes produced in this project were comparable to the previous researches; similar chemistry to R.Hong study but lower surface energy than H.M.S Iqbal, specially the polar component (30 mN/mm in this study compared to 55 mN/mm from the previous research), however another studied carried out by H.M.S Iqbal studied the effect of low pressure plasma on PPS and showed a polar component of 18 mN/mm with a failure mode on the substrate [13].

The polar component plays an important role in the adhesion performance since its main mechanism (molecular bonding) depends directly on the surface chemistry. As it was stated in Chapter 2, the polar component of the surface energy accounts for hydrogen interaction, dipole-dipole, dipole-induce dipole [43]. During the bonding step, these interactions give rise to chemical bonds whose strength and number are directly proportional to the strength of the adhesive joint. According to H.S. Lee et al [57], the bond

strength can be improved up to 3 order of magnitude in some configurations of substrate and plasma parameters.

In this project, the surface energy was only calculated the same day as the activation step; therefore it should have decreased over time since the contact angle using water increases. The initial lower value of the polar component and this decrease over time seemed to be the main aspects to detect if the bonding performance will be unsatisfactory.

6.2. Effect of hot/wet conditioning and high testing temperature

The evaluation of the durability of a bonded joint is essential since most of the in-service failures occur due to a degradation at the interface and this evaluation was carried out by the storage of samples in hot/wet conditions and high test temperature, simulating an accelerated ageing condition.

The adhesion properties change considerably with respect to the different adhesives and to a lesser extent with respect to the surface treatment. This is related to the fact that both treatments show similar fracture mode (mostly adhesive) and in some cases also similar mean values of adhesion properties. The effect of hot/wet conditioning and high test temperature are explained separately for each adhesive due to their different behaviour.

- EP_1 adhesive

EP_1 has the lowest viscosity among the adhesives studied being beneficial to obtain a more intimate contact with the adherend. The different test results are shown in Figure 6.2, where the values for dry samples are shown on the left and on the right are the results after conditioning.

The specimens tested in SLS show the same tendency for both treatments; after hot/wet storage the values decrease by a factor of 1/3. In both cases, this decrease is accompanied by a change in the fracture pattern but still adhesive failure is the predominant failure mode and this change may be attributed due to a plasticization or degradation of the adhesive. The bulk properties of the adhesive seem to be altered due to the high temperature, which is in agreement with a previous research study on the bulk properties of the adhesive made in the company [58], in which the E-modulus (MPa) decreased from 2100 to 30 MPa after hot/wet conditioning and high test temperature and the Tg also decreased from 92°C to to 55°C.

The environmental effects on an adhesive joint are also visible after DCB tests. In this case, at RT the adhesive is rigid and stiff, showing very low value of G_{IC} with an adhesive failure mode. But, after the storage in the climate chamber and high test temperature, the adhesive becomes softer and the interface is no longer the weakest link; for APP the failure is 100% cohesive and for sanded samples it is a mixed failure: adhesive + cohesive. In the last case, the cohesive area is always on the inside, suggesting a possible degradation of the interface at the edges.

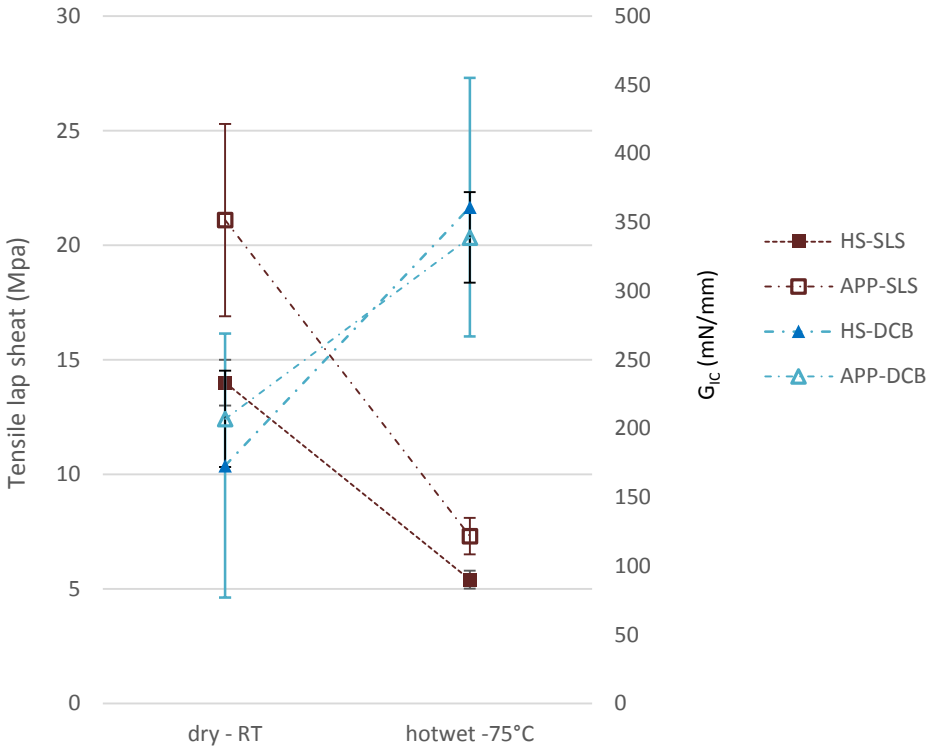

Figure 6.2: Test results for CF-PPS specimens bonded with EP_1 (HS: hand sanding and APP: atmospheric plasma treatment)

The softening of the adhesive appears to be the main reason for the behaviour after conditioning, which would lead to a decrease of the shear modulus with a more plastic behaviour increasing the fracture toughness.

- EP_2 adhesive

EP_2 is a rigid structural adhesive and had higher viscosity than the previous adhesive, making more difficult to spread the adhesive. According to its datasheet [35], it maintains its strength properties up to 177°C.

Samples bonded with this adhesive show lower values of shear strength and G_{IC} than EP_1 samples on the reference state (without conditioning), and all the failure modes are at the interface. There are some reasons that could explain this different behaviour with respect to the previous epoxy adhesive, such as lower intimate contact and worse interlocking due to its higher viscosity, less chemical bonds between the adhesive and the adherend which might have occurred due to the chemistry of the adhesive (being slightly different from EP_1) or due to the different mechanical properties of the adhesive. However, the joint maintains its initial strength showing barely any change after hot/wet conditioning. The results can be seen graphically in Figure 6.3.

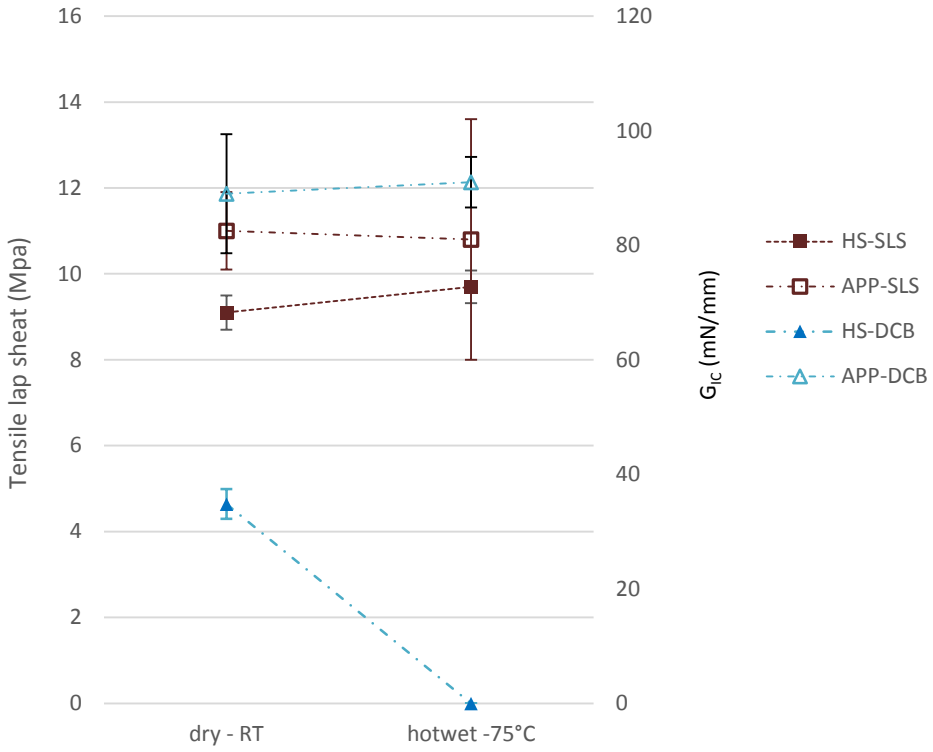

Figure 6.3: Test results for CF-PPS specimens bonded with EP_2 (HS: hand sanding and APP: atmospheric plasma treatment)

Shear strength and DCB values remained similar after hot/wet conditions and high test temperature. Although the samples show low value for both environmental conditions, the interface or adhesive does not seem to be degraded and it remains unaltered after the exposure at high temperature and humidity.

- PU

PU is a polyurethane sealant adhesive forming a flexible joint (low modulus and high ductility) in contrast with the epoxy structural rigid adhesives used as explained previously. The results are shown in Figure 6.4 and as it can be observed that all the values decrease after the conditioning; although the decrease varies to a large extent with respect to the mechanical test and surface treatment.

As it was stated, the primer and PU adhesive show good adhesion after hand sanding on the areas where the fibres are located and start to be exposed. This was observed only in dry conditions for both test configurations where the specimens failed 50% AF and 50% CF. However, the humidity and high temperature have a negative effect on the interface; it weakens the links between the substrate and the primer decreasing to a large extend the percentage of cohesive failure. After conditioning, the predominant failure mode occurs between the substrate and the primer, suggesting that the primer is not resistant to humidity and a weak interface consisting of big molecules of water could have been formed during storage. This explains the sharp decrease of the values, especially on the fracture toughness energy.

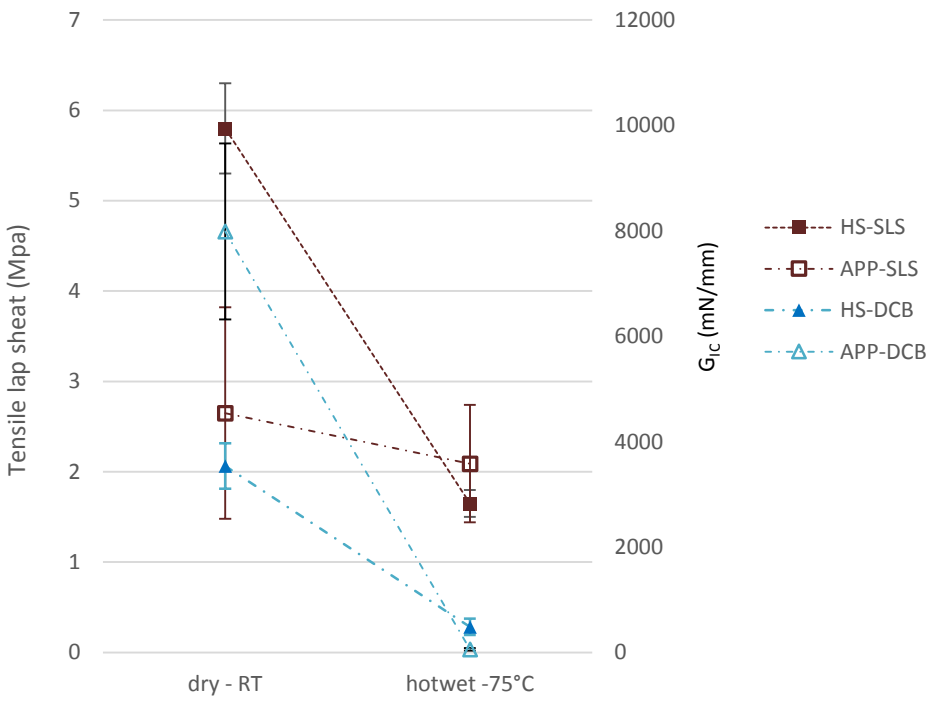

Figure 6.4: Test results from CF-PPS bonded with PU (HS: hand sanding and APP: atmospheric plasma treatment)

Plasma treated samples show different behaviour and it might be due to the plasma ageing effect since not all the samples were bonded the same day. SLS specimens were bonded 7 days after the treatment showing adhesive failure as the predominant failure mode, with cohesive failure mode in certain areas. The mean values were similar so the hot/wet conditions has little effect on the interface; in this case the interface between the substrate and the primer is stronger than after grinding and the degradation of this interface is partially hindered. Looking into plasma treated DCB samples, the bonded step was done after 2 and 7 days for dry and hot/wet respectively, and this is the main reason for this sharp drop.

Looking into the fracture toughness, when the failure is not 100% at the interface, the inherent flexibility of the PU produces extremely high values of fracture toughness; up to 3 orders of magnitude higher than epoxies as it was also observed by Y. Sekiguchi et al. [53]. According to the datasheet the elongation at break is greater than 500%; this elongation induces the necessity of a large deformation on the substrates to be able to propagate the crack so the applied load is very high. But when they fail at the interface, the values are then comparable with the epoxies specimens, having the same order of magnitude, since the adhesive does not undergo high deformations to propagate the crack.

6.3. Analysis of the adhesion performance: SLS and DCB

The performance of the adhesion can be determined by different mechanical tests, such as single lap shear, double cantilever beam, T-peel tests, floating roller peel etc. But, which is the best destructive method to assess the adhesion?

This question is difficult to answer because adhesion is a complex phenomenon involving several disciplines and the mechanical tests evaluate different properties of the adhesion. Among these tests, the most commonly used and found in previous literature research were single lap shear and double cantilever beam. In this section, an analysis of the similarities and differences is made with respect to these two surface treatments.

- Dispersion of the results

The dispersion of the DCB results is found to be greater than SLS tests. Several reasons can explain this difference such as the initial crack or the evaluation area. Additionally, the manual sanding and the ageing effect of APP are also a source of dispersion on the results due to the possible non-homogeneous surface activation.

The initial crack was created while the specimen was manually forced into the metal clamping, being the crack length depended on the adhesive, thickness of the adhesive, the interface etc. If the initial crack is larger, then the force needed to propagate the crack will be lower. Thus, the length of the pre-crack is a critical parameter on the performance of the tests, and since it can not be controlled different tests configuration had different initial crack lengths, making more difficult to give an accurate comparison.

Hand sanding was performed manually and although it was taken a special care on the activation of the surface, certain areas were inevitable more grinded than others, especially the centre compared to the edges. On plasma treated samples, the ageing effect might not have occurred uniformly on the surface and therefore the adhesion strength at the interface could have varied. This heterogeneity on the surface properties had greater effect on DCB specimens due to the larger area and type of loading at the interface, which result in a greater probability of detection of these variations.

- Different loading conditions at the interface

Single lap shear tests induce shear and peel stresses at the interface (mode I and II). The distribution of these stresses is not uniform across the surface, being higher at the edges. In contrast, double cantilever beam tests only induce peel stresses (mode I) at the interface. This difference on the type of loading has great influence on the fracture pattern.

Examples of this influence can be seen on the failure mode after plasma treatment and in dry condition. The substrate tested in shear is damaged showing perpendicular cuts on the matrix (as it is seen in Figure 6.1) due to shear stresses at the interface in contrast to DCB tests where adhesive failure is predominant with small areas failing by delamination. In hot/wet condition, the failure mode was also different and especially for EP_1; failing cohesively in peel tests and a mixed mode between cohesive and adhesive when it was loaded in shear.

Since adhesive joints are designed for shear stresses, peel forces are more critical for the interface. The critical load during testing differs in one order of magnitude between these two mechanical tests; for SLS tests it ranges from 2000 to 5000 N for epoxies and from 200N to 2000N for polyurethane adhesive whereas for DCB tests, the maximum load from 20N to 100N for epoxies and up to 600N for PU adhesive.

This difference is based on the type of stresses (mode I and/or II) and the area where the stresses are applied; for SLS the area corresponds to the overlap area, but for DCB the area is smaller corresponding to the crack of the tip. The smaller the area is, the higher the stresses are and therefore failure occurs earlier.

- Behaviour of rigid adhesive

In certain configurations, the calculation of fracture toughness energy was inadequate since the propagation of the crack was unstable. This occurred when the adhesive was brittle and the failure mode was at the interface, in this case using EP_1 at RT and EP_2 at RT and with hot/wet conditioning all after plasma treatment.

Especially with EP_1, the load-displacement graph obtained was a linear relation, the load increased linearly until it reached a certain critical load where the crack propagates catastrophically, ranging from 90 and 160 mm of the propagated crack length. Therefore the propagation of the crack is unstable. The failure mode was at the interface with small areas where the resin was debonded from the substrate except at the start of the crack, where it failed mostly on the interface but the adhesive presented damaged as it showed lighter colour due to the internal stresses and/or in some configuration it also showed delamination or cohesive failure (as it can be seen in Figure 6.5). However, this value was still used for comparison with respect to other test configurations and the maximum load gave an insight of the strength of the joint.

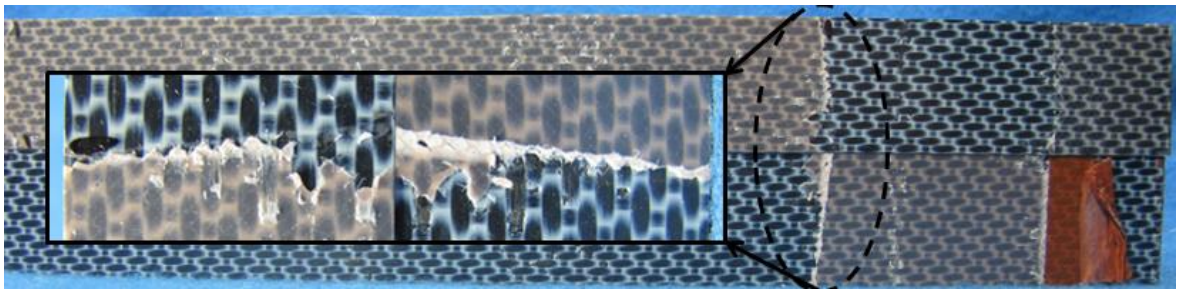

Figure 6.5: Fracture area of a specimen bonded with EP_1 treated with plasma and tested at RT and DCB

- Sensitivity of the surface properties

Wetzel et al [59] studied the sensitivity of the surface contamination level and different surface pre-treatments using the two mechanical tests studied in this project. It is concluded that DCB tests showed greater variations with respect to the different test configurations than SLS being DCB more sensitive to detect a weak interface and the surface treatments effects. The results obtained in this project using a similar adhesive can be seen in Figure 6.6 and are in agreement with this previous investigation even though the DCB specimens were bonded two weeks after the plasma surface activation.

Therefore, double cantilever beam tests appeared to be more sensitive to surface modifications, being easier to detect small changes on the surface compared to SLS, in which the same changes might not be detectable. This occurs in hot/wet condition where a similar shear strength mean value (9-11 MPa) after

the two pre-treatments and high standard deviation (±2.8) makes difficult to make reliable statements about the surface quality.

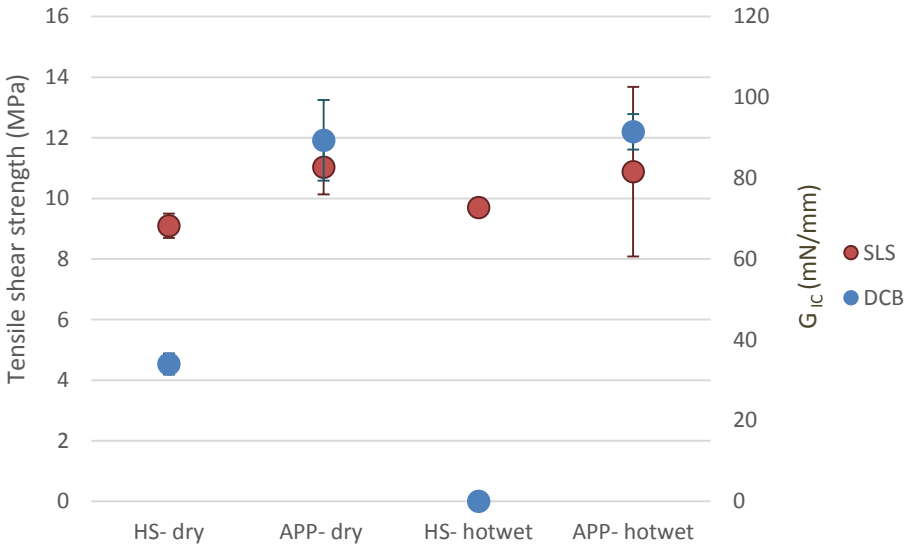

Figure 6.6: GIC and lap shear strength bonded with EP_2 for different surface treatments and storage conditions

However, this trend is hard to see using the other adhesives (Figure 6.7). In case of EP_1, the improvement after plasma is similar for both mechanical tests and moreover SLS shows lower standard deviation being more reliable the comparison between the different test series. This case contradicts the trend observed with EP_2 and Wetzel' study [59] since the difference between these two pre-treatments are more visible after SLS tests. With respect to PU adhesive, a reliable comparison cannot be made due to the fact that the samples were bonded 2 and 7 days after the pre-treatment and as it was stated, the ageing effect plays an important role on the adhesion performance.

This disagreement using EP_1 with respect to EP_2 can be explained looking into the failure modes. During DCB tests, certain considerations has to be taken into account with EP_1:

- The unstable propagation of the crack after plasma treatment in which the G_{IC} value represents the fracture energy for crack initiation rather than crack propagation. On the contrary, a stable crack growth was observed after hand sanding.
- After conditioning, both pre-treatments showed good adhesion properties showing cohesive failure at least on certain areas.
- Hand sanding specimens showed different failure modes within the same test series leading to high coefficient of variation (up to 55%).

These three aspects observed during testing makes difficult a reliable comparison of activation treatments using only DCB tests, and the information obtained from SLS is essential for assessing the surface quality.

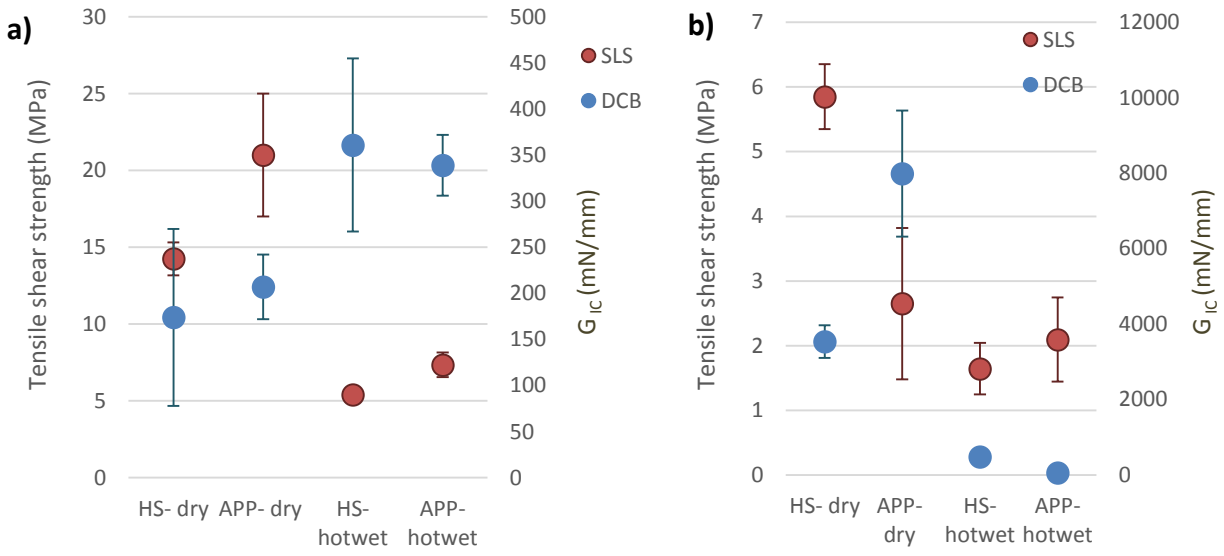

Figure 6.7: GIC and lap shear strength bonded with a) EP_1 and b) PU for different surface treatments and storage conditions

6.4. CF-PPS and CF-PEEK substrates

As it was stated before, adhesion performance is a surface phenomenon depending to a large extent on the properties of the substrates. The main research of this project was done using CF-PPS substrates, but a small evaluation was also carried out using another carbon fibre reinforced high performance thermoplastic PEEK. In this case, only the shear strength was evaluated for both pre-treatments and it could be observed the effect of the substrate in Figure 6.8, in which the results are plotted for PEEK and PPS substrates.

The most important aspect is that CF-PEEK substrate gives better results in all test series. In most cases, the predominant failure mode is still at the interface but the interatomic and interfacial forces between the adhesive and substrates are stronger. The performance depends on the surface properties and although the morphology was similar, the chemistry of the polymer differs; in case of PEEK, the molecular structure contains two ethers and one ketone. These functional groups are beneficial for the adhesion since the likelihood to form chemical interactions is higher as it can be observed on the higher polar component of the surface free energy of PEEK with respect to PPS.

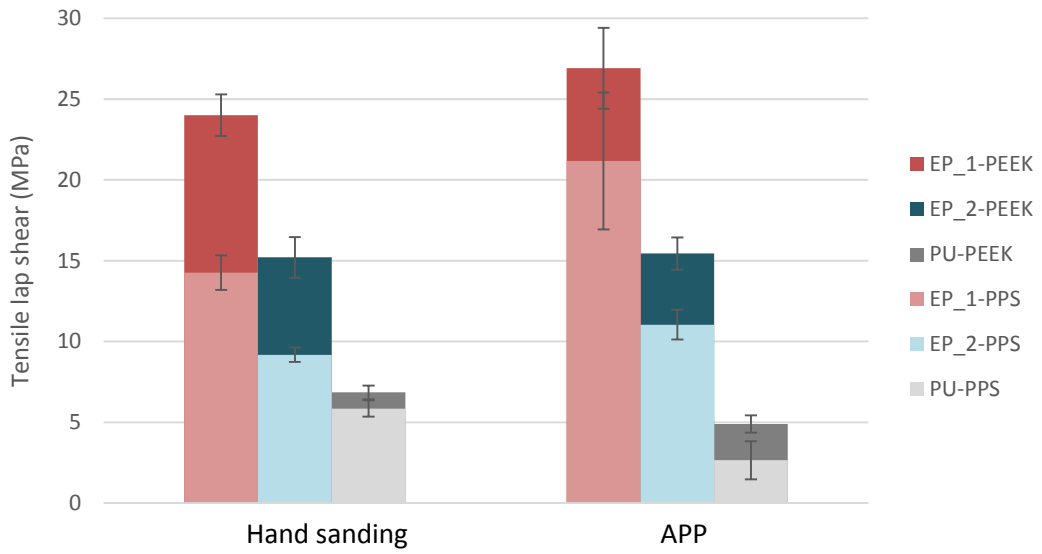

Figure 6.8: Shear strength values of CF-PPS and CF-PEEK substrates after hand sanding and APP

6.5. Comparison with thermoset substrates

The activation treatments were applied on CF-epoxy substrates in a previous internal investigation at Airbus Helicopters [58]. Hand sanding was carried out using the same internal instruction where the type of sandpaper, exhausting time of the acetone and cleaning steps are detailed, and with respect to APP treatment, a depth research was done to find the optimal parameters for CF-epoxy substrates, being the same used in this report.

The results using thermosets were performed using only the epoxies adhesives (EP_1 and EP_2) showing a satisfactory adhesion performance; DCB and SLS values were between a factor of 1.5 - 2 higher than CF-PPS with the failure modes cohesive or delamination in the substrate.

For thermoset composites, it was previous investigated by Kinloch [30] or H.M.S. Iqbal [13] among other the effect of hand sanding and solvent cleaning on the adhesion properties. This surface treatment gives satisfactory results with interlaminar or cohesive failure mode, analogous to the performance made at Airbus. The high wettability and the chemistry of the molecular chains with more functional groups compared to thermoplastics are the two main characteristics that ensure good bonding performance after a mechanical treatment such as hand sanding.

Airbus also study the effect of plasma treatment on thermoset composites due to a possible automation of the bonding process. The parameters chosen gave similar results than manual grinding and the failure mode was not at the interface, however the same parameters are inadequate for thermoplastic composites as it was seen in chapter 5. The plasma treatment on PPS was insufficient since the interface generally shows a small improvement with respect to hand sanding and the weakest link is still the interface. Although the surface changes observed showed potential for the improvement of the adhesion and were comparable to previous studies [31, 32], adhesive failure was still the predominant failure pattern.

This different behaviour can be explained because thermosets have higher polar component of the surface energy due to the chemistry of the molecular chains, therefore it is expected that with less intensity of plasma, the surface is modified slightly being sufficient for a change of the failure mode. But as it was stated, thermoplastics in general show more difficulties to achieve a strong bond [12, 30] and an activation treatment that produces more substantial changes on the surface should be necessary.

7. Conclusion and future work

Adhesion refers to a thin layer between the adhesive and substrate and implies all the interatomic forces and anchoring mechanisms to hold these two materials together [21], therefore the main parameters that define the adhesive performance are the adhesive, the substrate and the properties of its surface. To improve the adhesion performance, the properties of the surface can be changed by activation treatments such as hand sanding and/or plasma. The parameters used during activation modify the chemistry and topography of the surface which have a big influence on the behaviour of bonded joints.

Hand sanding treatment results in an unsatisfactory adhesion performance for CF-PPS and CF-PEEK since the adhesion properties are relatively low and they fail adhesively, which is an unacceptable failure mode. The main objective of abrasion is to roughen the surface, but due to the chemically inert composition of the substrates and considering molecular bonding as the main mechanism to achieve high strength, the likelihood of formation of strong covalent bonds is not high enough to avoid interfacial failure. As it was observed by R. Oosterom et al. in a research with UHMWPE (Ultra-high molecular weight polyethylene) [60], an important parameter of abrasion is the treatment time; concluding that the longer treatment time, the higher contact angle and shear strength. In this study with PPS, sanding was done manually without the measurement of the time and in this case the grade of the sandpaper influences the adhesion performance; coarser grains produced higher roughness which might lead to an increase of shear strength but care should be taken not to damage the fibres which will have a negative effect on the adhesion properties. Looking into the obtained results, it can be conclude that hand sanding is not an effective method to improve the adhesion on thermoplastic composites and should be used together with other energetic or chemical surface treatments, as it was studied by A.J. Kinloch [30] showing positive results.

Plasma treatment produces changes on the surface chemistry increasing the polar component of the surface free energy due to the insertion of functional groups (C-O, C=O, O-C=O S=O and O=S=O) leading to a better adhesion performance than hand sanding, which only roughens the surface. However, the optimum plasma parameters used on the surface activation for thermoset composites do not show good adhesion performance on thermoplastics.

An internal research at Airbus Helicopters was carried out to obtain the optimum parameters on plasma treatment with CF-epoxy substrates resulting in high values of tensile shear strength and adhesive fracture energy and avoiding the failure at the interface. However, CF-PPS and CF-PEEK do not exhibit good adhesion properties since their failure modes are predominantly at the interface. The main reason is an inadequate selection of plasma parameters since thermoplastics are inherent chemically inert and thus need greater surface changes than thermosets.

In case of plasma treatment, exposure time, power input and nozzle distance appear to be the main operational parameters to alter the surface properties. According to [60], increasing the exposure time and/or power input leads to a decrease on the contact angle up to a minimum, and then the angle increases slightly. The opposite behaviour occurs with the shear strength, reaching a maximum at certain parameters. Similar behaviour is observed in V.Fombuena's research [61] where the nozzle distance and

treatment rate were evaluated for PE substrates; decreasing the treatment rate or the nozzle distance leads to an increase of the surface energy and T-peel strength with a cohesive failure mode. Although in this project the nozzle distance and treatment rate were similar to the lowest value of the two parameters studied by V.Fombuena, the adhesive performance was different; being unsatisfactory for PPS. It should be then noted that not only the main operational parameters count, but also the characteristics of the generator, voltage and the type of equipment.

To achieve stronger changes, the parameters should have been optimized such as lower velocity of the cross-head inducing more treatment time on each area, lower distance nozzle or higher power input (as it was seen in [13, 49, 61, 62]). But, care should be taken not to overactivate the surface, since big functional molecules might be created that can be separated from the surface, resulting in a loss of the plasma effect as it was observed in [60] where the shear strength reaches a maximum and then decreases with increasing treatment time. The ageing effect also results in a loss of the surface modifications because the polymer will try to minimize its surface free energy being non-favourable for the adhesion performance, and in this project the bonding step was mainly carried out during the following week of the surface activation step.

Single lap shear and double cantilever beam tests have been performed to evaluate the surface modifications on the adhesion performance. Previous researches [59] concluded that DCB was more sensitive to surface changes, however, that trend was not always observed in this project. On the contrary, for the EP_1 adhesive, SLS is more sensitive. This occurs because during DCB tests, the crack propagation was unstable with an increase of its value between 90 and 150 mm so the calculation of the fracture energy is not completely adequate. In addition, hand sanding specimens tested in DCB show different failure patterns within the same test series, and as a result the coefficient of variation is higher than on SLS tests reaching the value of 55%. This high variation together with the unstable propagation of the crack makes very impossible to evaluate the modification of the surface properties with the fracture energy for mode I.

Future work

This study has evaluated two surface treatments to improve the adhesion performance on CF-PPS and CF-PEEK; two high performance thermoplastic materials. Although the results are not satisfactory in certain configurations, plasma treatment usually results in higher adhesion properties than hand sanding and shows high potential on the development of a strong interface and the avoidance of adhesive failure mode.

In this project, the parameters used on plasma treatment were expected to provide good adhesion performance based on the results of previous researches carried out in Airbus. However, as it was seen the adhesion behaviour depends to a large extent on the substrates used; and an extensive research for each material should be done with the analysis of the surface and performance of destructive tests. It is important to include both aspects of the investigations for these particular substrates, since in this case the surface after plasma treatment seemed very promising but it was insufficient for avoiding the interface to be the weakest link. An extensive research of the plasma process parameters such as power input, exposure time or velocity of the rotor should be studied in greater depth to obtain the optimum parameters for the adhesive performance.

As it has been seen, thermoplastic composites are more difficult to bond than thermosets and a simple abrasion treatment is not enough to change the failure mode. For this reason, thermoplastics should undergo to stronger changes than thermoset and the plasma parameters used on this project appear not to be strong enough. Therefore with plasma treatment, it is expected that with more aggressive parameters such as higher exposure time, lower nozzle distance or higher power input will produce better adhesion performance as long as the surface is not overactive. According to R. Oosterom et al. [60], the shear strength increases up to a maximum with respect to time or power input; therefore it is important to discover those parameters to reach the maximum shear strength and be able to optimize the process.

In addition, it should be noted that adhesives, substrates or the interface would change their properties when the samples are subjected to a simulated ageing condition. As it has been seen, there was not a general trend of this behaviour since it depends to a large extent on the adhesive used and mechanical test performed. Therefore, a study of the adhesive and its response to hot/wet conditioning should be made in order to obtain a complete understanding on the degradation of bonded joints in service.

8. Appendix

DSC spectrum –CF/PPS

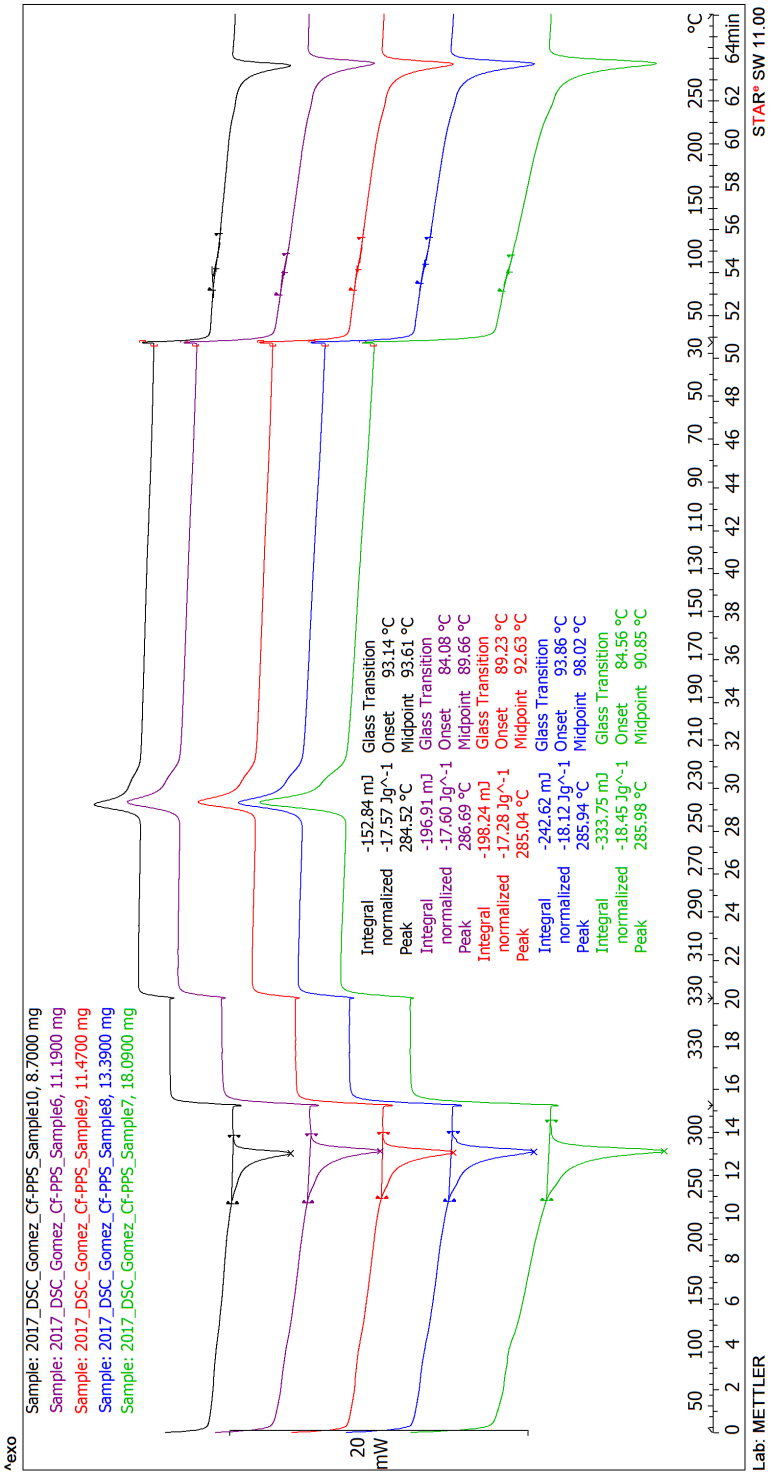

Figure 8.1: DSC spectrum from CF-PPS specimens

DSC spectrum –CF/PPS

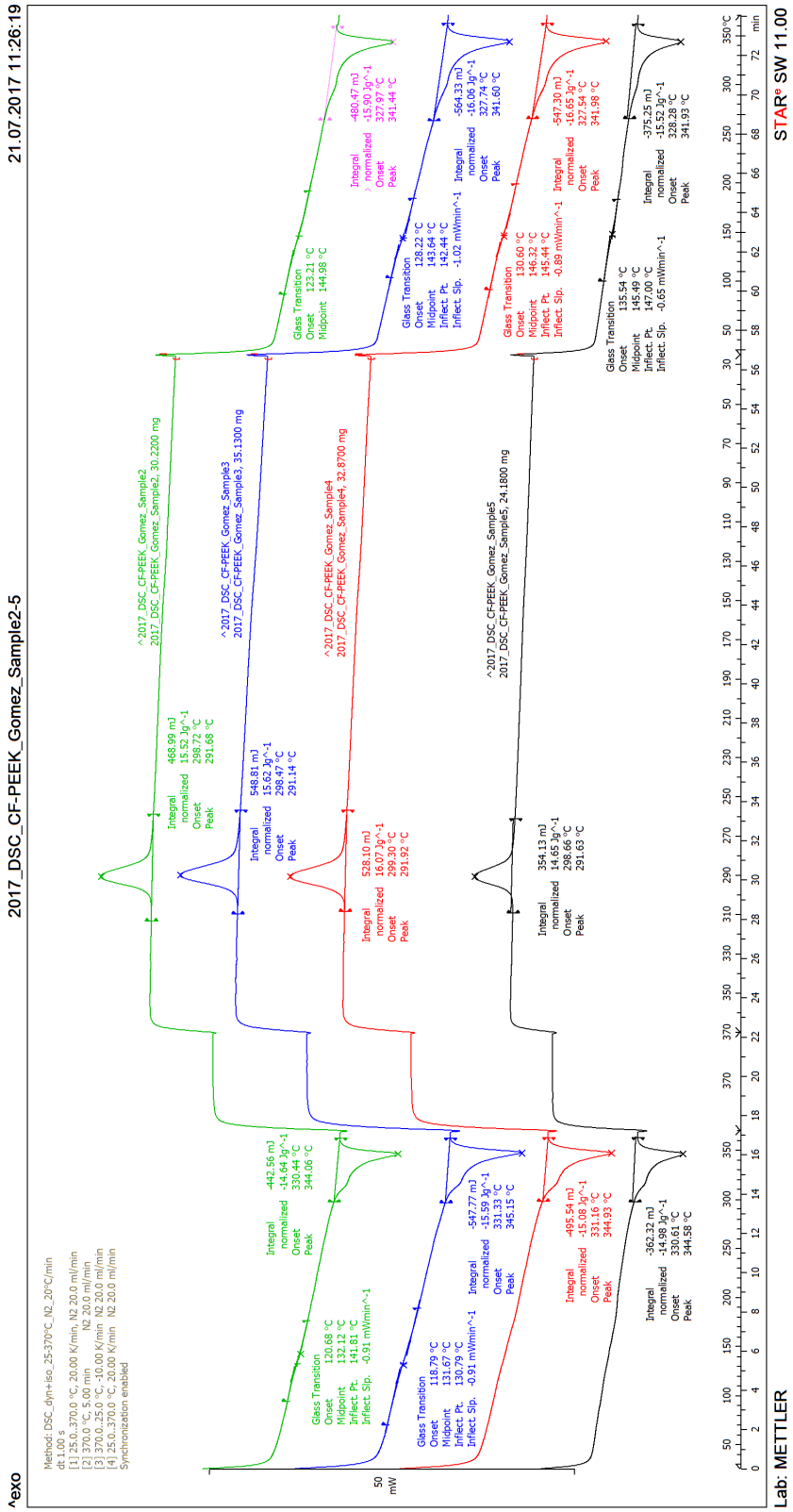

Figure 8.2: DSC spectrum from CF-PEEK specimens

Calculation of the surface energy

The average values of the contact angle are shown in Table 8.1 with the standard deviation; for each test configuration, three different liquids were used. The contact angle was measured at least 6 times for each configuration, and for each drop the program measured 10 times the left and right angle giving the mean and standard deviation for each drop. According to the standard EN 828:2013 at least three different liquids should be used and they should have different ratios of disperse and polar components of the surface energy.

Table 8.1: Contact angle measurements

Substrate	Surface treatment	Liquid	Average value (°)	STD
CF-PPS	Ref	H2O	79.05	1.31
		C2H6O2	57.02	1.97
		CH2I2	36.55	3.31
	Hand sanding	H2O	96.52	4.08
		C2H6O2	33.48	2.72
		MI	3.2	5.68
	APP	H2O	30.41	3.06
		C2H6O2	7.77	1.25
		MI	44.36	3.85
CF-PEEK	Ref	H2O	76.53	4.33
		C2H6O2	63.7	4.32
		CH2I2	54.49	10.1
	Hand sanding	H2O	75.38	10
		C2H6O2	29.84	2.7
		MI	16.15	1.54
	APP	H2O	20.91	9.00
		C2H6O2	5.32	1.94
		MI	39.46	3.27

The Owens-Wendt-Rabel-Kaelble equation (eq. 4.4) offers a relation between the surface energy of the solid (divided into its polar and disperse component), the surface tension of the liquid and the contact angle. The unknown values are the polar and disperse component of the surface energy of the solid, which as it can be seen correspond to the square of the slope and the square of the axis ordinate respectively.

$$\underbrace{\frac{(1+\cos\theta)\gamma_{LV}}{2\sqrt{\gamma_{LV}^{d}}}}_{y} = \underbrace{\sqrt{\gamma_S^P}}_{m} \cdot \underbrace{\frac{\sqrt{\gamma_{LV}^P}}{\sqrt{\gamma_{LV}^d}}}_{x} + \underbrace{\sqrt{\gamma_S^d}}_{b}$$

The value of the terms 'x' and 'y' are obtained from the contact angle and the surface properties of the liquid. In this case, three values were obtained for each configuration as it can be seen in Figure 8.3, and the equation of the straight line was obtained by linear regression using Excel.

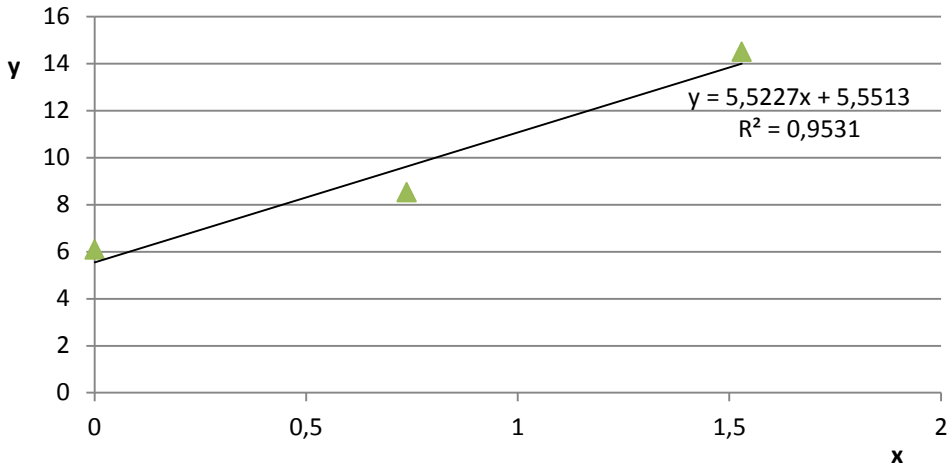

Figure 8.3: Linear relationship between the two terms of Owens-Wendt-Rabel-Kaelble equation

All the values from the Owens-Wendt-Rabel-Kaelble equation are presented in Table 8.2 and the surface free energy in Table 8.3.

Table 8.2: Data from Owens-Wendt-Rabel-Kaelble equation

Substrate	Surface treatment	Liquid	x	y	b	m
CF-PPS	Ref	H2O	1.53	9.28	6.02	1.88
		C2H6O2	0.74	6.63		
		CH2I2	0.00	6.43		
	Hand sanding	H2O	1.53	6.91	7.42	0.15
		C2H6O2	0.74	7.87		
		MI	0.00	7.12		
	APP	H2O	1.53	14.52	5.55	5.52
		C2H6O2	0.74	8.54		
		MI	0.00	6.11		
CF-PEEK	Ref	H2O	1.53	9.61	5.16	2.62
		C2H6O2	0.74	6.19		
		CH2I2	0.00	5.63		
	Hand sanding	H2O	1.53	9.76	6.88	1.82
		C2H6O2	0.74	8.01		
		MI	0.00	6.99		
	APP	H2O	1.53	15.08	5.63	5.76
		C2H6O2	0.74	8.56		
		MI	0.00	6.32		

Table 8.3: Values of surface free energy

		Surface Disperse Proportion	Surface Polar Proportion	Surface Free Energy
CF-PPS	Ref	36.26	3.54	39.80
	Hand sanding	54.99	0.02	55.01
	APP	30.82	30.50	61.32
CF-PEEK	Ref	26.67	6.88	33.54
	Hand sanding	47.32	3.31	50.63
	APP	31.73	33.18	64.91

Fracture analysis – DCB – CF/PPS

a)

b)

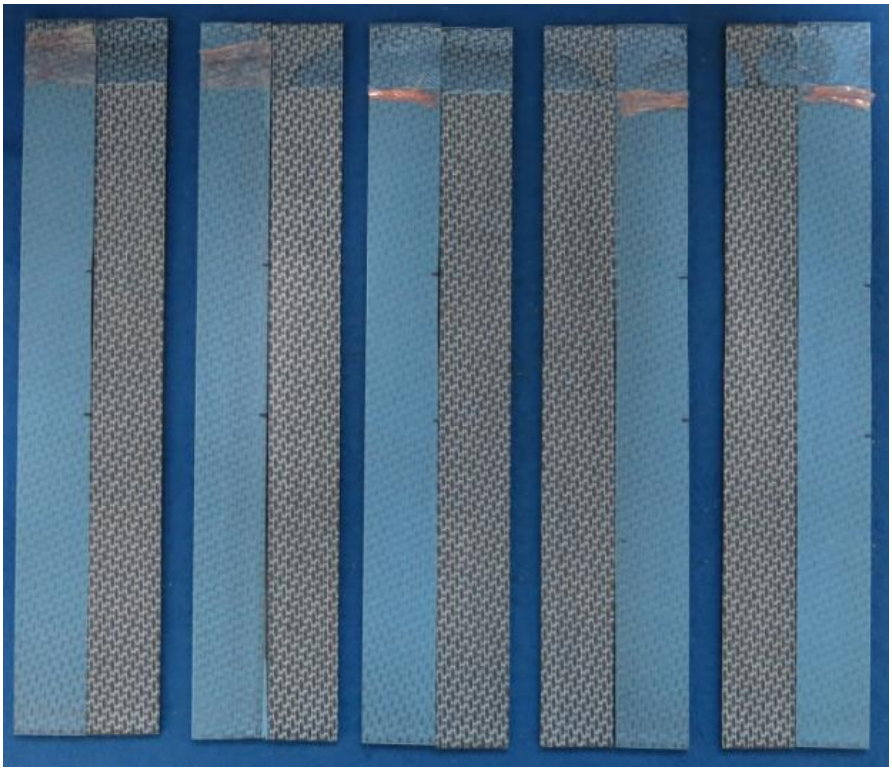

c)

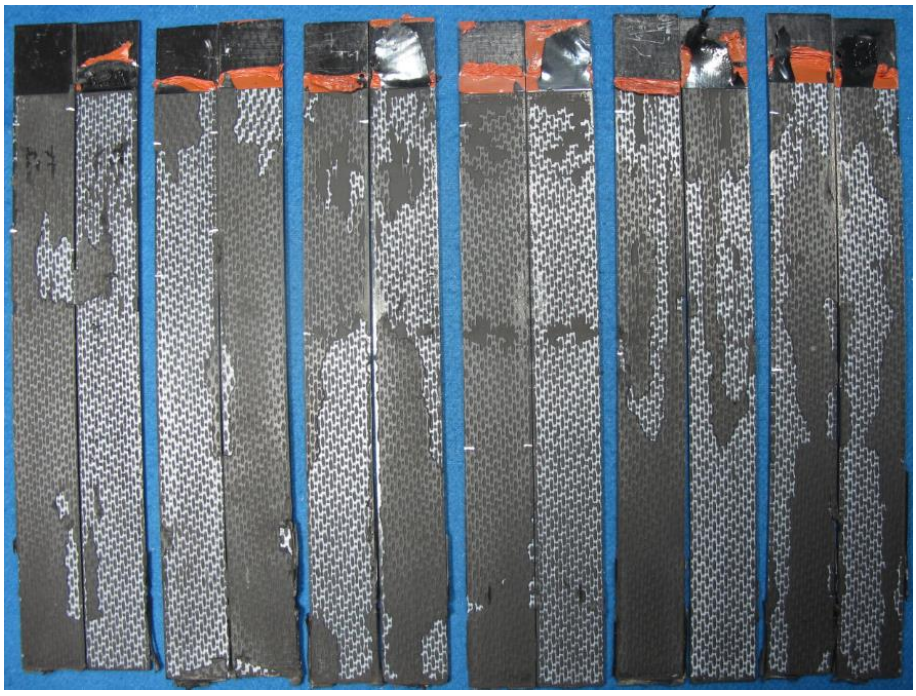

Figure 8.4: Fracture pattern DCB-sanding- dry-RT- bonded with a) EP_1, b) EP_2 and c) PU

a)

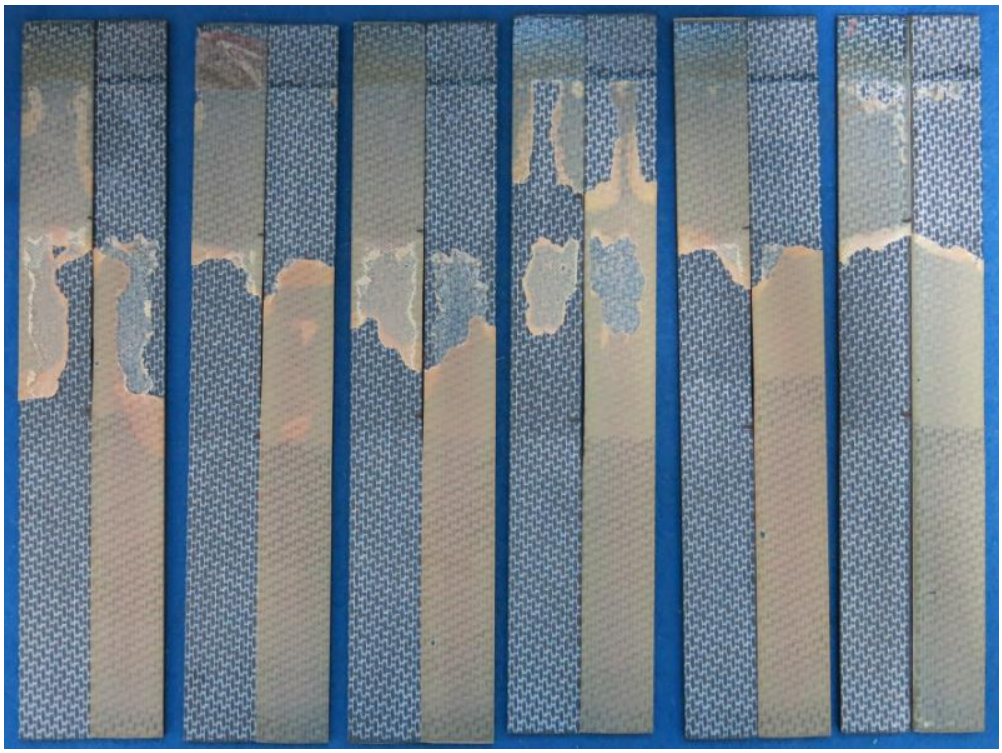

b)

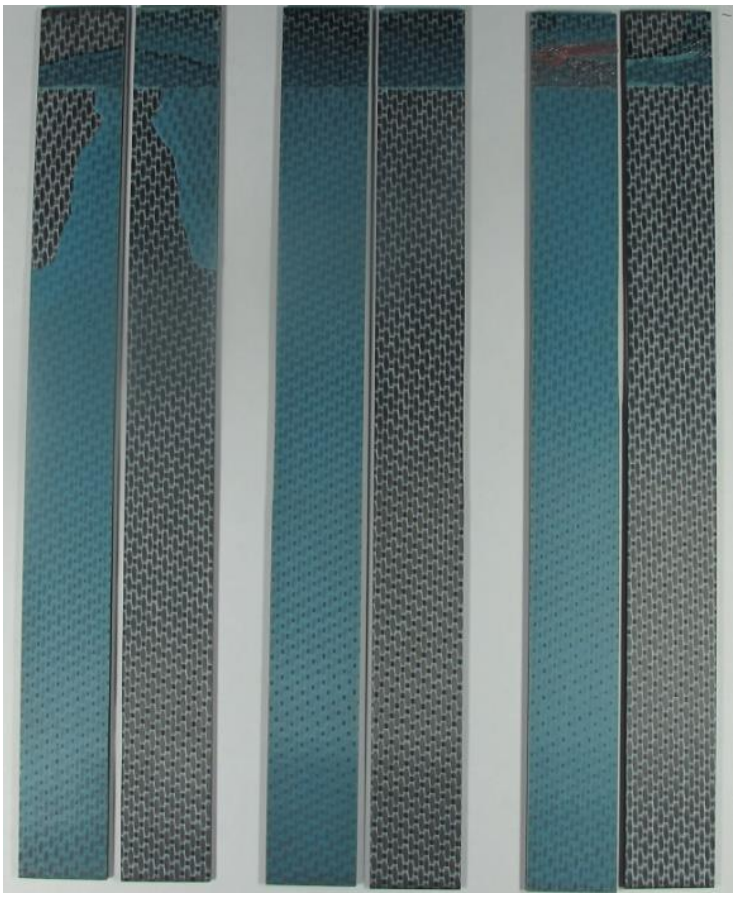

c)

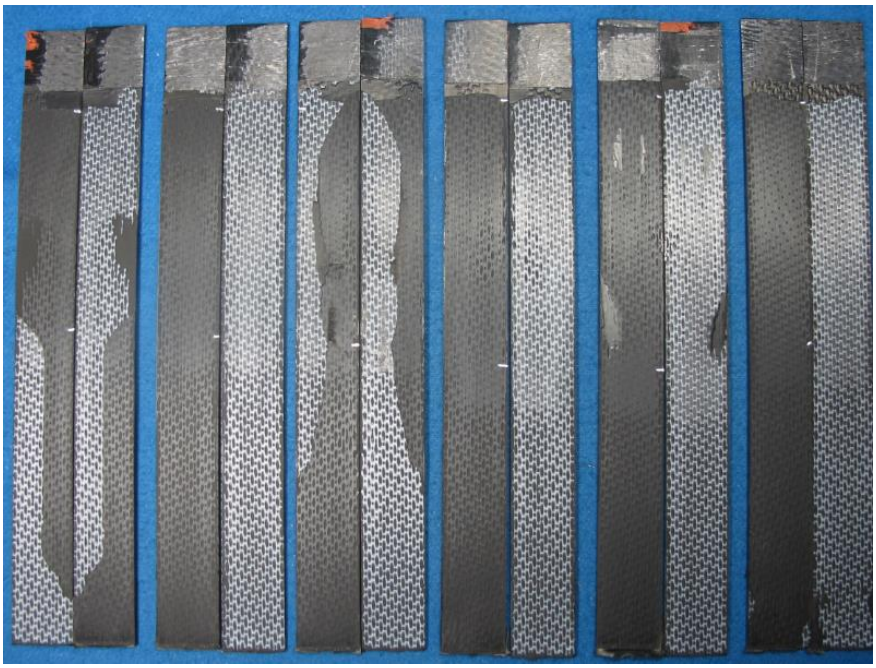

Figure 8.5: Fracture pattern SLS-grinding- hotwet-75°C bonded with a) EP_1, b) EP_2 and c) PU

a)

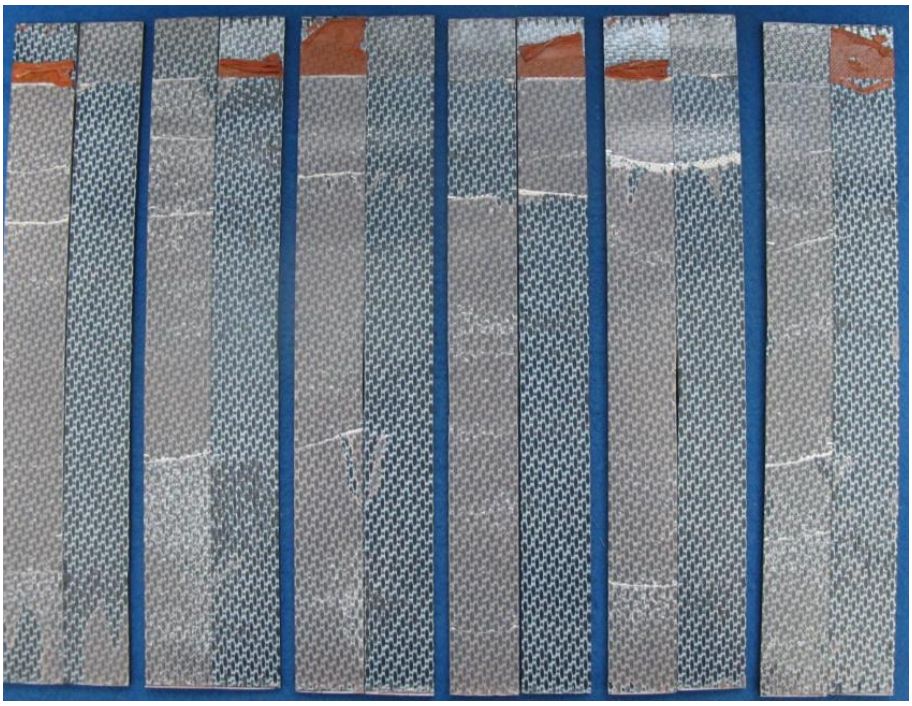

b)

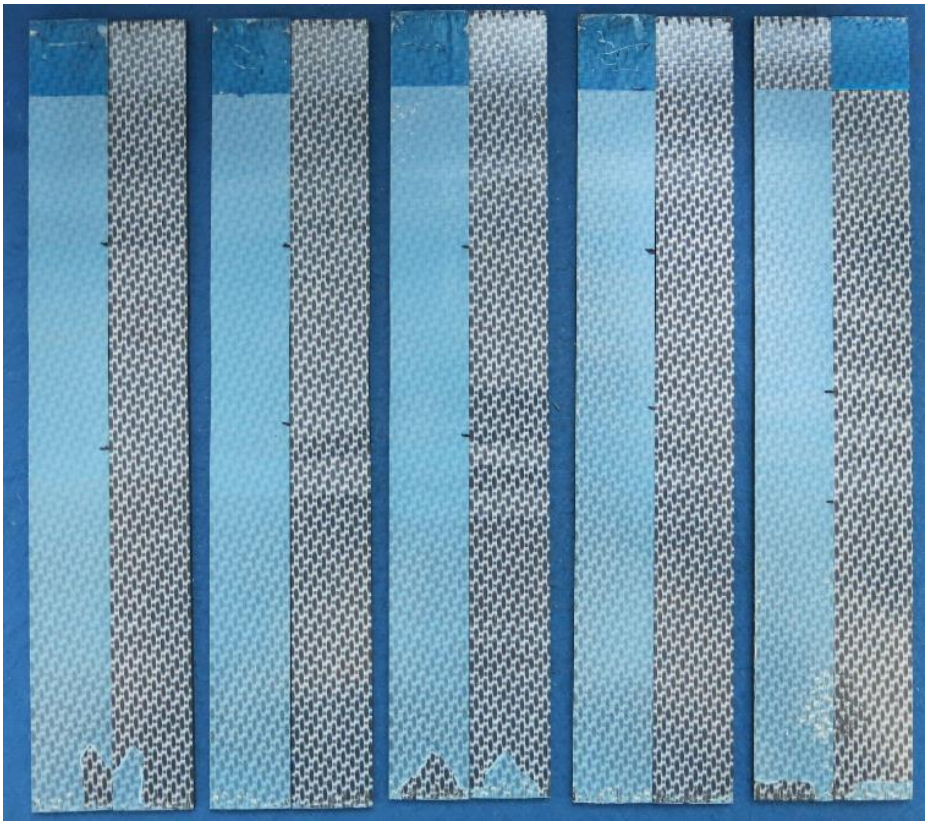

c)

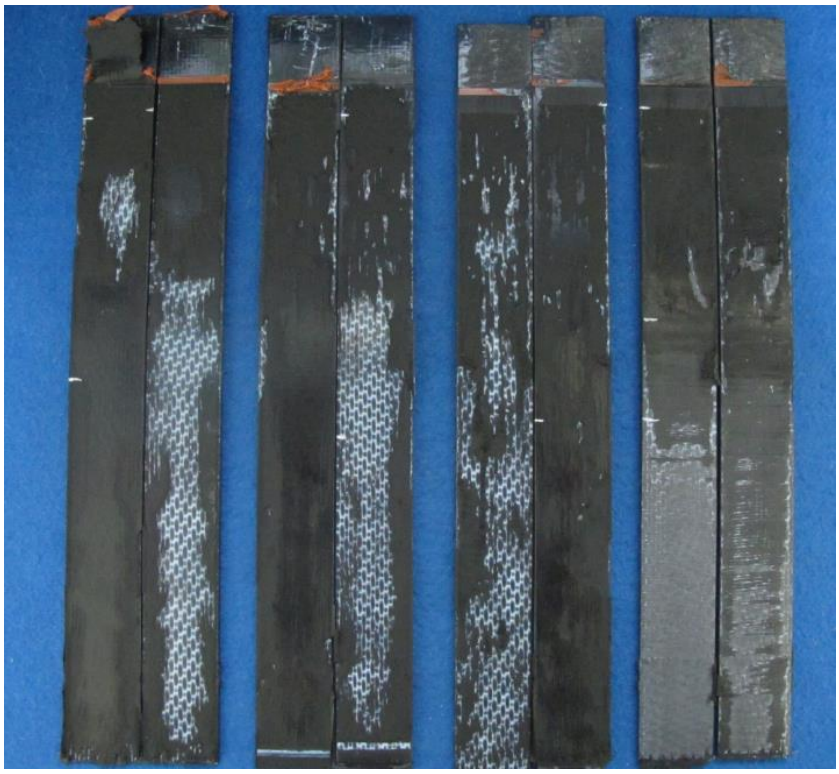

Figure 8.6: Fracture pattern DCB-APP- dry-RT- bonded with a) EP_1, b) EP_2 and c) PU

a)

b)

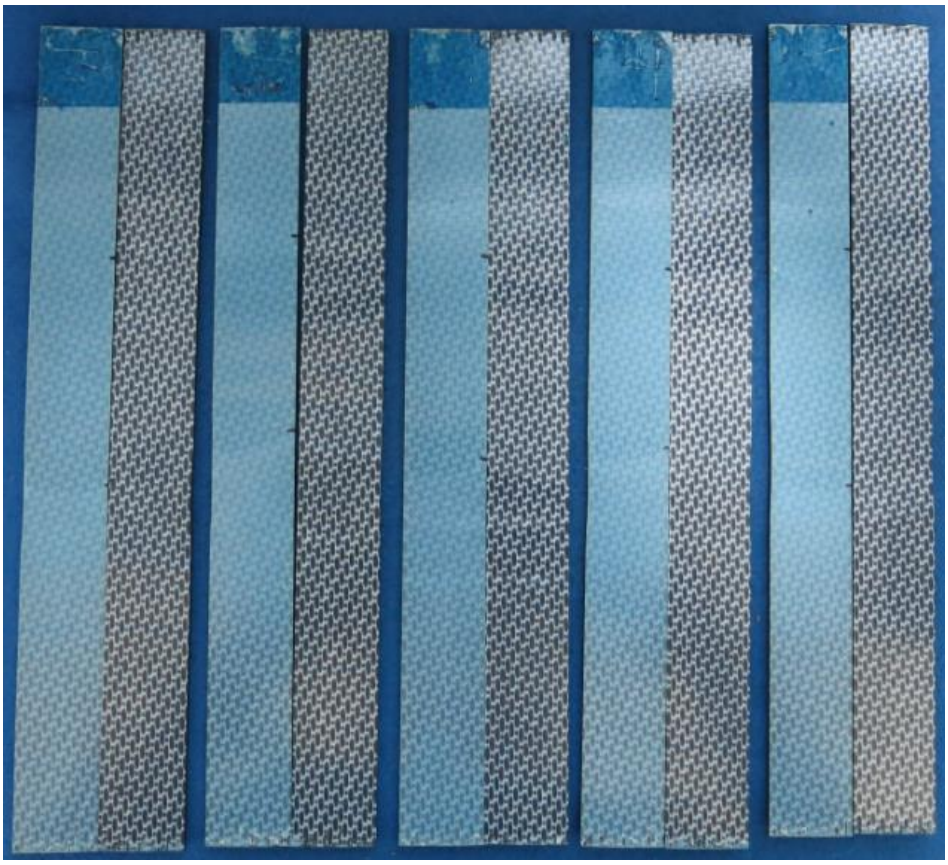

c)

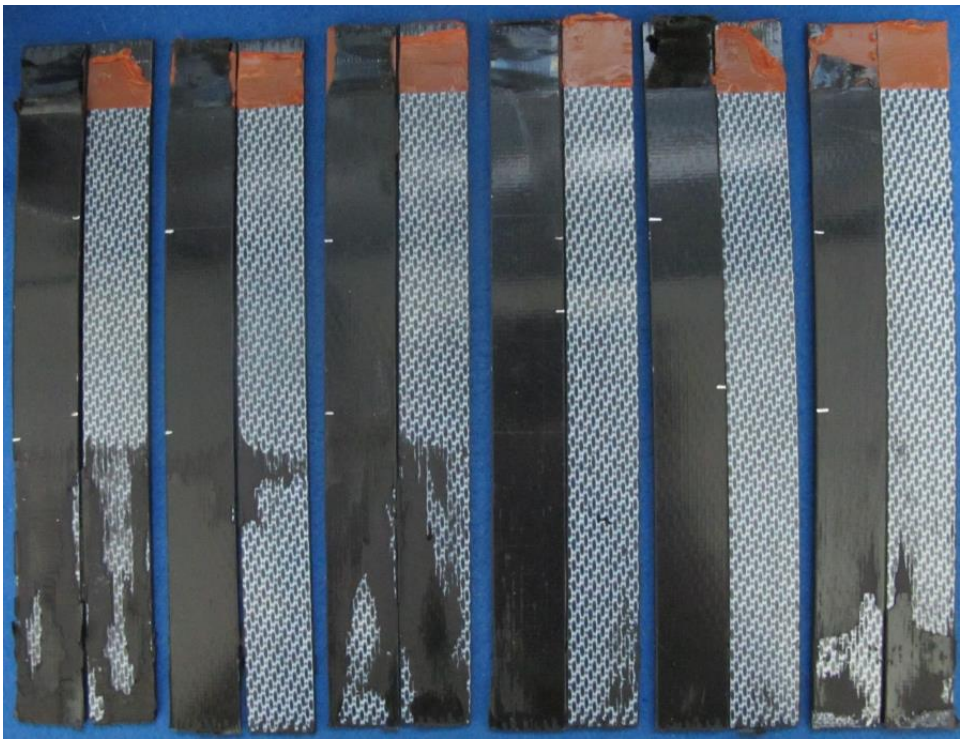

Figure 8.7: Fracture pattern DCB -APP- hotwet-75°C bonded with a) EP_1, b) EP_2 and c) PU

Fracture analysis – SLS – CF/PPS

- **Hand sanding – dry**

a)

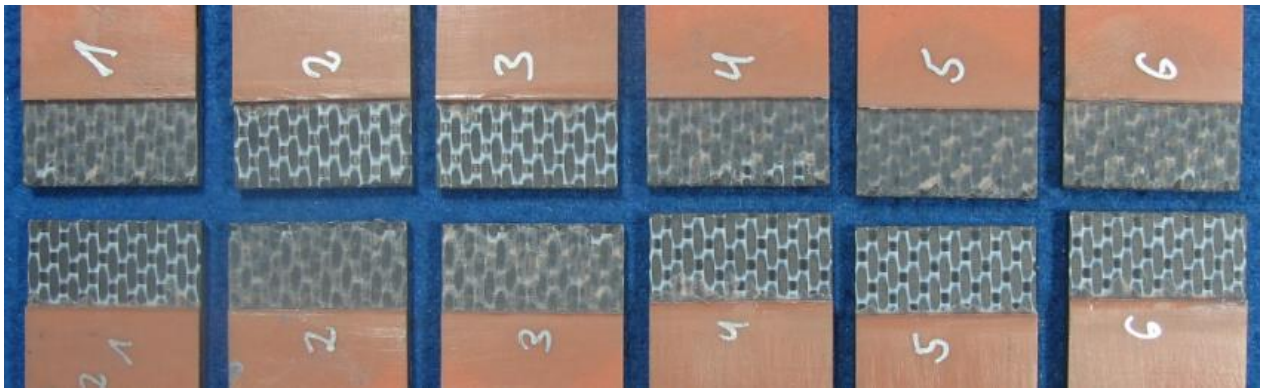

b)

c)

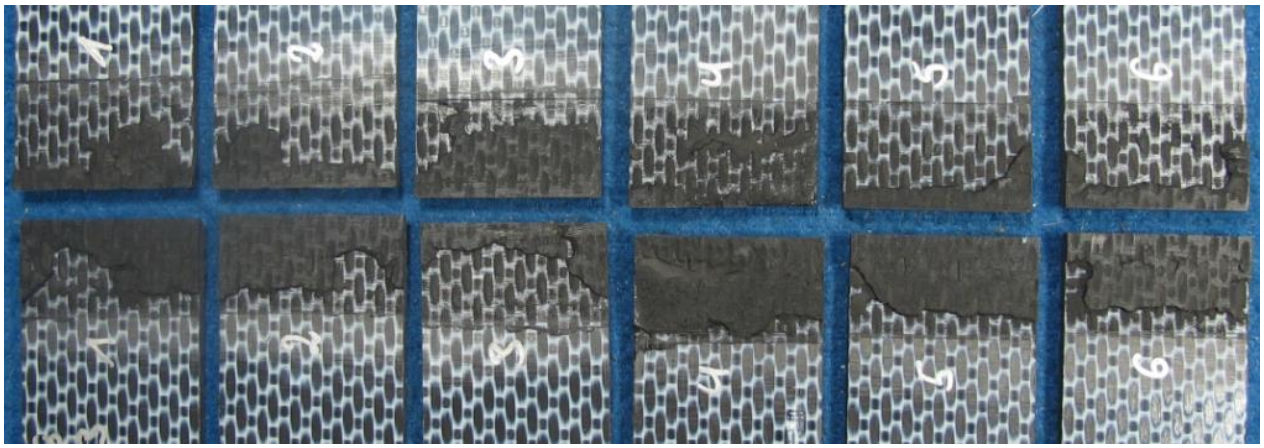

Figure 8.8: Fracture pattern SLS-sanding- dry-RT- bonded with a) EP_1, b) EP_2 and c) PU

- **Hand sanding – hot/wet conditioning**

a)

b)

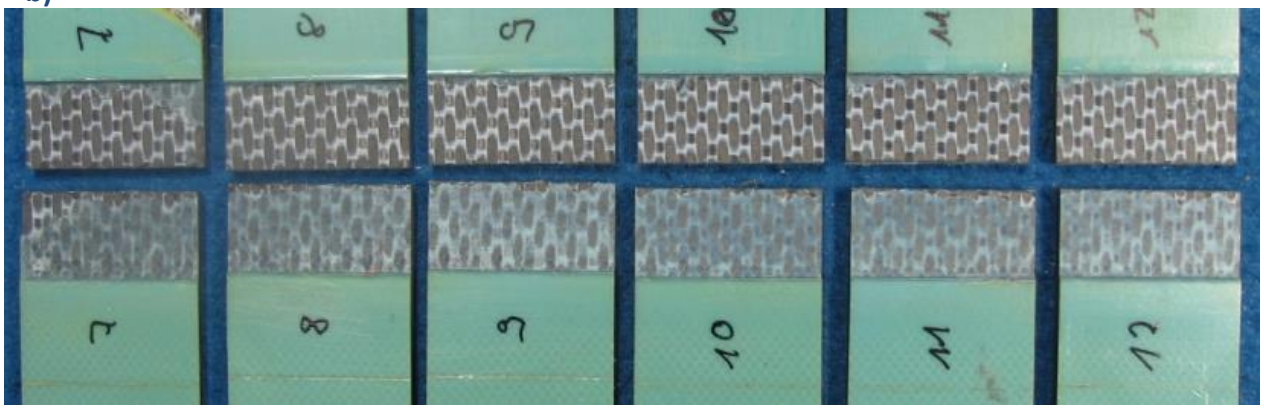

c)

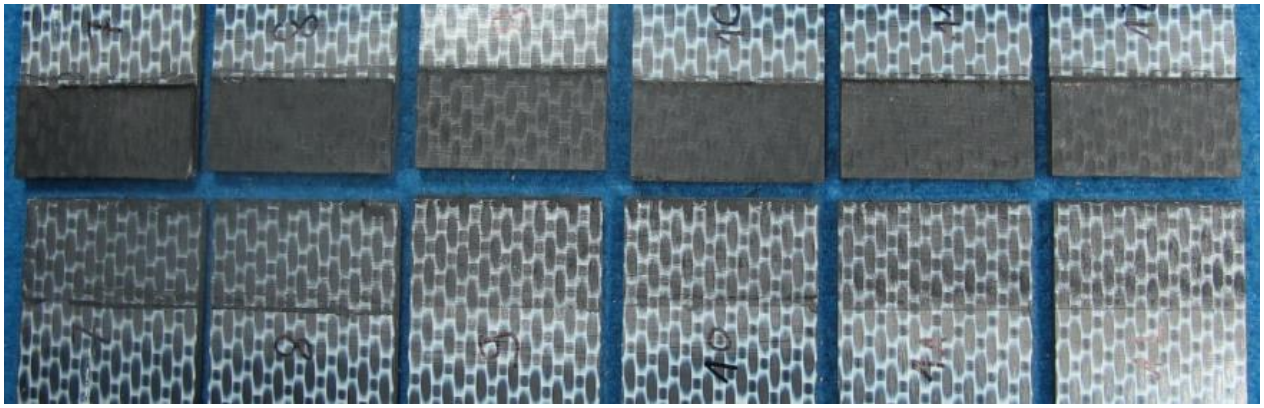

Figure 8.9: Fracture pattern SLS-sanding-hotwet-75°C bonded with a) EP_1, b) EP_2 and c) PU

- **APP – dry**

a)

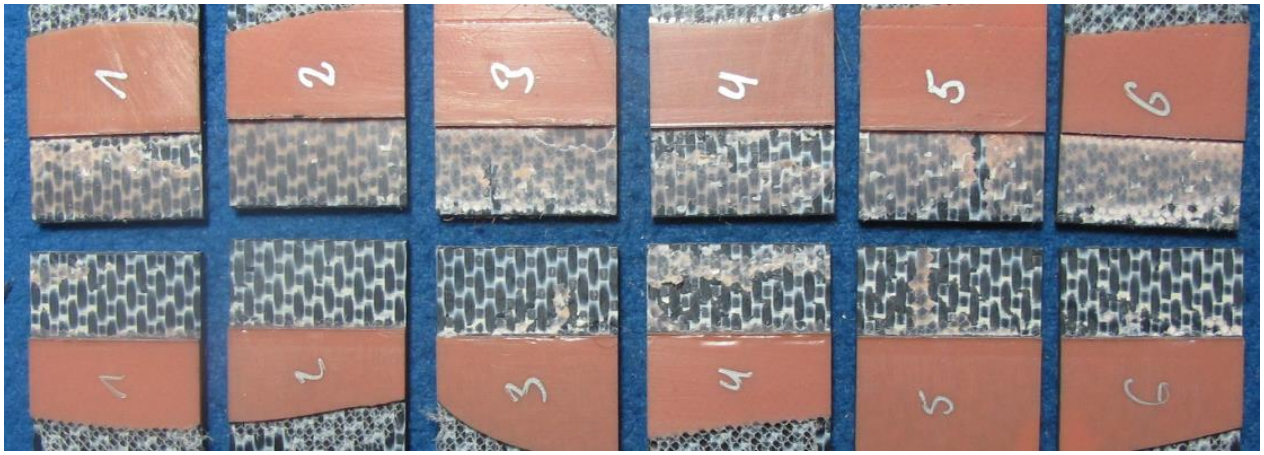

b)

c)

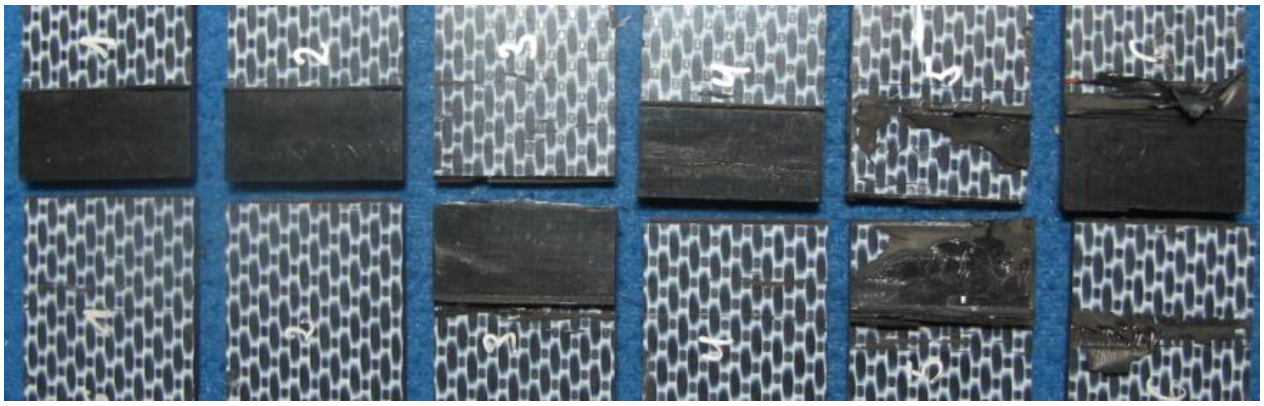

Figure 8.10: Fracture pattern SLS-APP- dry-RT bonded with a) EP_1, b) EP_2 and c) PU

- **APP – hot/wet conditioning**

a)

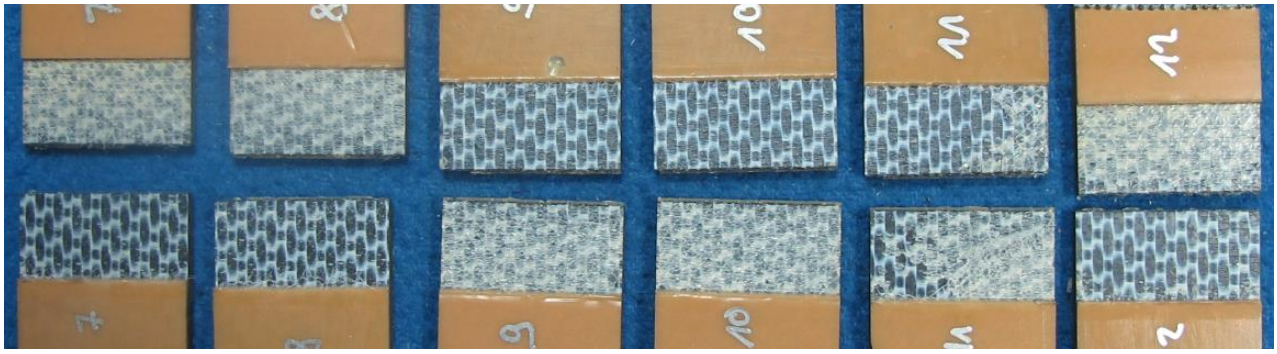

b)

c)

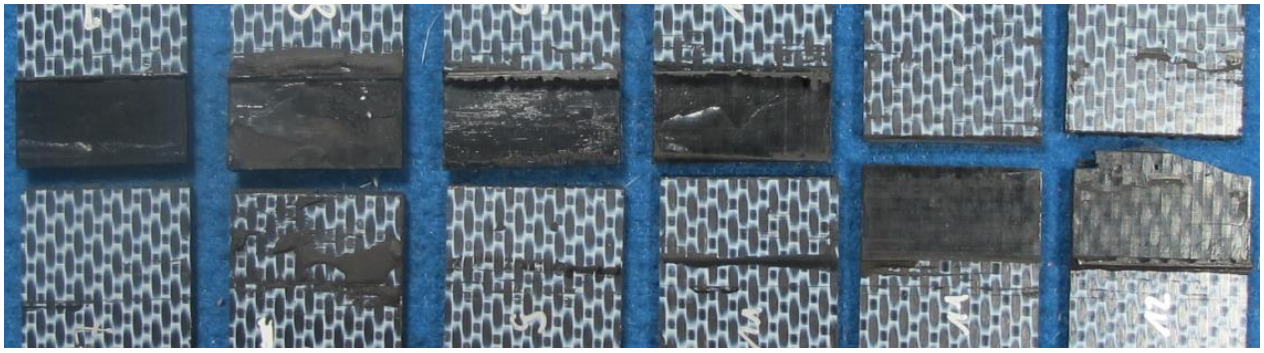

Figure 8.11: Fracture pattern SLS-APP- hotwet-75°C bonded with a) EP_1, b) EP_2 and c) PU

Fracture analysis – SLS CF/PEEK

a)

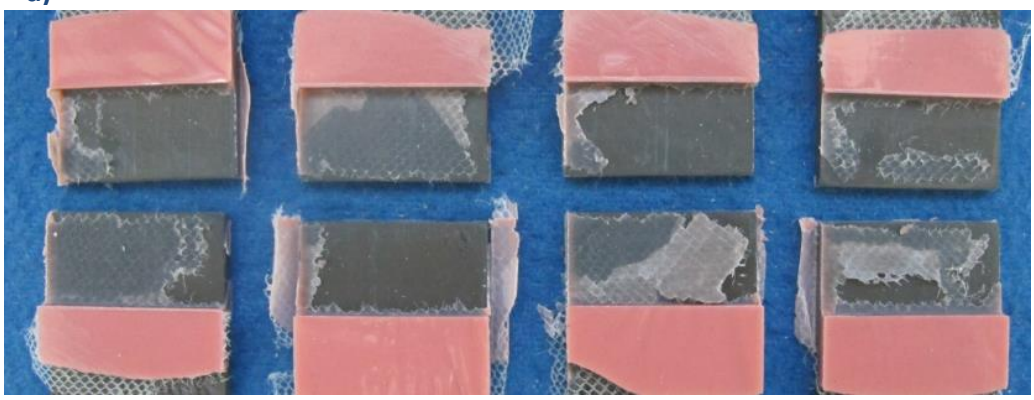

b)

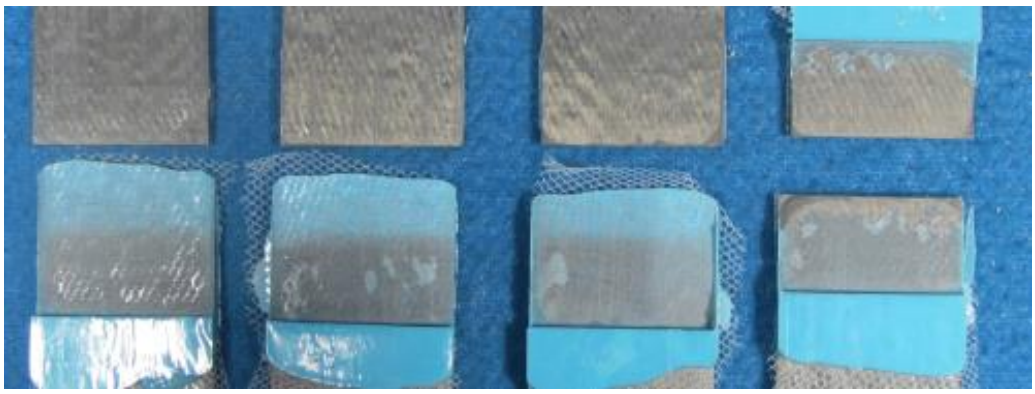

c)

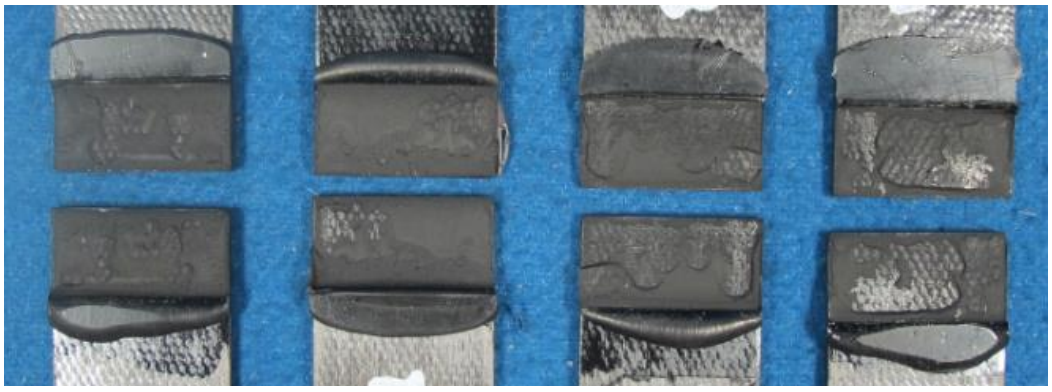

Figure 8.12: Fracture pattern CF-PEEK-SLS-grinding- dry-RT- bonded with a) EP_1, b) EP_2 and c) PU

a)

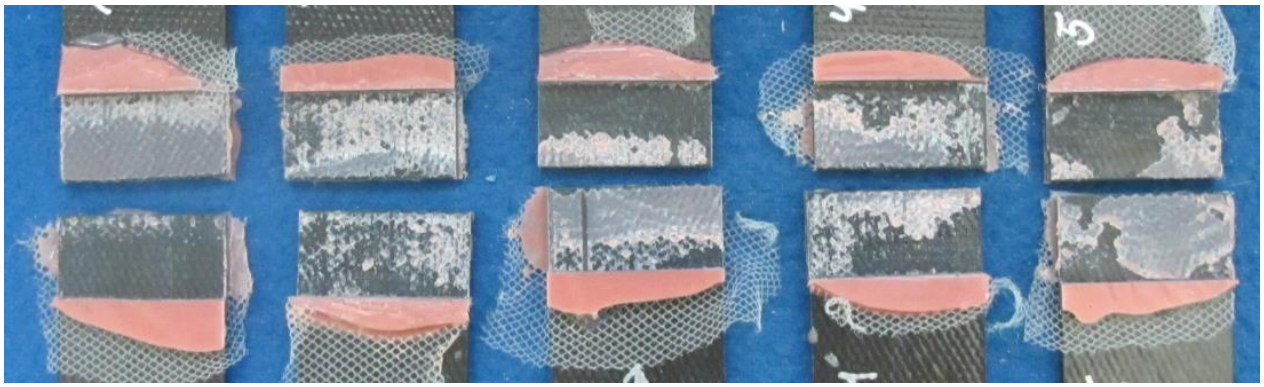

b)

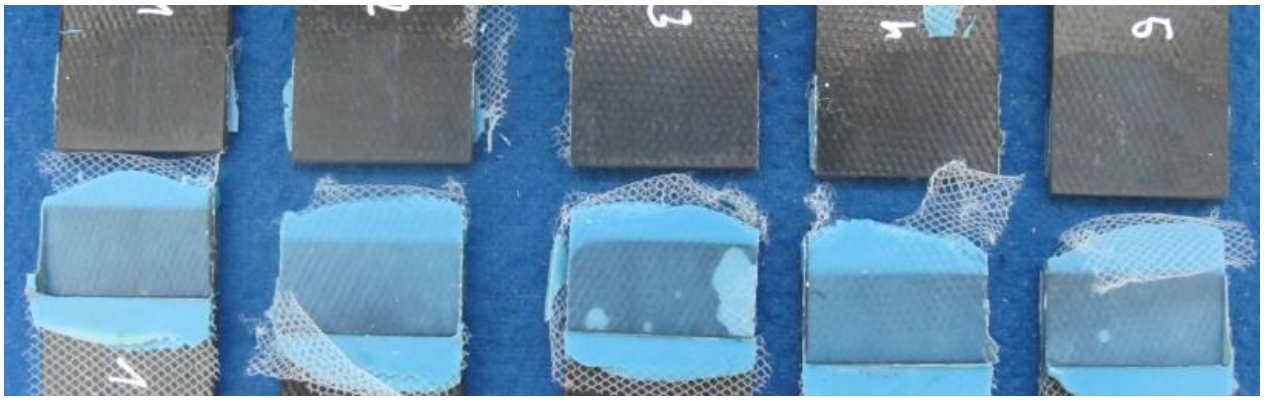

c)

Figure 8.13: Fracture pattern CF-PEEK-SLS-APP- dry-RT- bonded with a) EP_1, b) EP_2 and c) PU

9. References

1. *Fokker and partners win innovation award for thermoplastic tailplane of the AgustaWestland AW169 new-generation helicopter*. 2013; Available from: http://www.fokker.com/node/120.

2. Mash, G., *Reinforced thermoplastics, the next wave?* Reinforced Plastics, 2014. **58**(4): p. 24-48.

3. P.P Parlevliet, C.W., *Thermoplastic high performance composites: Environmental requirements on future helicopter airframes.* 18th International conference on composite materials.

4. Leeser, D. *Thermoplastic Composites- A proven Composite Material Technology Generates New Interest*. Helicopter Maintenance 2012; Available from: http://www.helicoptermaintenancemagazine.com/article/thermoplastic-composites.

5. Airbus. *The future is now! Airbus Helicopters unveils its all-new H160 as the benchmark for medium-class rotorcraft*. 2015; Available from: https://www.airbushelicopters.com/website/en/press/The-future-is-now-Airbus-Helicopters-unveils-its-all-new-H160-as-the-benchmark-for-medium-class-rotorcraft_1714.html.

6. S. Rana, R.F., *Advanced composite materials for aerospace engineering : processing, properties and applications*. 2016, Elsevier.

7. Red, C. *The outlook for thermoplastic in Aerospace composites, 2014-2023*. High-performance composites 2014]; Available from: http://www.compositesworld.com/articles/the-outlook-for-thermoplastics-in-aerospace-composites-2014-2023.

8. Black, S. *Structural adhesives, Part II: Aerospace*. CompositesWorld 2016; Available from: http://www.compositesworld.com/articles/structural-adhesives-part-ii-aerospace.

9. EASA, *Composite Aircraft Structure AMC 20-29*. 2010: https://www.easa.europa.eu/system/files/dfu/Annex%20II%20-%20AMC%2020-29.pdf.

10. M.D. Banea, L.F.M.d.S., *Adhesively bonded joints in composite materials: an overview.* Materials: Design and application, 2008. **223**(L).

11. Gardiner, G. *Certification of bonded composite primary structures*. Composites World 2014; Available from: http://www.compositesworld.com/articles/certification-of-bonded-composite-primary-structures.

12. Favaloro, M., *PPS for continuous fiber composites aerospace applications.* Celanese, 2013.

13. H.M.S. Iqbala, S.B., R. Benedictus, *Study on the effect of surface morphology on adhesion properties of polybenzimidazole adhesive bonded composite joints.* International Journal of Adhesion & Adhesives, 2017. **72**: p. 43-50.

14. *Rython PPS; thermal stability, dimensional stability, chemical resistance and inherent flame retardancy*. Available from: http://www.solvay.com/en/markets-and-products/featured-products/Ryton-PPS.html.

15. Kazunaka Endo, S.S., Nobuhiko Kato, Tomonori Idaa, *Analysis of valence XPS and AES of (PP, P4VP, PVME, PPS, PTFE) polymers by DFT calculations using the model molecules.* Journal of Molecular Structure, 2016. **1122**: p. 341-349.

16. Béland, S., *High performance thermoplastic resins and their composites*. Institute for Aerospace research. National research council of Canada.

17. *TRP company - Polyphenylene sulfide (PPS)*. Available from: http://www.rtpcompany.com/products/product-guide/polyphenylene-sulfide-pps/.

18. Nabil Anagreh, L.D., Christine Bilke-Krause, *Low-pressure plasma treatment of polyphenylene sulfide (PPS) surfaces for adhesive bonding* International journal of Adhesion and Adhesives, 2007. **28**.

19. muller, D.a. *What is PEEK?* ; Available from: http://www.dollfus-muller.com/en/FAQ-General/what-is-peek.html.

20. Fluorocarbon. *Material overview: PEEK*. Available from: http://www.fluorocarbon.co.uk/products/material-overview/peek.

21. Adhesive, G.a.S. *Definition of Adhesion*. Available from: http://www.adhesiveandglue.com/adhesion-definition.html.

22. M.Petrie, E., *Choosing Adhesive Bonding Over Other Fastening Methods- Weighing the Options.* 2008.

23. transportation, U.S.D.o., *Best Practice in Adhesive-Bonded Structures and Repairs*, F.A. Administration, Editor. 2007.

24. Soo-Jin Park, M.-k.S., *Interface Science and Composites*, ed. I. University. Vol. 18. 2011: Elsevier.

25. Baldan, A., *Adhesion phenomena in bonded joints.* International Journal of Adhesion & Adhesives, 2012. **38**: p. 95-116.

26. Firas Awajaa, M.G., Georgina Kelly, Bronwyn Fox, Paul J. Pigram, *Adhesion of polymers.* Progress in Polymer Science, 2009. **34**.

27. Ebnesajjad, S., *Surface Treatment of Materials for Adhesion Bonding*, ed. W.A. Publishing. 2006.

28. M J Shenton, M.C.L.-H.a.G.C.S., *Adhesion enhancement of polymer surfaces by atmospheric plasma treatment.* JOURNAL OF PHYSICS D: APPLIED PHYSICS, 2001. **34**: p. 2754-2760.

29. E.M. Liston, L.M., M.R. Wertheimer, *Plasma surface modification of polymers for improved adhesion: a critical review.* Journal of Adhesion Science and Technology, 1993. **7**(10): p. 1091-1127.

30. A. J. Kinloch, G.K.A.K.a.J.F.W., *The Adhesion of Thermoplastic Fibre Composites.* Philosophical Transactions: Physical Sciences and Engineering, 1992. **338**: p. 83-112.

31. H.M.S. Iqbal, S.B., R.Benedictus, *Surface modification of high performance polymers by atmospheric pressure plasma and failure mechanism of adhesive bonded joints.* International Journal of Adhesion & Adhesives, 2010. **30**: p. 418-424.

32. Rui Hong, D.X., Xiaojun Wang, Shengru Long, Gang Zhang and Jie Yang, *Effect of air dielectric barrier discharge plasma treatment on the adhesion property of sanded polyphenylene sulfide.* High performance polymers, 2015: p. 1-10.

33.

Data sheet adhesives: CONFIDENTIAL

34.

35. M. Kilinc, S.C., C. Eyupoglu, D. Kut, *The Evaluation with Statistical Analyses of the Effect of Different Storage Condition and Type of Gas on the Properties of Plasma Treated Cotton Fabrics.* Procedia - Social and Behavioral Sciences 2015. **195**: p. 2170-2176.

36. E.Moritzer, C.B., C. Leister, *Effect of atmospheric pressure plasma pre-treatment and aging conditions on the surface of thermoplastics.* Weld World, 2015. **59**: p. 23-32.

37. Scientific, T.F. *Learn XPS. Analysis of Surfaces and Thin Films*. 2013-2016; Available from: http://xpssimplified.com/whatisxps.php.

38. D.Y. Kwok, A.W.N., *Contact angle measurement and contact angle interpretation.* Advances in Colloid and Interface Science, 1999. **81**: p. 167-249.

39. K-Y. Law, H.Z., *Surface Wetting: Characterization, Contact Angle, and Fundamentals* 2016: Springer International.

40. E.L. Decker, B.F., Y. Suo, S. Garoff, *Physics of contact angle measurement.* Colloids and Surfaces. A, 1999. **156**: p. 177-189.

41. Y. Yuan, T.R.L., *Contact Angle and Wetting Properties*, in *Surface Science Technique*. 2013, Springer Berlin Heidelberg.

42. *KRÜSS Advancing your surface science*. Available from: https://www.kruss.de/services/education-theory/glossary/youngs-equation/.

43. Wendt, D.K.O.a.R.C., *Estimation of the Surface Free Energy of Polymers.* Journal of applied polymer science, 1969. **13**: p. 1741-1747.

44. R.M Lopes, R.D.S.G.C., F.J.G da Silva, T.M.S Faneco, *Comparative evaluation of the Double-Cantilever Beam and Tapered Double-Cantilever Beam tests for estimation of the tensile fracture toughness of adhesive joints.* International Journal of Adhesion & Adhesives, 2016. **67**: p. 103-111.

45. Standard, E., *Aerospace series - Carbon fibre reinforced plastics - Test method - Determination of interlaminar fracture toughness energy - Mode I - GIC*. 2015.

46. *AdhesivesToolkit*. Available from: http://www.adhesivestoolkit.com/Docs/test/MECHANICAL%20TEST%20METHOD%201%20-%20Shear%20Tests.xtp.

47. S. Guo, D.A.D., R.H. Plaut, *Effect of boundary conditions and spacers on single-lap joints loaded in tension or compression.* International Journal of Adhesion & Adhesives, 2006. **26**: p. 629-638.

48. Stojilovic, N., *Why Can't We See Hydrogen in X-ray Photoelectron Spectroscopy?* Journal of Chemical Education, 2012. **89**: p. 1331-1332.

49. B.R.K. BLACKMAN, A.J.K.a.F.W., *The plasma treatment of thermoplastic fibre composites for adhesive bonding.* Composites, 1994. **25**(5): p. 332-340.

50. U. Cvelvar, M.M., I. Junkar, *Oxygen plasma functionalization of poly(p-phenilene sulphide).* Applied Surface Science, 2007. **253**: p. 8669-8673.

51. H.J. Busscher, A.W.J.V.P., P. De Boer, *The effect of surface roughening of polymers on measured contact angles of liquids* Colloids and Surfaces, 1984. **9**: p. 319-331.

52. R.C. Chatelier, X.X., T.R. Gengenbach, H.J. Griesser, *Quantitative Analysis of Polymer Surface Restructuring* Langmuir, 1995. **11**: p. 2576-2584.

53. Y. Sekiguchi, M.K.a.C.S., *Experimental study of the mode I adhesive fracture energy in DCB specimens bonded with a polyurethane adhesive.* The journal of adhesion, 2017. **93**(3): p. 235-255.

54. J. Comyn, L.M.a.G.X., *Corona-discharge treatment of polyetheretherketone (PEEK) for adhesive bonding.* International Journal of Adhesion & Adhesives, 1996. **16**: p. 301-304.

55. C. Mandolfino, E.L., C. Gambaro, M. Bruno, *Improving adhesion performance of polyethylene surfaces by cold plasma treatment.* Meccanica, 2014. **49**: p. 2299-2306.

56. W. Leahy , V.B., M. Buggy , T. Young , A. Mas , F. Schue , T. McCabe & M.Bridge, *Plasma Surface Treatment of Aerospace Materials for Enhanced Adhesive Bonding.* The Journal of Adhesion, 2001. **77**: p. 215-249.

57. Han S, L.Y., Kim u H, ho Kim G, Lee J, Yoon JH, et al. , *Polymer surface modification by plasma source ion implantation.* Surf Coat Technol, 1997. **93**: p. 261-264.

58. Helicopters, A., *ECD – TN – EDVLO – 2013-031*. 2016.

59. M. Wetzel, J.H., J.Gudladt, J.V.Czarnecki *Sensitivity of double cantilever beam test tos urface contamination and surface pretreatment.* International Journal of Adhesion & Adhesives, 2013. **46**: p. 114-121.

60. R. Oosterom, T.J.A., J.A. Poulis, H.E.N. Bersee, *Adhesion performance of UHMWPE after different surface modification techniques.* Medical Engineering & Physics, 2005. **28**: p. 323-330.

61. V. Fombuena, J.B., T. Boronat, L. Sánchez-Nácher, D. Garcia-Sanoguera, *Improving mechanical performance of thermoplastic adhesion joints by atmospheric plasma.* Materials and Design, 2013. **47**: p. 49-56.

62. T. Zeiler, P.P., M. Kürner and H. Münstedt, *Improvement of adhesive bonding of thermoplastics polymers by different surface treatments.* Macromol. Symp, 1997. **126**.